Aus der

Abteilung für Hand-, Plastische und Ästhetische Chirurgie

Klinikum der Ludwig-Maximilians-Universität München

Optimization of novel photosynthetic biomaterials and design of a hibernation-like process for their preservation

Dissertation

zum Erwerb des Doctor of Philosophy (Ph.D.)

an der Medizinischen Fakultät

der Ludwig-Maximilians-Universität München

vorgelegt von

Rocio Corrales Orovio

aus

Madrid / Spanien

Jahr

2024

Mit Genehmigung der Medizinischen Fakultät der
Ludwig-Maximilians-Universität München

Erstes Gutachten:	Prof. Dr. Thilo Schenck
Zweites Gutachten:	Prof. Dr. Thomas Egana
Drittes Gutachten:	Prof. Dr. Sebastian Baumbach
Viertes Gutachten:	Priv. Doz. Dr. Elias Volkmer

Dekan: Prof. Dr. med. Thomas Gudermann

Tag der mündlichen Prüfung: 23.09.2024

Affidavit

LMU LUDWIG-MAXIMILIANS-UNIVERSITÄT MÜNCHEN | Promotionsbüro Medizinische Fakultät | MMRS

Affidavit

Corrales Orovio, Rocío

Surname, first name

I hereby declare, that the submitted thesis entitled:

Optimization of novel photosynthetic biomaterials and design of a hibernation-like process for their preservation

is my own work. I have only used the sources indicated and have not made unauthorised use of services of a third party. Where the work of others has been quoted or reproduced, the source is always given.

I further declare that the dissertation presented here has not been submitted in the same or similar form to any other institution for the purpose of obtaining an academic degree.

Santiago, 20-10-2024

place, date

Rocio Corrales Orovio

Signature doctoral candidate

Confirmation of congruency

LMU LUDWIG-MAXIMILIANS-UNIVERSITÄT MÜNCHEN

Promotionsbüro
Medizinische Fakultät

MMRS

Confirmation of congruency between printed and electronic version of the doctoral thesis

Corrales Orovio, Rocío

Surname, first name

I hereby declare, that the submitted thesis entitled:

Optimization of novel photosynthetic biomaterials and design of a hibernation-like process for their preservation

is congruent with the printed version both in content and format.

Santiago, 20-10-2024

place, date

Rocio Corrales Orovio

Signature doctoral candidate

Acknowledgements

All the work behind this PhD thesis would not have been possible without the support and guidance of some very special people:

First, I would like to express my deepest gratitude to my PhD supervisor, Prof. Dr. med. Thilo Schenck, for his guidance and unconditional support during this PhD journey, which made this thesis possible. I would also like to extend my gratitude to my doctoral advisors: Prof. Dr. Tomás Egaña, for his mentoring and guidance which has significantly influenced my development as a researcher; and Dr. Nicholas Möllhoff, for his continuous support, and insightful comments and suggestions over the years.

I would also like to deeply thank the MMRS team, especially Dr. Antje Hentrich, for their time and support during the entire PhD process. Their guidance has been indispensable, especially during the pandemic era.

I am also extremely grateful to all the co-authors of the published works that arose along the PhD journey: their expertise, knowledge, support, and engaging discussions have played a significant role in the advancement of this project and in my career as a researcher.

I am truly grateful to my cherished colleagues, *The Wisconsins*, for their unconditional encouragement and cheering which make life and research incredibly fun. Their support and friendship have been a guiding light during these years.

My heartfelt appreciation goes to my family, who support even my wildest decisions. I am grateful every day to have such an incredible family. This thesis is dedicated to each one of you.

Table of contents

List of abbreviations

a.u.: arbitrary units

bp: base pairs

C.r.: *Chlamydomonas reinhardtii*

CS: Control scaffold

DMSO: Dimethyl sulfoxide

DMEM: Dulbecco's Modified Eagle Medium

ELISA: Enzyme-linked immunosorbent assay

F-PS: Fresh photosynthetic scaffold

FDA: Food and Drug Administration

GAGs: Glycosaminoglycans

GDL: Gluconolactone

GelMA: Gelatin-methacryloyl

HBOT: Hyperbaric oxygenation therapy

HDFn: Human dermal fibroblasts, neonatal

HG: Hydrogel

IFN: Interferon

IL: Interleukin

ISO: International Organization for Standardization

MCP-1: Monocyte chemoattractant protein 1

mRNA: Messenger ribonucleic acid

MTT: 3-(4,5-dimethylthiazol-2-yl)-2,5-diphenyltetrazolium bromide

ns: non-significant

OD: Optical density

P-PS: Preserved photosynthetic scaffold

PBS: Phosphate buffered saline

PFA: Paraformaldehyde

PSI: Primary skin irritation

PTFE: Polytetrafluoroethylene

PVA: Polyvinyl alcohol

RBCL: ribulose bisphosphate carboxylase oxygenase, large subunit

ROS: Reactive oxygen species

RuBisCo: Ribulose bisphosphate carboxylase oxygenase

RT: Room temperature

RT-PCR: Reverse transcription polymerase chain reaction

SEM: Scanning electron microscopy

SD: Standard deviation

SPI: Score of primary irritation

TNF: Tumor necrosis factor

TAP: Tris-acetate phosphate

TOT: Topical oxygenation therapy

VEGF: Vascular endothelial growth factor

List of publications

Publications contributing to the cumulative dissertation:

Corrales-Orovio R & Carvajal F, Holmes C, Miranda M, González-Itier S, Cárdenas C, Vera C, Schenck TL, Egaña JT. Development of a photosynthetic hydrogel as potential wound dressing for the local delivery of oxygen and bioactive molecules. Acta Biomaterialia (2023) 155:154–166.

Corrales-Orovio R, Castillo V, Rozas P, Schenck TL, Egaña JT. Development of a Hibernation-Inspired Preservation Strategy to Enhance the Clinical Translation of Photosynthetic Biomaterials. Advanced Therapeutics (2023) 6:2300299.

Additional publications:

Ortega JS & Corrales-Orovio R, Ralph P, Egaña JT, Gentile C. Photosynthetic microorganisms for the oxygenation of advanced 3D bioprinted tissues. Acta Biomaterialia (2023) 165:180–196.

Ehrenfeld C, Veloso-Giménez V, **Corrales-Orovio R**, Rebolledo R, Boric MP, Egaña JT. Microalgae share key features with human erythrocytes and can safely circulate through the vascular system in mice. Applied Microbiology and Biotechnology (2023) 107:4621–4633.

Castillo V, Díaz P, **Corrales-Orovio R**, San Martín S, Egaña T. Comprehensive characterization of mouse skin derived from regenerative versus reparative stages: a comparative analysis. Cells (2023) 12:9.

Obaíd ML, Carvajal F, Camacho JP, **Corrales-Orovio R**, Martorell X, Varas J, Calderón W, Guzmán CD, Brenet M, Castro M, Orlandi C, San Martín S, Eblen-Zajjur A, Egaña JT. Case report: Long-term follow-up of a large full-thickness skin defect treated with a photosynthetic scaffold for dermal regeneration. Frontiers in Bioengineering and Biotechnology (2022) 10.

Veloso-Giménez V, Escamilla R, Necuñir D, **Corrales-Orovio R**, Riveros S, Marino C, Ehrenfeld C, Guzmán CD, Boric MP, Rebolledo R, Egaña JT. Development of a Novel Perfusable Solution for ex vivo Preservation: Towards Photosynthetic Oxygenation for Organ Transplantation. Frontiers in Bioengineering and Biotechnology (2021) 9:1287.

Obaíd ML, Camacho JP, Brenet M, **Corrales-Orovio R**, Carvajal F, Martorell X, Werner C, Simón V, Varas J, Calderón W, Guzmán CD, Bono MR, San Martín S, Eblen-Zajjur A, Egaña JT. A First in Human Trial Implanting Microalgae Shows Safety of Photosynthetic Therapy for the Effective Treatment of Full Thickness Skin Wounds. Frontiers in Medicine (2021) 8:2088.

Montero A, Valencia L, **Corrales-Orovio R**, Jorcano JL, Velasco D. Smart polymer gels: properties, synthesis, and applications. In M. R. Aguilar, J. San Román, Smart Polymers and Their Applications, 2nd edition. Woodhead publishing, Elsevier (2019), 279-322.

1. Introductory summary

This cumulative dissertation synthesizes insights from two individual yet interconnected articles that were published over the course of the PhD. The general objective of the doctoral research project was to develop new photosynthetic biomaterials and to study if a technological platform could be established to preserve photosynthetic biomaterials in a clinically compatible setting. In order to fulfill the general objective, the following specific objectives were defined:

1. To develop a novel hydrogel-based photosynthetic biomaterial.
2. To study if the photosynthetic microalgae *Chlamydomonas reinhardtii* can be preserved under hibernation-like conditions, optimizing a protocol for their storage.
3. To validate the protocol for microalgae preservation in an already established photosynthetic biomaterial *in vitro*.
4. To evaluate safety of preserved photosynthetic biomaterials in an *in vivo* model for tissue regeneration.

The subsequent sections of this introductory summary address the topics of wound healing and management, the significance of oxygen in the healing process, and the development of photosynthetic biomaterials for the advanced oxygenation of tissues. The first published work presented in this dissertation (**Publication I**) corresponds to the results obtained from specific objective 1, and contributes to the aforementioned topics by introducing a biocompatible photosynthetic hydrogel-based wound dressing designed to release oxygen and other bioactive molecules to enhance the wound healing process (1). Additionally, this dissertation discusses the clinical feasibility and preservation challenges associated with photosynthetic biomaterials. The second published article (encompassing results from specific objectives 2, 3 and 4; **Publication II**) proposes a novel solution for the preservation challenge by generating a hibernation-inspired preservation protocol for photosynthetic biomaterials (2). Concluding this section, the contributions and future directions of the presented research findings are discussed.

1.1 Skin damage and clinical wound management

Skin wounds are defined as the disruption or injury of the normal structure and function of the tissue (3), and can be caused by both external and/or internal factors. External causes include physical trauma, chemical exposure, or burns. On the other hand, internal causes can include pathological conditions such as autoimmune disorders or chronic diseases. Wounds can also be classified based on their depth, as superficial (affecting epidermis only), partial-thickness (affecting epidermis and dermis) or full-thickness (affecting all layers of the skin) (4). In addition, wounds are generally classified as acute or chronic based on the time and progression of the healing process (5).

Under normal conditions, the process of wound healing is a complex body response of overlapping events known as the wound healing cascade, which aims to repair the injured

tissues. This response involves four phases: hemostasis, inflammation, proliferation, and remodeling (6). In the initial hemostasis phase, platelets aggregate to form a plug at the injury site, releasing growth factors that facilitate blood clot formation. This activates the subsequent inflammation phase, where immune cells are attracted to the site, tasked with the removal of debris and pathogens. Next, tissue repair takes place in the proliferation phase, through processes such as cell division, collagen synthesis, and angiogenesis. Finally, in the remodeling phase, the newly formed collagen fibers undergo reorganization, increasing tissue strength and ending in the formation of a scar (7). While the wound healing cascade is a natural body process occurring in acute wounds, several factors can arise, impeding its normal progression. Underlying health conditions (such as diabetes or vascular diseases) are typical risk factors that can cause systemic complications such as inflammation, infection, and local hypoxia, leading to the formation of chronic wounds (8).

Therefore, during the course of wound healing, correct patient care and wound management is essential for optimal tissue regeneration and avoiding prolonged complications. To date, wound care involves a spectrum of approaches, ranging from traditional to advanced wound dressings (9). Traditional dressings, such as gauzes, provide a physical barrier to protect the wound bed and avoid infections. Advancements in wound care have introduced modern solutions such as hydrocolloids or hydrogels, which offer benefits such as moisture control, enhanced healing environment, and the ability to manage various wound types. The choice between traditional and advanced dressings depends on several factors, including individual patient's needs, wound type, size, and depth. In cases of extensive skin damage or full thickness wounds, traditional and advanced dressings may be insufficient for optimal wound healing. In this case, skin substitutes (including natural or synthetic scaffolds) are commonly used, as they offer a structured and supportive environment for the wound healing process, enhancing cell migration, tissue granulation, and angiogenesis (5).

In order to further promote wound healing, functional biomaterials have been also generated by incorporating bioactive molecules, including therapeutical drugs, antimicrobial agents, and growth factors into wound dressings and scaffolds (10). These biomaterials are capable of locally releasing specific molecules onto the wound site, enhancing the wound healing process.

Despite the significant advancements in wound management in the last decades, this field remains as a global clinical and scientific challenge. Therefore, the development of advanced wound dressings and scaffolds is an active field of research. This cumulative thesis encompasses two different wound care treatments within the context of photosynthetic biomaterials. The first publication describes the generation of a novel hydrogel as potential wound dressing, designed for superficial and partial-thickness skin wounds. On the other hand, the second publication describes the development of a preservation strategy to enhance the clinical translation of photosynthetic scaffolds for the treatment of full-thickness skin wounds.

1.2 Oxygen and wound healing

Oxygen is known to be a critical component of many biological processes, and stands out as a key factor for wound healing, as it is involved in all phases of the wound healing cascade (Figure 1) (11,12). During hemostasis, oxygen is crucial for effective platelet aggregation and formation of blood clots at the wound site. Next, during inflammation, oxygen supports immune cell function, particularly neutrophils and macrophages, facilitating the generation of reactive oxygen species (ROS) and cytokines to eliminate pathogens and regulate the inflammatory response. In the proliferation phase, oxygen is key for various cellular processes involved in new tissue formation, including cell division, collagen synthesis, and angiogenesis. Finally, in the remodeling phase, oxygen plays a pivotal role in supporting fibroblast activity and therefore proper collagen alignment, contributing to the maturation and organization of the healing tissue (11).

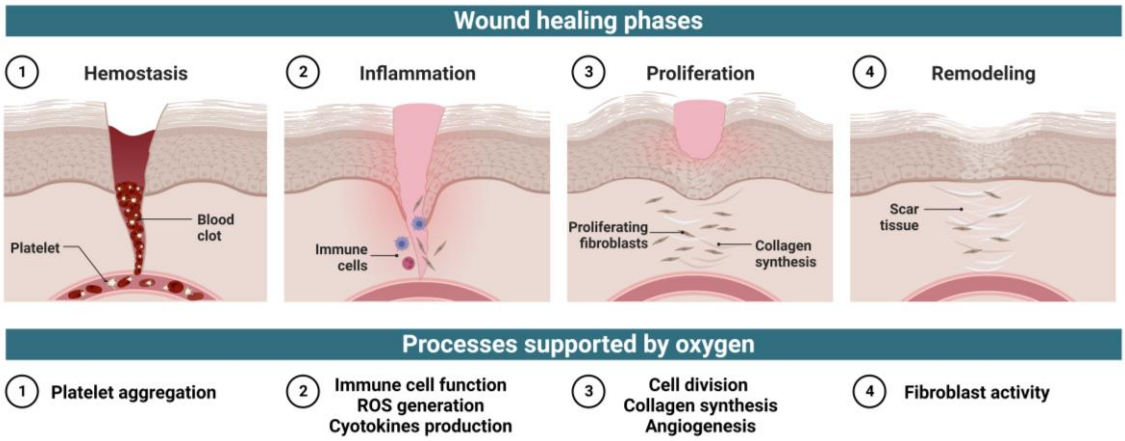

Figure 1: Role of oxygen in the wound healing process. Schematic shows wound healing phases (hemostasis, inflammation, proliferation, and remodeling), and mechanisms supported by oxygen in every wound healing phase. Created with Biorender.

While acute hypoxia acts as an initial signal to promote wound healing, prolonged and chronic hypoxia is responsible for non-healing chronic wounds. Optimizing oxygen levels in the wound promotes a favorable healing environment and enhances the chances of successful wound closure. Hence, significant efforts have been made to advance the development of novel therapies capable of delivering oxygen to wounds, whether through systemic or local approaches (13). Systemic approaches, such as hyperbaric oxygen therapies, represent a complex and expensive clinical approach, and have shown variable outcomes to date (14). On the other hand, local or topical oxygen therapies, including mechanical devices or oxygen delivering dressings, have shown to promote wound healing by enhancing cell proliferation and vascularization (15,16).

1.3 Photosynthetic biomaterials for wound oxygenation

In the context of topical oxygen delivering systems, the use of photosynthetic microorganisms has been investigated in order to increase the local oxygen concentration in wounds via photosynthetic oxygenation *in situ* (17). This approach offers distinct advantages over alternative oxygenation methods. First, photosynthetic microorganisms enable a constant production and delivery of oxygen. By modulating the illumination settings, photosynthetic activity can be effectively controlled. This dynamic adjustment enables the precise delivery of specific concentrations of oxygen to address diverse wound requirements. Moreover, photosynthetic microorganisms can be genetically engineered to produce and deliver specific bioactive molecules, including growth factors, which could be potentially used to enhance the wound healing process (18–20).

This photosynthetic oxygenation method has been also proposed for other medical fields, including cancer therapies, ischemia treatment and organ preservation (21). However, its application in wound healing has garnered greatest attention in the last years (17). This has led to the development of various biomaterials, which combine the use of a structural substrate (natural or synthetic) with photosynthetic microorganisms, including microalgae or cyanobacteria. Upon illumination, these photosynthetic biomaterials produce and release oxygen, aiming to reduce tissue hypoxia and to enhance the wound healing process. These designed biomaterials include scaffolds (22,23,18,24–26), topical hydrogels (1,27–31), patches (32,33), and sutures (20), each of them designed for specific wound types (Table 1).

Table 1: Photosynthetic biomaterials designed for wound oxygenation.

Biomaterial type	Biomaterial composition	Photosynthetic microorganism	Main findings	Reference
Scaffolds for dermal regeneration	Bovine Collagen and GAGs	*Chlamydomonas reinhardtii*	• Reduced hypoxia *in vitro.*	(22)
	Bovine Collagen, GAGs, and fibrin	*Chlamydomonas reinhardtii*	• Biocompatibility *in vivo* in athymic nude mice.	(23)
	Bovine Collagen, GAGs, and fibrin	*Chlamydomonas reinhardtii*	• Recombinant human VEGF release. • Biocompatibility *in vivo.*	(18)
	Bovine Collagen, GAGs, and fibrin	*Chlamydomonas reinhardtii*	• Safety validation after implantation in human full thickness skin wounds.	(24,25)
	Alginate, GelMA, and $CaCl_2$	*Chlorella pyrenoidosa*	• *In situ* bioprinting strategy enhanced wound healing *in vivo.*	(26)
Topical hydrogels	Alginate, $CaCO_3$, GDL and $CaCl_2$	*Chlamydomonas reinhardtii*	• Oxygenation of tissues. • Growth factor and antibiotic release. • Safety in healthy human skin.	(1)
	Hyaluronic acid	*Synechococcus elongatus*	• Enhanced healing in burn and ischemic wound model *in vivo.*	(27)
	Chitosan	*Spirulina platensis*	• Photosynthetic and photodynamic effect. • *In vitro* and *in vivo* validation.	(28)
	Chitosan, alginate, genipin, and berberine	*Spirulina platensis*	• Oxygen and antibacterial molecules release. • Enhanced healing in infected diabetic wounds *in vivo.*	(29)
	Hyaluronic acid	*Chlorella sp*	• Oxygenation upon illumination, inactivation of chlorella respiration at night. • *In vitro* and *in vivo* validation in diabetic wound models.	(30)
	Pluronic powder and polydopamine	*Chlorella pyrenoidosa*	• Oxygen production promoted *Bacillus subtilis* growth and eliminated pathogenic bacteria. • Enhanced wound healing *in vivo.*	(31)
Topical patches	Alginate encapsulated in a PTFE membrane	*Synechococcus elongatus*	• Effective penetration of oxygen in skin. • *In vitro* and *in vivo* validation.	(32)
	PVA and GelMA microneedles	*Chlorella vulgaris*	• Enhanced wound healing *in vivo.*	(33)
Surgical sutures	Polylgactin surgical sutures	*Chlamydomonas reinhardtii*	• Oxygen and recombinant growth factor release *in vitro.*	(20)

Within this topic, the first work presented in this cumulative dissertation (**Publication I**) describes the development of a photosynthetic hydrogel for the local release of oxygen and other bioactive molecules as a potential wound dressing (Figure 2) (1).

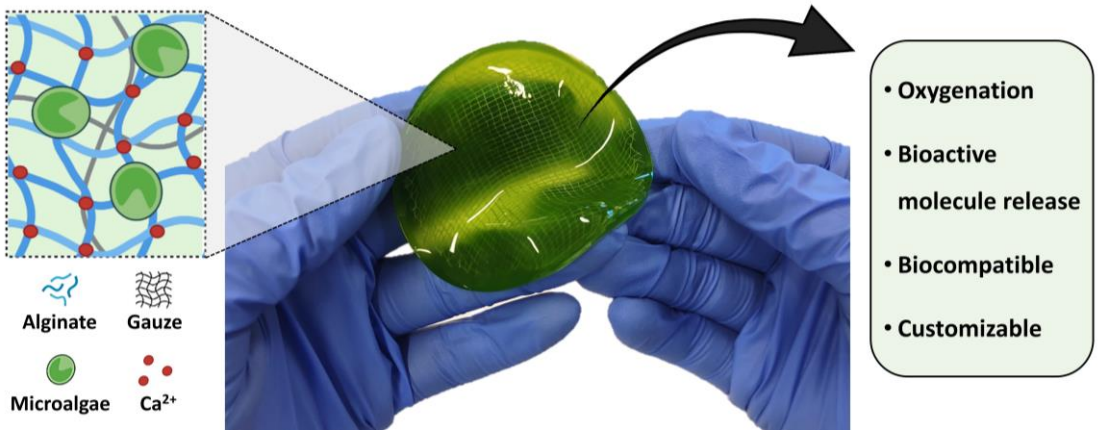

Figure 2: Development of a photosynthetic hydrogel wound dressing for the release of oxygen and other bioactive molecules. Graphical abstract from Publication I (1). Reproduced with permission. © 2022, Elsevier Ltd.

Ideally, a wound dressing should fulfill specific criteria, including biocompatibility, moisture control, prevention of microbial contamination, adequate mechanical strength to sustain integrity during use, and allow a painless and easy removal (34). Therefore, in this first published work, particular attention was given to all these parameters. Alginate was selected due to its known biocompatibility, and because of its mechanical and chemical properties, as it can absorb wound exudate, and maintain a physiologically moist environment. Moreover, a novel strategy to improve the mechanical properties of the dressing was designed, where a single layer of sterile gauze was embedded within the alginate hydrogel. This optimized the strength and handling of the dressing, which enabled a painless application and removal from the skin. In comparison to the other published topical hydrogels described in Table 1, the presented approach used microalgae *C. reinhardtii*, as they are the only photosynthetic microorganisms that have shown clinical safety in human patients to date (24). Results showed biocompatibility of the dressings *in vitro*, *in vivo*, and in healthy skin of human volunteers, following ISO -10993-10-2010 guidelines. Finally, this published work described the potential of the dressing to become a customizable platform for the release of oxygen as well as other therapeutic drugs such as antibiotics and recombinant growth factors.

1.4 Clinical translation of photosynthetic biomaterials

While the potential of photosynthetic biomaterials in wound healing and medical applications holds great promise and has garnered increased attention in the last decade, their current clinical translation is limited by the short half-life of photosynthetic microorganisms within the materials. Moreover, these biomaterials require specific and strictly controlled culture and transport conditions to maintain their viability until clinical use.

These limitations extend to other engineered constructs, such as fresh cellularized skin substitutes, which have a shelf life of less than one week, restricting their practicality and

commercial potential (35). For this reason, cryopreservation methods are commonly implemented for human cell treatments (36). Indeed, several FDA-approved cellular scaffolds now employ cryopreservation methods to extend their shelf life from days to months and even years (37). This advancement enables the production of larger quantities, enhances quality control, and extends shelf lives, leading to the development of more reliable, scalable, and cost-effective technologies (38). However, cryopreservation methods use highly toxic cryoprotective agents, such as dimethyl sulfoxide, which must be properly removed before biomaterial use (36).

Concerning the preservation of photosynthetic microorganisms, various techniques have been explored to date, including cryopreservation, vitrification and lyophilization. These techniques have shown different performances depending on the microorganisms preserved (39). In the case of microalgae *C. reinhardtii*, cryopreservation stands out as the most used method for their extended storage, which has been mainly described for strain maintenance and culture applications (40,41).

Interestingly, several photosynthetic cells, including microalgae *C. reinhardtii* have the ability to enter a dormant state under harsh or hibernation-like environmental conditions, which include lack of light, nutrients, and low temperatures (42,43). The second publication presented in this cumulative thesis (**Publication II**) describes the development of a preservation method based on hibernation-inspired conditions to increase the clinical translation of photosynthetic biomaterials (Figure 3) (2).

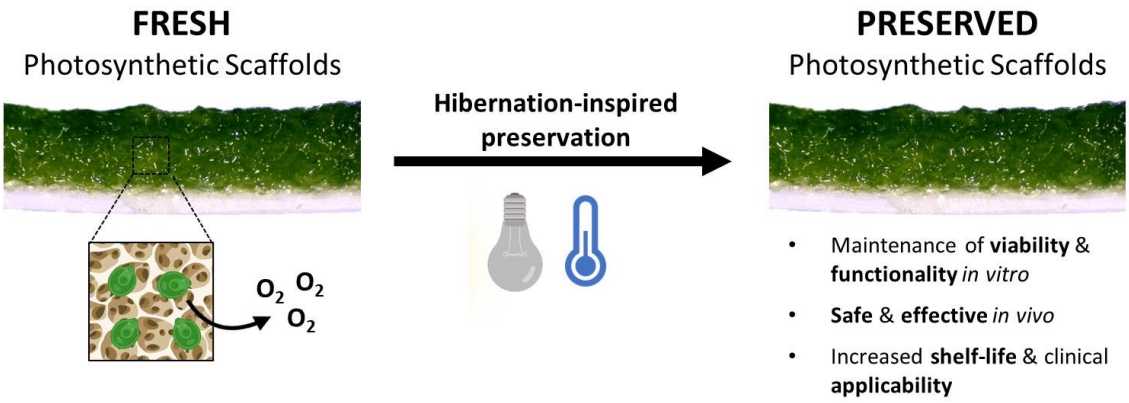

Figure 3: Development of a hibernation inspired preservation strategy for photosynthetic biomaterials. Graphical abstract from Publication II (2). Reproduced with permission. © 2023, John Wiley & Sons, Inc.

In the study, a protocol to preserve *C. reinhardtii* was optimized, and then applied to photosynthetic scaffolds. The scaffolds selected for this work had been previously designed by the research group (22,23), and had been also used in a Phase I Clinical Trial evaluating the safety of implanting photosynthetic microorganisms in human patients (24). The preservation protocol demonstrated that the structure (collagen and fibrin integrity), viability (chlorophyll content and growth capacity) and functionality (oxygen production) of the biomaterial was maintained for

up to 6 weeks. To evaluate the clinical viability and safety of the developed preservation approach, fresh and preserved photosynthetic scaffolds were implanted in a mouse full-thickness skin defect model and studied by several means, including clinical parameters, histological assays, and local and systemic molecular analysis.

1.5 Contributions to the field and future directions

Based on available bibliography, it becomes evident that photosynthetic therapies and biomaterials represent an emerging and promising field of research (17,21). Although the global publication rate within these research domains have experienced a substantial growth over the past years (Figure 4), it is important to note that the field is still in its early stages. Consequently, several key aspects remain to be studied before its widespread clinical implementation. The publications presented in this cumulative thesis contribute to the development and optimization of photosynthetic therapies for biomedical applications, specifically in the topic of wound healing.

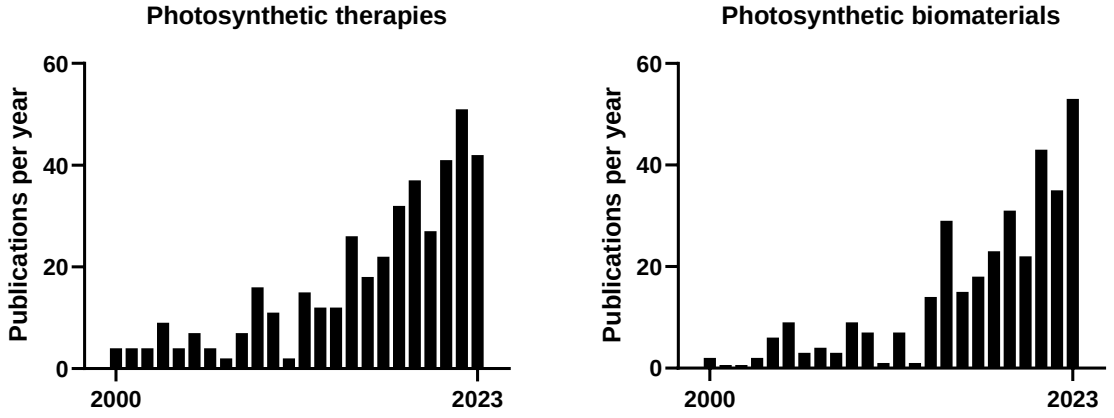

Figure 4: Publications per year in the topic of photosynthetic therapies and photosynthetic biomaterials. Graphs created with data extracted from PubMed®, using search queries ''photosynthetic therapies'' and ''photosynthetic biomaterials'' in December 2023.

As previously explained, the first article proposed the use of alginate-based hydrogels as wound dressings, that could locally act as personalized bioreactors to promote wound healing by the controlled delivery of oxygen and other bioactive molecules *in situ* (1). Further studies should evaluate efficacy of these dressings in relevant preclinical wound models, and continue with clinical trials in human patients.

The second article presented in this thesis designed a preservation method to increase the operational timeframe of photosynthetic biomaterials based on hibernation-inspired conditions, without the need of toxic cryopreservation chemicals (2). This method allows to reduce manufacturing times and costs, enabling mass production, standardization, and significantly increasing the shelf-life and applicability of photosynthetic biomaterials in a clinical

context. Altogether, these results could have a tremendous impact on the clinical translation of photosynthetic biomaterials. While this preservation strategy has been validated in a specific photosynthetic scaffold, this technology could be adapted to all different photosynthetic biomaterials, including those presented in Table 1, such as hydrogels, patches, and sutures. Moreover, it should also be evaluated and adapted to different photosynthetic microorganisms that have shown to be promising for photosynthetic therapies.

Altogether, this cumulative dissertation contributes to the growing field of photosynthetic therapies, supporting the use of photosynthetic biomaterials through advanced, sustainable, scalable, and biocompatible solutions for regenerative medicine.

2. Contribution to the publications

2.1 Contribution to paper I

The first paper presented in this cumulative thesis is entitled *"Development of a photosynthetic hydrogel as potential wound dressing for the local delivery of oxygen and bioactive molecules",* and was published in the journal Acta Biomaterialia in January 2023 (available online since November 2022). The full published manuscript can be found in Section 3.

Conceptualization and design

I actively participated in the conceptualization and design of the research, which was performed in collaboration with several members of the team, including the shared first co-author. We formulated the research questions and outlined the study objectives as follows:

1. To design a novel and mechanically stable photosynthetic hydrogel.
2. To study and characterize the biocompatibility of the photosynthetic hydrogel.
3. To validate the oxygenation capacity of the hydrogel.
4. To validate the hydrogel as a platform for the delivery of other bioactive molecules.

Once the main objectives of the study were clear, I designed the experimental approach, which was discussed and adjusted with the team before execution.

Execution of the research activities

I oversaw the practical implementation of the research plan, taking personal responsibility on the fabrication of photosynthetic hydrogels. This involved coordinating laboratory activities, ensuring proper protocols were followed by all co-authors, and solving issues that arose during the execution of the research activities. In the following paragraphs, an in-depth description of my contribution to the research activities is described.

The initial formulation of the hydrogel was designed in collaboration with the shared first co-author, where alginate-based photosynthetic hydrogels containing microalgae *C. reinhardtii* and a thin layer of sterile gauze were created. The protocol involved an internal crosslinking technique using calcium carbonate ($CaCO_3$) and gluconolactone (GDL), which ensured homogeneous hydrogel density, pore size and distribution of microalgae. However, after preliminary mechanical tests, we observed poor mechanical properties and therefore, handling difficulties (data not shown in the published article). At this point, I personally worked on improving the stability of the hydrogels by performing an additional external crosslinking with calcium chloride. This final fabrication protocol can be observed in the Figure 1A of the published article (1).

Once the fabrication protocol was optimized, I performed the structural and mechanical analysis of the photosynthetic hydrogel. First, I optimized a protocol for the fixation and preparation of

hydrogels for scanning electron microscopy (SEM). Once I obtained the SEM images, I analyzed them by calculating the pore size and distribution using Fiji Software. In parallel, I also performed swelling and compressive tests to study the mechanical properties of the photosynthetic hydrogels. Next, I assessed the stability of the hydrogels over time by means of microalgae distribution, chlorophyll content and oxygenation capacity.

Once mechanically stable hydrogels were obtained and fully characterized, their biocompatibility was assessed *in vitro* (co-culture with human endothelial cells) and *in vivo* (acute exposure to zebrafish larvae). I personally fabricated the hydrogels for every test, and then performed the *in vitro* and *in vivo* assays with the support of several co-authors of the work. As the combination of alginate, $CaCO_3$, GDL and *C. reinhardtii* had not been described previously in clinics, I adapted the Primary Skin Irritation (PSI) test from ISO-10993-10-2010 guidelines, to study the biocompatibility of the photosynthetic hydrogels on healthy skin of human volunteers. As human volunteers were involved, I previously wrote the corresponding research protocol (including detailed methodology, informed consent document, assessment scales and self-questionnaires) for its ethical approval. Once the research protocol was approved by the corresponding ethical authorities, volunteers were recruited. I fabricated the hydrogels, and a qualified nurse (co-author of the work) was in charge of applying them on each volunteer and assessing their skin irritation after hydrogel application. In parallel, I recovered the hydrogels after removal from volunteers' skin, to assess their overall integrity, mass reduction and microalgae viability after application.

Next, metabolic coupling assay assays were carried out to study if the oxygen released by the photosynthetic hydrogels was able to fulfill the metabolic requirements of zebrafish larvae and mice skin explants. I fabricated the hydrogels for each test, and the assay was performed in collaboration with several co-authors, who supported in the breeding and handling of zebrafish larvae and in the obtention of mice skin explants, as well as in the overall coupling assay.

Finally, I performed several proof-of-concept tests to validate the use of the photosynthetic hydrogels as platforms for the delivery of other bioactive compounds beside oxygen, such as growth factors or antibiotics. I first fabricated the hydrogels by incorporating a strain of *C. reinhardtii* expressing recombinant human-VEGF, and quantified VEGF production and release with an ELISA kit. Secondly, I also fabricated photosynthetic hydrogels containing 1% cefazolin, and measured its release over time. Functionality of the released antibiotic in *E. coli* and *S. aureus* was performed with the support of one of the co-authors.

Data collection, analysis, and interpretation

I actively participated in data collection, including data from assays performed by co-authors, which involved overseeing and supervising all experiments. Additionally, I conducted the whole analysis of the collected data, applying appropriate statistical methods with GraphPad Prism 8

Software. Next, approval and interpretation of the analyzed data was performed and discussed with co-authors.

Manuscript preparation

As first author of the published work, I led the writing of the manuscript, drafting the initial version. I acted as the primary contact for co-authors, incorporating all their feedback through the preparation process. Once the manuscript was finished, I ensured it adhered to the specific guidelines of the journal (Acta Biomaterialia), including formatting and citation style. I also prepared additional documents such as the graphical abstract and supplementary materials for the submission.

2.2 Contribution to paper II

The second published article presented in this cumulative thesis is entitled *"Development of a Hibernation-Inspired Preservation Strategy to Enhance the Clinical Translation of Photosynthetic Biomaterials",* and was published in the journal Advanced Therapeutics in December 2023 (available online since October 2023). The full published manuscript can be found in Section 4.

Conceptualization and design

I actively participated in the conceptualization of the project, and played a central role in the design of the research plan. Together with other members of the team, we formulated the research questions and outlined the primary study objectives:

1. To establish a protocol for the preservation of microalgae *C. reinhardtii*.
2. To validate the established preservation protocol in an already existing photosynthetic biomaterial.
3. To study the safety and feasibility of the preservation approach in an *in vivo* model.

Once the objectives were clearly defined, I designed the experimental approach, which was a collaborative task involving discussions with the research team, and subsequent approval of the proposed design.

Execution of research activities

I played a leading role in all research activities. I was in charge of organizing, scheduling, and executing experiments. Given that the main goal of this work was to design a preservation protocol for photosynthetic biomaterials, meticulous pre-planning was key to ensure that after each time point of the preservation process, all planned analysis and characterizations of the preserved biomaterials could be performed seamlessly.

After performing extensive bibliographic research in the topic of microalgae preservation, I designed a preservation protocol based on hibernation-inspired conditions, aiming to reduce the metabolic activity of the microalgae while being preserved. This protocol was based on harsh

conditions, including cold temperatures, lack of light and nutrients. Once the protocol was defined, it was validated *in vitro*. I preserved microalgae *C. reinhardtii* for up to 8 weeks, and at different time points analyzed microalgae morphology by means of microscopy and cell cytometry. In parallel, I assessed the oxygen production capacity of the microalgae, as well as their growth capacity by means of agar plating. Finally, I also studied the viability of the microalgae by cell cytometry.

After establishing a hibernation-inspired preservation protocol for microalgae *C. reinhardtii*, it was essential to validate it in an already existing photosynthetic biomaterial. Therefore, I fabricated photosynthetic scaffolds for dermal regeneration based on previously published works from our group (18,23). These were then preserved for up to 8 weeks based on the established preservation protocol. At each specific time point, I studied overall morphology and structure of the scaffolds by macroscopic, fluorescent, and SEM imaging. In parallel, and to assess the functionality of the preserved scaffolds, I quantified chlorophyll content, oxygen production and growth capacity of the microalgae. Moreover, as a proof of concept, I also assessed the preservation of scaffolds containing a strain of *C. reinhardtii* expressing recombinant human-VEGF protein. This included the fabrication of the scaffolds and quantification of the expressed and released VEGF after preservation at all time points.

These results showed that photosynthetic scaffolds could be preserved for up to 6 weeks. Based on the bibliographic research performed at the start of the project, we knew that certain microalgae could produce and release harmful compounds and cold-shock proteins in response to environmental stressors. Due to the potential implications of these factors in the clinical translation of the proposed preservation approach, a main goal of this work was to evaluate and validate the safety of hibernation-inspired preserved photosynthetic biomaterials in an *in vivo* model. Therefore, I planned the *in vivo* experiments based on a full skin defect model previously described by the group, where scaffolds are implanted on bilateral defects created on the back of mice (18,23,44). Before starting the *in vivo* assays, I wrote a research protocol which was sent to the corresponding Scientific Ethical Committee for Animal Care. This document included all methodology, surgery details, sample processing and animal follow up protocols, including Grimace and health assessment scales. Once the research protocol was approved, I organized and scheduled the *in vivo* assays, which were performed with the support of several co-authors, as surgical procedures required a highly organized team. After surgically implanting the scaffolds, I performed animal maintenance for 10 consecutive days, including administration of analgesics, and assessing animal weight, overall animal welfare and wound evolution. After euthanasia of all animals, tissues (including blood samples, implanted scaffolds and lymphoid

organs) were processed. I led all the characterization of the obtained tissues, with the significant support of co-authors for an efficient and optimal analysis.

Data collection, analysis, and interpretation

I performed data collection, including all *in vitro* and *in vivo* experiments. Additionally, I conducted the analysis of the collected data, applying appropriate statistical methods which were previously discussed with the co-authors of the work. Finally, interpretation of the analyzed data was performed and discussed with co-authors.

Manuscript preparation

As first author of the published work, I was in charge of writing and generating the initial draft version of the manuscript. After the review of all co-authors, I incorporated their feedback through several correction rounds. Once the manuscript was finished, I ensured it adhered to the specific guidelines of the journal (Advanced Therapeutics), including formatting and citation style. I also prepared supplementary documents such as the graphical abstract and the statement of significance for the final manuscript submission.

3. Paper I

Title	Development of a photosynthetic hydrogel as potential wound dressing for the local delivery of oxygen and bioactive molecules.
Authors	Corrales-Orovio R & Carvajal F, Holmes C, Miranda M, González-Itier S, Cárdenas C, Vera C, Schenck TL, Egaña JT.
Journal	Acta Biomaterialia
Year	2023 (available online on November, 2022)
Issue	155
Pages	154-166
DOI	10.1016/j.actbio.2022.11.036

Copyright notices

The following pages present a publication as originally published, reprinted with permission from the corresponding publisher. The copyright of the original publications is held by the respective copyright holders:

© 2022, Elsevier Ltd. Reprinted with permission. The original publication is available at: https://www.sciencedirect.com/science/article/pii/S1742706122007656?via%3Dihub.

Acta Biomaterialia 155 (2023) 154–166

Contents lists available at ScienceDirect

Acta Biomaterialia

journal homepage: www.elsevier.com/locate/actbio

Full length article

Development of a photosynthetic hydrogel as potential wound dressing for the local delivery of oxygen and bioactive molecules

Rocío Corrales-Orovio[a,b,1], Felipe Carvajal[b,1], Christopher Holmes[b], Miguel Miranda[b,c], Sergio González-Itier[b], Camila Cárdenas[b], Constanza Vera[b], Thilo L. Schenck[a], José Tomás Egaña[b,*]

[a] Division of Hand, Plastic and Aesthetic Surgery, University Hospital, LMU Munich, Munich, Germany
[b] Institute for Biological and Medical Engineering, Schools of Engineering, Medicine and Biological Sciences, Pontificia Universidad Católica de Chile, Santiago, Chile
[c] Facultad de Medicina Veterinaria y Agronomía, Universidad de las Américas, Santiago, Chile

ARTICLE INFO

Article history:
Received 3 August 2022
Revised 4 November 2022
Accepted 16 November 2022
Available online 23 November 2022

Keywords:
Wound dressing
Photosynthetic hydrogel
Oxygen delivery
Microalgae
Drug release

ABSTRACT

The development of biomaterials to improve wound healing is a critical clinical challenge and an active field of research. As it is well described that oxygen plays a critical role in almost each step of the wound healing process, in this work, an oxygen producing photosynthetic biomaterial was generated, characterized, and further modified to additionally release other bioactive molecules. Here, alginate hydrogels were loaded with the photosynthetic microalgae *Chlamydomonas reinhardtii*, showing high integration as well as immediate oxygen release upon illumination. Moreover, the photosynthetic hydrogel showed high biocompatibility *in vitro* and *in vivo*, and the capacity to sustain the metabolic oxygen requirements of zebrafish larvae and skin explants. In addition, the photosynthetic dressings were evaluated in 20 healthy human volunteers following the ISO-10993-10-2010 showing no skin irritation, mechanical stability of the dressings, and survival of the photosynthetic microalgae. Finally, hydrogels were also loaded with genetically engineered microalgae to release human VEGF, or pre-loaded with antibiotics, showing sustained release of both bioactive molecules. Overall, this work shows that photosynthetic hydrogels represent a feasible approach for the local delivery of oxygen and other bioactive molecules to promote wound healing.

Statement of significance

As oxygen plays a key role in almost every step of the tissue regeneration process, the development of oxygen delivering therapies represents an active field of research, where photosynthetic biomaterials have risen as a promising approach for wound healing. Therefore, in this work a photosynthetic alginate hydrogel-based wound dressing containing *C. reinhardtii* microalgae was developed and validated in healthy skin of human volunteers. Moreover, hydrogels were modified to additionally release other bioactive molecules such as recombinant VEGF or antibiotics. The present study provides key scientific data to support the use of photosynthetic hydrogels as customizable dressings to promote wound healing.

© 2022 Acta Materialia Inc. Published by Elsevier Ltd. All rights reserved.

1. Introduction

Wound management and healing remain as a global clinical and scientific challenge. Therefore, the development of advanced wound dressings is an active field of research, and several products have been recently introduced to promote healing in patients [1]. An ideal wound dressing should meet specific criteria, which include being biocompatible, maintaining local moisture, avoiding microbial contamination, having sufficient mechanical strength to maintain its integrity during its use, and allow an easy removal [2]. In this context, hydrogels have gained popularity due to their outstanding mechanical and biochemical properties, and nowadays represent one of the most commonly used dressings in clinical practice [3].

Compared to other dressings, such as gauzes or synthetic films, which attempt to avoid further complications by providing a tem-

* Corresponding author.
E-mail address: jte@uc.cl (J.T. Egaña).
[1] Both authors have equally contributed.

https://doi.org/10.1016/j.actbio.2022.11.036
1742-7061/© 2022 Acta Materialia Inc. Published by Elsevier Ltd. All rights reserved.

porary barrier to wounds, hydrogels have attracted increased clinical attention, as they can provide an optimal physiological microenvironment, accelerating the process of wound healing [4]. Another advantage of using hydrogels is that they can be easily modified in order to meet the specific requirements of diverse wounds. Therefore, parameters such as composition, moisture, pore size or mechanical strength can be optimized based on the type of the wound [3,5]. Hydrogels can be further activated by incorporating bioactive molecules, including therapeutical drugs [6,7], antimicrobial agents [8,9], and growth factors [10,11] which can be locally released providing a customizable platform to improve wound healing. The release of these biomolecules can be further controlled based on the mechanical properties and pore size of the hydrogels, where larger pores will enable a more rapid molecule release [2]. Moreover, hydrogels can be easily applied onto irregular and deep wounds due to their flexibility and ability to crosslink *in situ* [12]. Finally, excess exudate, metabolic waste products, and proinflammatory molecules that are present in the surface of the wounds can be absorbed by these dressings, which can then be easily removed and replaced, acting as cleaning systems and enhancing autolytic debridement [13].

Among the key molecules of the wound healing process, oxygen is described to be crucial in its success, being involved in several critical steps including aerobic cell metabolism, angiogenesis, collagen maturation, and oxidative killing of bacteria [14,15]. Although it has been well described that despite acute hypoxia acts as an initial signal to promote wound healing, prolonged and chronic hypoxia plays a major role in non-healing chronic wounds [16]. Hence, several efforts have been made to provide oxygen to wounds either systemically or locally, including hyperbaric oxygen therapy (HBOT) or topical oxygen therapy (TOT), but larger studies are still needed, as no consistent or significant results have been obtained [16–18]. In addition, dressings have been designed to deliver oxygen in the wound site by incorporating different chemical compounds such as hydrogen peroxide, calcium peroxide or perfluorocarbons, representing a promising approach for the local oxygenation of wounds [19]. However, these artificial oxygen carriers present several limitations, including local toxicity, poor stability, and short term oxygen delivery [20].

Recently, the use of photosynthetic microorganisms has been suggested as an alternative approach to increase local oxygen concentration in several medical fields including antitumor therapies [21–24], stroke and ischemia treatment [25–28], organ preservation [29,30], and wound healing [31–35]. In the case of wound healing, scaffolds containing *Chlamydomonas reinhardtii* microalgae cells have shown to decrease tissue hypoxia *in vitro* [31], and further studies have shown their safety in both animal models [36], and human patients [37]. Moreover, the generation of genetically engineered photosynthetic microalgae and cyanobacteria has been studied, aiming to additionally provide freshly produced recombinant bioactive molecules *in situ*, such as growth factors [34,36] and glycosaminoglycans [38].

Taking all this into consideration, in this work a biocompatible photosynthetic hydrogel-based wound dressing was developed to release oxygen as well as other bioactive molecules to wounds.

2. Materials and methods

2.1. Microalgae strains and culture

Cell-wall deficient *C. reinhardtii* microalgae (cw15-30-derived UVM4 [39]) were grown photomixotrophically at 20 °C and constant illumination (30 $\mu E/m^2 \cdot s$) on either solid Tris Acetate Phosphate medium (TAP) with 1.5 % (w/v) agar or in liquid TAP with constant agitation (180 rpm) [40]. For growth factor release experiments, a genetically modified *C. reinhardtii* UVM4-human VEGF producing strain was used (UVM4-VEGF) [36], and cultured as described above.

2.2. Alginate hydrogel fabrication

Stock solutions of 1.67% sodium alginate (PanReac Applichem, Germany) and 128.5 mM calcium carbonate ($CaCO_3$) (Merck, Germany) were prepared, and autoclaved for sterilization. Right before hydrogel preparation, 320 mM D-(+)-Gluconic acid δ-lactone (GDL) (Sigma, Germany) dissolved in TAP was prepared, and sterilized with a 0.22 µm filter. Microalgae *C. reinhardtii* (*C.r.* in figures) were used at a concentration of $5{\cdot}10^7$ microalgae/ml of hydrogel, which was established after preliminarily assessing densities from $1{\cdot}10^7$ to $2.5{\cdot}10^8$ microalgae/ml. For the preparation of 1 ml of hydrogel, 600 µl of sodium alginate were added to a sterile tube, followed by the addition of 117 µl of $CaCO_3$. Next, $5{\cdot}10^7$ microalgae resuspended in 183 µl of TAP were added to the mixture (for control hydrogels, 183 µl of TAP without microalgae were used). In order to initiate polymerization, 100 µl of GDL were finally added to the mixture. Standard commercially available woven cotton sterile gauze (Cat: AAGAALE5, Reutter, Chile) was cut into 20 mm in diameter single layer disks and placed in a 12-well cell culture plate, followed by the addition of 800 µl of hydrogel mixture, obtaining hydrogels of 2 mm in height. After overnight gelation, hydrogels were submerged into 2% calcium chloride ($CaCl_2$; Sigma, Germany) for 30 seconds, and placed in properly sealed culture plates, to avoid drying of the hydrogel. Hydrogels were maintained for up to seven days at room temperature (RT) and constant illumination, without any additional medium.

2.3. Hydrogel imaging

Photosynthetic hydrogels were macroscopically imaged using a standard stereoscope (Leica S6D, Germany) coupled to a digital camera. Hydrogels were also analyzed by fluorescence microscopy, where chlorophyll autofluorescence was observed using Texas Red filter (Cytation 5, BioTek, USA). For scanning electron microscopy (SEM) imaging, hydrogels were fixed in 2% glutaraldehyde and frozen at -80 °C overnight. Then, samples were freeze dried at -80 °C for 24 hours, mounted, sputtered with gold and analyzed using 15 kV accelerating voltage (Hitachi TM3000, Japan). Pore size was measured from SEM images using Fiji Software [41].

2.4. Swelling assay

Semi-dried hydrogels to half of their initial weight were placed in 35 mm plates and covered with 3 ml of 0.9% saline. Then, samples were incubated at 30 °C, and mass was recorded at different time points: 0, 15, and 30 minutes, 1, 2, 4, 6, 8, and 24 hours. Swelling ratio was calculated as follows:

$$Swelling\ ratio = \frac{m_{swollen}}{m_{initial}}$$

Where initial ratio for time 0 equals 1.

2.5. Mechanical characterization

Compression tests were performed using a TA-XT plus texture analyzer (Stable Micro Systems, UK) in compression mode. A cylindrical probe (10 mm diameter) was used, and hydrogels were compressed reaching 70% strain, while stress values were calculated using Exponent software (Stable Micro Systems, UK). Compressive young modulus was calculated as the slope of the linear region of the stress-strain curve.

2.6. Chlorophyll quantification

Hydrogel samples of 2 cm^2 were stored individually at -20 °C until analysis. Then, 500 µl of DMSO (Sigma, Germany) were added to each thawed sample, disrupted with a plastic pestle, and incubated for 40 minutes in agitation, covered from direct light. After incubation, absorbance was measured at 665 and 648 nm using Epoch microplate reader (BioTek, USA), and total chlorophyll content was calculated as follows [42]:

$$Chlorophyll\ (\mu g/ml) = 7.49 \cdot A^{665} + 20.34 \cdot A^{648}$$

2.7. Cell culture and incubation with hydrogels

Human neonatal dermal fibroblasts (HDFn) were kindly provided by Dr. Ignacia Fuentes (Universidad del Desarrollo, Santiago, Chile), and were maintained under standard cell culture conditions (37 °C, 5% CO_2) in DMEM (Biological Industries, Israel) supplemented with 10% Fetal Bovine Serum (Pan Biotech, Germany) and 1% penicillin/streptomycin (Sigma, Germany). For the incubation assay, cells were seeded on 12-well plates ($2{\cdot}10^5$ cells/well for viability assays or $1{\cdot}10^5$ cells/well for immunofluorescence) and cultured overnight. Then, 6 mm in diameter hydrogels were placed in 8 µm transwell inserts on top of the seeded cells, covered with cell culture media, and incubated for 24 hours under constant illumination with blue light (455 nm).

2.8. Cell viability assays

After 24 hours of incubation, hydrogels were removed, and MTT metabolic assay of HDFn was performed following the manufacturer's protocol (Abcam, UK). Briefly, cell culture media was replaced by 1 ml of MTT (500 µM), followed by 2 hours of incubation. Then, 500 µl of DMSO (Sigma, Germany) were added to stop the reaction and incubated at room temperature for 15 minutes. Finally, 200 µl of supernatant were transferred to a 96 well plate and absorbance was measured at 570/650 nm. Microalgae viability after 24 hours of incubation with HDFn was determined by examining growth after 7 days of inoculation in agar plates.

2.9. Cell morphology

After 24 hours of incubation with the hydrogels (see Section 2.7), inserts were removed and cells were washed once with PBS $Ca2^+$/$Mg2^+$, fixed with 4% paraformaldehyde and then incubated with PBS-Triton X-100 0.1% for 10 minutes. After washing, cells were stained with Hoechst 1 µg/ml (Life Technologies, USA) and Phalloidin-AF546 (Life Technologies, USA) for 40 minutes at RT and protected from direct light. Images were obtained using a fluorescence microscope (Leica DM500, Germany) equipped with a digital camera (MS60).

2.10. In vivo *biocompatibility assays*

To evaluate the biocompatibility of the photosynthetic hydrogels *in vivo*, a well described acute toxicity zebrafish model was used [43]. *Danio rerio,* (TAB5 strain) embryos were obtained from our zebrafish breeding facility as described before [44]. All embryos were collected by natural spawning and raised at 28.5 °C in E3 medium (5 mM NaCl, 0.17 mM KCl, 0.33 mM $CaCl_2$, 0.3 mM $MgSO_4$) adjusted to pH 7. The embryos were maintained in an incubator with 14-10 hours of light-dark cycles, and E3 medium was changed daily.

For this assay, 5 zebrafish larvae at 5 days post fertilization (dpf) were placed in a 6-well plate and covered with 2.5 ml of E3 medium. Next, control hydrogels (HG) or hydrogels containing microalgae (HG + *C.r*) were added to the wells. In order to maintain larvae in optimal conditions, incubations were performed in a 14-10 hours light-dark cycles. After 24 hours of exposure, survival was evaluated when heartbeats were detected, and expressed as the percentage of live larvae. For morphological imaging, larvae were anesthetized in 4.2% (w/v) tricaine (Sigma, Germany), mounted in 1% low-melt point agarose [45] and imaged with a stereoscope (Leica S6D, Germany) equipped with a digital camera.

2.11. Skin irritation test

Primary skin irritation (PSI) test was performed according to the guidelines of ISO-10993-10-2010 [46] on healthy skin of 20 human volunteers who provided signed informed consent. Procedures were carried out in accordance with the ethical standards, and protocols were previously approved by the Scientific Ethics Committee for Health Sciences at Pontificia Universidad Católica de Chile (No: 220128002). Control and photosynthetic hydrogels were fabricated as described above (20 mm in diameter), applied onto the forearms of volunteers, and covered with a transparent dressing (Tegaderm, 3M, USA). The control site corresponded to the skin covered with Tegaderm alone. 24 hours after application, hydrogels were recovered and Score of Primary Irritation (SPI) was evaluated by a qualified nurse at 0, 1, 2, 24, 48 and 72 hours after hydrogel removal for each volunteer. The observed reaction was defined as erythema and/or edema, and classified as absent (0), very slight (1), defined (2), moderate (3) or severe (4). SPI was calculated as:

$$SPI = \left[\frac{\sum E_{0h} + E_{1h} + E_{2h} + E_{24h} + E_{48h} + E_{72h}}{6}\right]_T - \left[\frac{\sum E_{0h} + E_{1h} + E_{2h} + E_{24h} + E_{48h} + E_{72h}}{6}\right]_C$$

Where E stands for edema/erythema, T for treated site (with control or photosynthetic hydrogel) and C for control site. The Primary Irritation Index (PII) was calculated as the arithmetical mean of the SPI values from all volunteers. PII categories were defines as: negligible ($\leq$0), slightly irritating (0.1-0.9), moderately irritating (1-2.7) and severely irritating (2.8-4). Additionally, volunteers completed a self-evaluation questionnaire to evaluate pain intensity (0-10), itching (0-3), burning (0-3) and skin palpitation (0-3) in the treated sites and control sites at 0, 1, 2, 24, 48, and 72 hours after hydrogel removal.

Hydrogel weight was measured before and after application, and viability of the microalgae from the photosynthetic hydrogels once recovered from volunteer's arms was determined by examining growth after 7 days of inoculation in agar plates.

2.12. Oxygraphy

Metabolic activity or oxygen production of the photosynthetic hydrogels was measured using a Oxygraph+ System (Hansatech Instruments, UK). Samples were introduced in the electrode chamber and covered with 2 ml of 0.9% saline, and subjected to 10 minutes of darkness, followed by 10 minutes of illumination with blue light (455 nm, 300 $\mu E/m^2{\cdot}s$). Oxygen production rate in the illuminated phase was calculated from the slope of the oxygen concentration curves.

For metabolic coupling experiments, 10 zebrafish larvae at 5 dpf or 10 mm in diameter mice skin explants were introduced in the electrode chamber of the Oxygraph+ System, and covered with 1 or 2 ml of 0.9% saline respectively. Oxygen concentration evolution was recorded for 5 minutes in darkness, followed by 5 minutes of

blue light (455 nm, 300 µE/m^2·s). Then, 10 mm in diameter photosynthetic hydrogel was added to the chamber, and the oxygen evolution was recorded for the next 10 minutes in the same lighting condition, followed by 10 minutes of darkness. Oxygen metabolic rates were calculated from the slopes of the oxygen concentration curve. All oxygraphy measurements were carried out at 30 °C.

2.13. Growth factor release

Hydrogels containing strain UVM4-VEGF of *C. reinhardtii* were prepared as described above in Section 2.2. At time points 0, 3, and 7 days, hydrogels were washed thrice with 0.9% saline for 5 minutes, placed in 12-well culture plates, and covered with 500 µl of saline. Samples were then incubated for 2 hours at RT and with direct exposure to light. Saline supernatant with released VEGF was removed from the wells and stored at -80 °C until analysis. For growth factor release quantification, Quantikine® ELISA Human VEGF (R&D Systems, MN, USA) was used, following manufacturer's instructions.

2.14. Cefazolin release and bacterial growth inhibition assay

Hydrogels were prepared as described in Section 2.2 with slight modifications. For 1 ml of hydrogel, microalgae were resuspended in 100 µl of TAP (100 µl of TAP alone were used for control hydrogels), while the remaining 83 µl of TAP were used to dissolve 10 mg of sodium cefazolin (Vitalis, Colombia). After overnight gelation and further immersion in 2% $CaCl_2$, hydrogels were covered with 1 ml of saline (0.9% NaCl) and incubated at 30 °C. Supernatant was recovered at different incubation time points: 15 and 30 minutes, 1, 2, 4, 6, 8, 24, 48 and 72 hours, and substituted for new saline at each time point. Absorbance at 272 nm of the recovered saline was measured at each time point using V-730 Spectrophotometer (Jasco, UK) [47], and cumulative cefazolin release was calculated.

In order to study the functionality of the released antibiotic, hydrogels containing cefazolin were covered with 1 mL of saline (0.9% NaCl) and incubated at 30 °C for 8 and 72 hours. Supernatants were recovered, and 500 µl were added to a 24 well plate, followed by 500 µl of bacterial suspension (*Staphylococcus aureus* ATCC 25923 or *Escherichia coli* ATCC 25922) with initial optical density (OD) = 0.15, prepared in Luria Bertani broth, from bacterial cultures in the exponential phase of growth. Samples were incubated for 24 hours at 30 °C. Next, bacterial OD was determined by measuring absorbance at 600 nm, using Luria Bertani broth as blank and freshly prepared 1% cefazolin in saline as control of the antibiotic's activity.

2.15. Statistical analysis

All assays were performed in at least three independent experiments. GraphPad Prism 8 software was used for statistical analyses. Error bars in graphs correspond to SEM, and comparison of conditions was performed by t-test, One-way or Two-way ANOVA with Tukey's multiple comparison test when necessary (unless stated otherwise). Differences between groups were considered significant at $p \leq 0.05$. Details are specified at each figure legend.

3. Results

3.1. Photosynthetic hydrogel fabrication and characterization

Photosynthetic hydrogels were fabricated as described in the materials and methods section (Fig. 1**A**), leading to the formation of a regular hydrogel network with homogeneously distributed microalgae cells (Fig. 1**B**). Moreover, results show that the incorporation of this single layer of sterile gauze followed by an immersion step of the hydrogel in 2% $CaCl_2$, provided sufficient strength and flexibility to the material, further allowing an easy manipulation (Fig. 1**B**) and good adhesion to skin (Supplementary Video 1). A metabolic characterization of freshly produced photosynthetic hydrogels was performed and showed optimal oxygen production capacity at $5{\cdot}10^7$ microalgae/ml. Results show that, in the absence of light, oxygen was consumed at a rate of 8.5 ± 2.1 nmol/cm^2·min, while, upon illumination, it was produced at a rate of 11.2 ± 2.5 nmol/cm^2·min (Fig. 1**C**). Preliminary data obtained during the optimization steps showed 30% and 70% less oxygenation capacity of the hydrogels containing the lowest ($1{\cdot}10^7$ microalgae/ml) and highest ($2.5{\cdot}10^8$ microalgae/ml) microalgae densities respectively.

The structural and mechanical properties of the photosynthetic hydrogels (HG + *C. reinhardtii*) were studied and compared to control hydrogels, which were prepared without microalgae (HG). SEM was performed to study the microstructure of the hydrogels, where a homogeneous polymer arrangement with high porosity was observed for both conditions (Fig. 2**A**). SEM images also evidence that the gauze layer was integrated in the polymer structure, as it was entirely embedded in the hydrogel without affecting alginate crosslinking pattern (Fig. 2**A,** upper pictures). Moreover, the polymer surface was smooth for the control hydrogels, while it was rough in the photosynthetic ones, showing that the microalgae were fully encapsulated in alginate (Fig. 2**A,** lower pictures). A quantitative analysis showed similar average pore diameters for control and photosynthetic hydrogels, being 252.9 ± 8.5 µm and 249.1 + 7.8 µm respectively. Similar results were obtained for the pore distribution, which was also unaffected by the presence of the algae, ranging between 100 and 400 µm for both hydrogels, with maximum frequency between 250 and 300 µm (Fig. 2**B**). Further, the potential effect of the algae in the swelling capacity of the hydrogels was also studied, evaluating their rehydration dynamics in saline for up to 24 hours. No differences were observed between control and photosynthetic hydrogels where, in both cases, a maximum swelling capacity was observed after four hours of incubation, reaching 95% of their original weight by that time point (Fig. 2**C**). Finally, the response of the hydrogels to mechanical forces was studied by a uniaxial compression test, where the compressive Young's modulus was quantified by linear regression analysis of the stress-strain curve. Once more, results showed that the presence of the microalgae did not affect the Young's modulus of the hydrogels, indicating that photosynthetic hydrogels have equal mechanical properties than standard alginate hydrogels (Fig. 2**D**).

Next, stability of the photosynthetic hydrogels was assessed by studying its morphology and functionality for up to seven days with constant illumination and without medium supplementation. Results showed that the overall appearance of the photosynthetic hydrogel remains stable for up to seven days (Fig. 3**A**, top view). Moreover, in order to better evaluate microalgae distribution across the photosynthetic hydrogel overtime, cross sections were analyzed by standard light microscopy, as well as by fluorescent imaging. Here, results showed a homogeneous distribution of the microalgae along the Z axis of the samples for up to seven days, which was evidenced by both methods at all the analyzed times (Fig. 3**A**, bottom panels). In addition, results also suggested that microalgae did not invade the gauze layer, as cotton fibers appear in white using transmitted light microscopy, while they were observed as dark segments in the fluorescence images (Fig. 3**A**). As hydrogels seemed to be slightly greener at day 7, chlorophyll content was quantified overtime but no differences were observed at the different time points (Fig. 3**B**). Finally, functionality of the hydrogels was also assessed in regard to their oxygen production capacity. Here, photosynthetic hydrogels were placed in an oxygraphy chamber, and the oxygen concentration was evaluated upon illumination, calculating the oxygen production rate from the slopes of the curve. Results showed that the oxygen release capacity of the

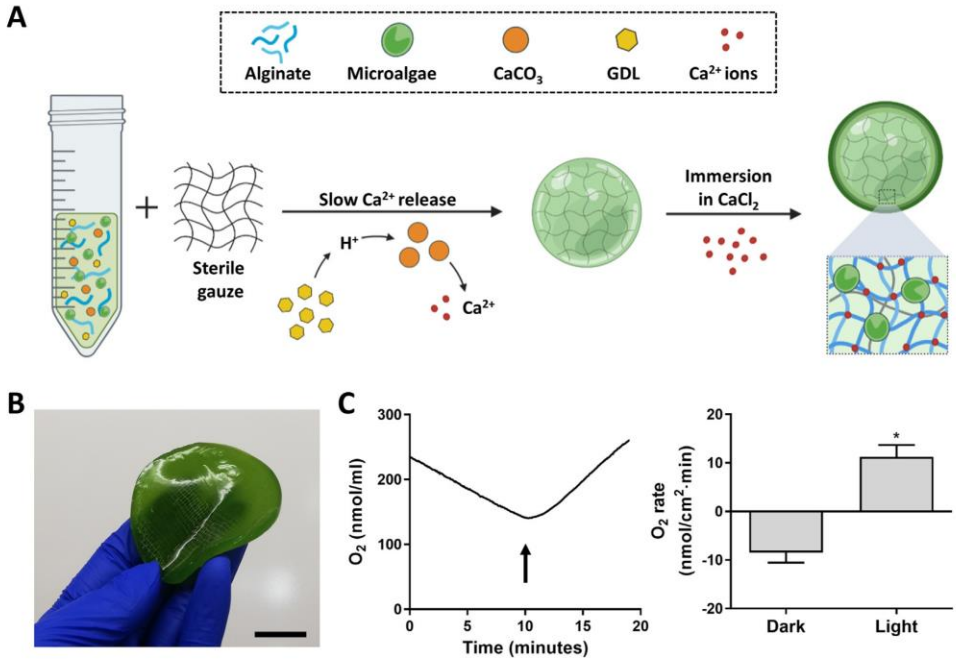

Fig. 1. Photosynthetic hydrogel fabrication. (**A**) Alginate based photosynthetic hydrogels were prepared by combining sterile gauze with alginate, microalgae, $CaCO_3$ and GDL, and crosslinked overnight. Next, a step of immersion in $CaCl_2$ was performed to improve handling of the material. (**B**) Macroscopic image of the hydrogel shows homogeneous composition and flexibility. (**C**) Oxygen concentration evolution in dark or light conditions (left), and hydrogel metabolic rates (right). Schematic in (A) was created using Biorender (https://biorender.com/). Scale bar in (B) represents 2 cm. Arrow (C, left) indicates start of illumination phase. Graph (C, left) is representative of at least three independent experiments, and data (C, right) is expressed as mean ± SEM; $^*p < 0.05$ (t-test).

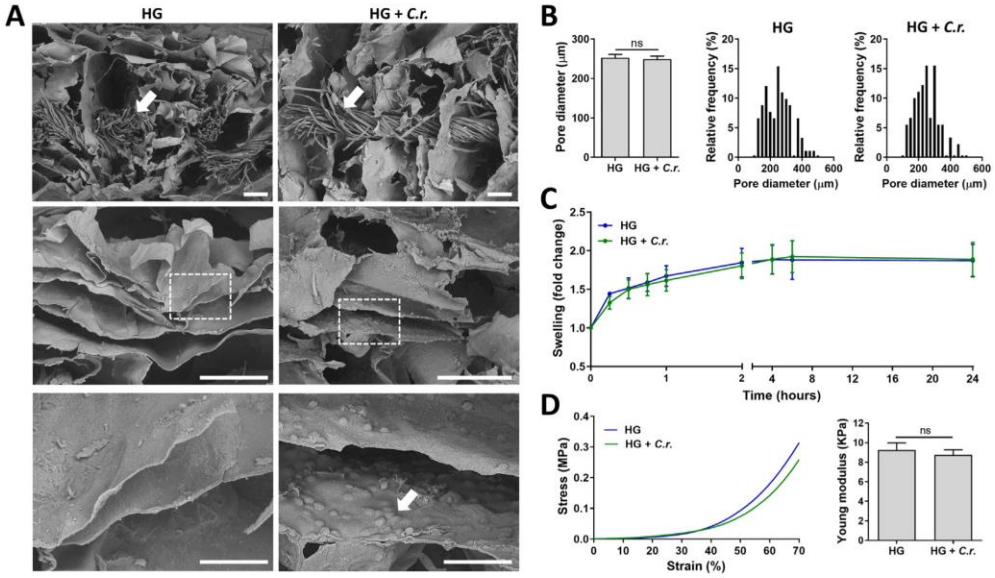

Fig. 2. Structural and mechanical characterization. (**A**) SEM imaging of control alginate hydrogels (HG) or seeded with the microalgae *C. reinhardtii* (HG + *C.r.*) are shown. White arrows indicate gauze (top row) and microalgae (bottom row, right). (**B**) Pore diameter (B, left) and distribution (B, right) in HG and HG + *C.r.* were compared. (**C**) Swelling in saline 0.9% at 30 °C was characterized for up to 24 hours in HG and HG + *C.r.*, reaching maximum swelling capacity after four hours. (**D**) Compression test was performed and representative curves (D, left) as well as Young modulus were compared (D, right). Scale bars in A represent 200 μm (top and middle) and 50 μm (bottom). Data are expressed as mean ± SEM; N ≥ 3; ns: non-significant (t-test).

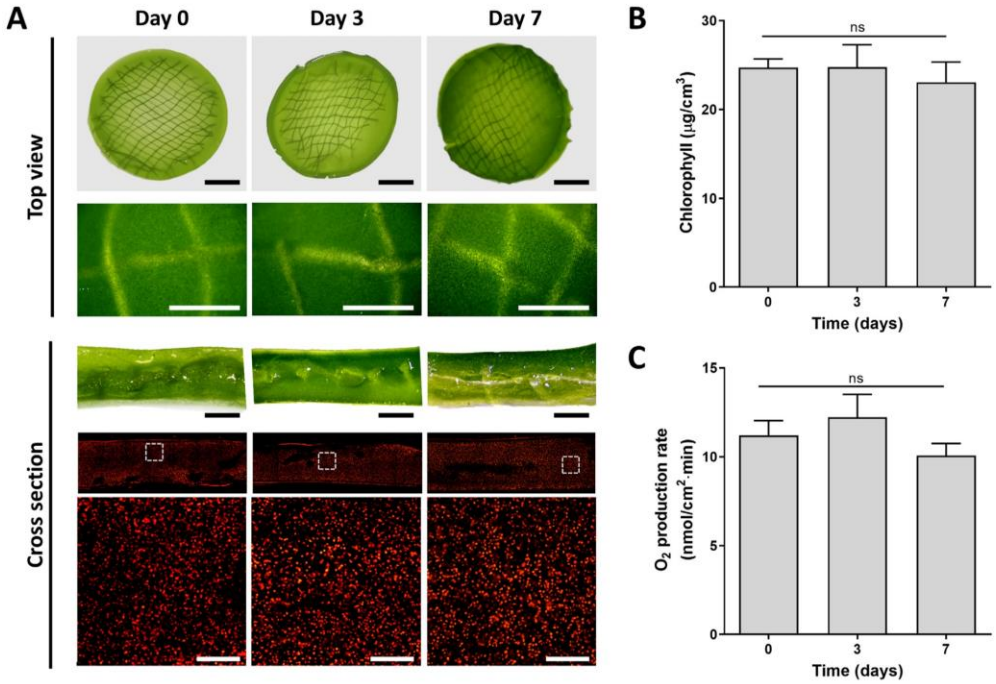

Fig. 3. Photosynthetic hydrogel stability and functionality over time. (**A**) Hydrogels were prepared and analyzed at different time points (days 0, 3 and 7). Macroscopic view of the hydrogel is shown by light imaging (A, upper), while microalgae integrity and distribution are visualized by fluorescence microscopy of the cross sections (A, lower). (**B**) Chlorophyll content and (**C**) oxygen production rate were also quantified overtime. Scale bars in A represent 5 mm (top view, top), 1 mm (top view, bottom and cross section, top) and 250 µm (cross section, bottom). Microalgae appear in red due to the chlorophyll autofluorescence. Data are expressed as mean ± SEM; N = 3; ns: non-significant (one-way ANOVA). (For interpretation of the references to colour in this figure legend, the reader is referred to the web version of this article.)

photosynthetic hydrogels was maintained for at least seven days (Fig. 3**C**).

3.2. Biocompatibility

To assess the biocompatibility of the photosynthetic hydrogel, a toxicological profile was performed *in vitro* and *in vivo*. Moreover, a metabolic coupling assay was carried out to study if the oxygen released by the hydrogel was able to fulfill the metabolic requirements of zebrafish larvae and mice skin explants. First, an *in vitro* co-culture system was established to evaluate the potential release of toxic molecules from control (HG) or photosynthetic hydrogels (HG + *C.r*). Here, HDFn were seeded in a multiwell plate, and hydrogels were located in a transwell insert, therefore no direct contact between cells and the hydrogels was established, but the exchange of soluble components was allowed. After 24 hours in co-culture, morphology of the HDFn cells was unaffected by the hydrogels, as shown by phalloidin staining of the actin cytoskeleton (Fig. 4**A**). Moreover, the viability of HDFn cells was quantified by MTT reduction metabolic assay, and no differences were observed among groups (Fig. 4**B**). As optimal microalgae culture conditions are strongly different than the setting established for the co-culture experiments (DMEM cell culture media, 37 °C and 5% CO_2 atmosphere), viability of the microalgae after co-culture was confirmed by evaluating their capacity to proliferate in TAP-Agar media plates, observing normal proliferation (Fig. 4**C**). Afterwards, toxicity *in vivo* was evaluated using a well-established zebrafish larvae model. Here, larvae were incubated for 24 hours in presence of hydrogels, and changes in morphology (Fig. 4**D**) and survival (Fig. 4**E**) were analyzed. As expected from the *in vitro* co-culture assays, no changes were observed in either group or parameter, confirming that photosynthetic hydrogels and microalgae were non-toxic for a whole living organism.

3.3. Human skin irritation test

After studying the biocompatibility of the biomaterial both with *in vitro* and *in vivo* models, it was necessary to assess whether the hydrogel dressing was irritating in healthy skin from human volunteers. Hydrogels were applied for 24 hours, and evaluation (Table 1) and imaging (Fig. 5**A**) of the skin was performed at 0, 1, 2, 24, 48 and 72 hours after hydrogel removal, and compared to the control skin, which was only covered by the transparent dressing. Skin reaction was defined as edema and/or erythema, and was classified as absent (0), very slight (1), defined (2), moderate (3) or severe (4). Most of the volunteers showed no irritation at any site and time point. However, very slight irritation was detected for several volunteers after short time in the control site (Table 1). One of the volunteers (V4) showed defined erythema at 48 and 72 hours after removal of both HG and HG + *C. reinhardtii.* SPI and PII were calculated as described in the materials and methods section. PII values were -0.06 for HG and -0.01 for HG + *C. reinhardtii* (Table 1). Self-evaluation of the patients revealed no pain or burning sensation at any time point. Itching was described by 3 volunteers at the control site among different time points, and by 2 volunteers in the HG + *C. reinhardtii* site one hour after hydrogel removal. Palpitations were described by only one volunteer in the control site after 48 and 72 hours (Fig. 5**B**). After application, hy-

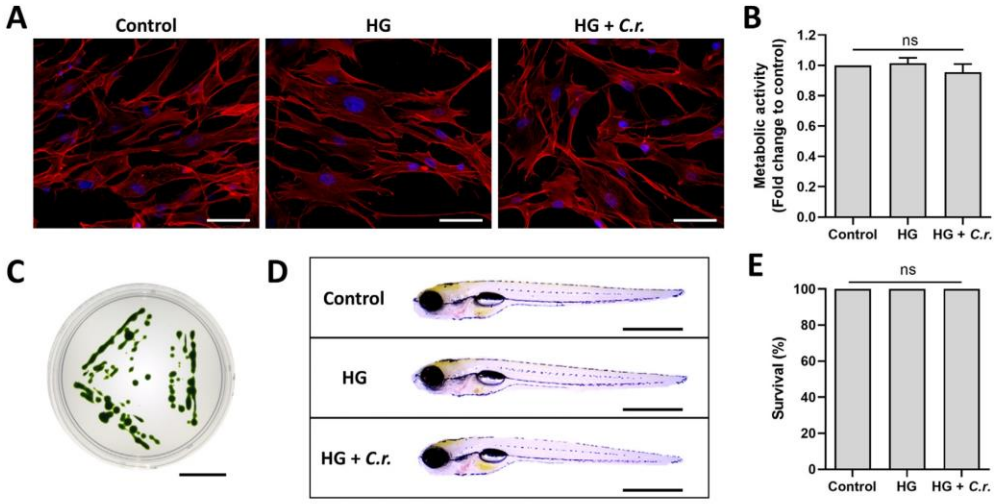

Fig. 4. Hydrogel biocompatibility *in vitro* and *in vivo*. (**A**) Neonatal human dermal fibroblasts were cultured alone (Control) or co-cultured for 24 hours with the control hydrogel (HG) or hydrogel containing *C. reinhardtii* (HG + *C.r.*). Morphology of the cells is shown by Phalloidin (red, actin) and Hoechst (blue, nuclei) staining. (**B**) Viability of the cells was assessed by MTT assay. (**C**) Viability and growing capacity of the microalgae in the photosynthetic hydrogel after coculture with human fibroblasts was studied by agar plating. (**D-E**) Acute toxicity assays *in vivo* were performed by exposing zebrafish larvae for 24 hours to their standard growth media alone (Control), with the control hydrogel (HG) or in the presence of the photosynthetic hydrogel (HG + *C.r.*), and morphology of the larvae and survival were assessed. Scale bars in A, C and D represent 100 µm, 1 cm and 1 mm respectively. Data are expressed as mean ± SEM; results were obtained from three independent experiments; for D and E, a total of 30 larvae were used per condition; ns: non-significant (one-way ANOVA). (For interpretation of the references to colour in this figure legend, the reader is referred to the web version of this article.)

drogels were recovered to assess overall integrity and mass change. As shown in Fig. 5**C**, hydrogels did not show any damage in the borders or surfaces, emphasizing their optimal mechanical properties, which enable an easy and successful application. However, hydrogels showed a 60% to 70% mass loss compared to their mass before application. To study microalgae viability in HG + *C. reinhardtii* after application in volunteers, hydrogels were then seeded in TAP agar plates. After seven days, agar plates were imaged, showing microalgae growth for all HG + *C. reinhardtii* applied in volunteers. A representative image of one of the plated hydrogels is shown in Fig. 5**D**.

3.4. Oxygenation capacity and bioactive molecules release

Once it was established that the photosynthetic hydrogels did not exert acute toxic effects in both *in vitro* and *in vivo* models, and neither triggered irritation in healthy human skin, the capacity of the photosynthetic hydrogel to supply enough oxygen to sustain the metabolic requirements of a heterotrophic biological system was evaluated. A closed-loop metabolic coupling assay was performed, where the photosynthetic capacity of the hydrogels was tested using zebrafish larvae or skin explants (Fig. 6**A**). First, ten zebrafish larvae were placed in an oxygraphy chamber filled with saline, and the oxygen concentration was measured in the absence or presence of light. Results showed that oxygen concentration decreased overtime, without varying in the presence of light, indicating that such high oxygen consumption was independent of illumination (Fig. 6**B, C,** segments I, II). Next, a 10 mm in diameter photosynthetic hydrogel was added to the chamber in the presence of light, and oxygen concentration showed a sustained increase over time, implying that the oxygen produced by the photosynthetic hydrogel exceeded the metabolic need of the ten larvae in the closed system (Fig. 6**B, C**, segment III). Finally, the light was turned off and a negative slope with a metabolic rate greater than segments I and II was observed, indicating that both larvae and photosynthetic hydrogels consumed oxygen in the dark (Fig. 6**B, C,** segment IV). To validate this data with a more relevant model for wound healing, the same setting was applied to freshly isolated mouse skin biopsies (Fig. 6**D, E**). Similar results were obtained, as skin samples consumed oxygen in segments I and II, indicating high metabolic activity of the isolated tissue, which was reverted in segment III once photosynthetic hydrogels were introduced and illuminated in the closed system. Finally, after turning the light off in segment IV, the slope turned negative again with a statistically lower value compared to segments I and II (Fig. 6**D, E**).

Hydrogels have been broadly described for their capacity to release bioactive molecules *in situ*, and genetically modified microalgae have been previously proposed as a tool for the local release of recombinant growth factors. Hence, hydrogels were prepared with VEGF-producing microalgae and the concentration of the released recombinant molecule was measured over time, showing a constant release for at least seven days *in vitro* (Fig. 7**A**). Moreover, control (HG) or photosynthetic hydrogels (HG + *C. reinhardtii*) were loaded with cefazolin and its cumulative release was quantified, showing similar behaviors among groups, reaching around 68% of drug release within the first two hours, 75% after eight hours, and 80% after 72 hours (Fig. 7**B**). As microalgae could have potentially affected drug bioactivity, its antibiotic capacity was measured in a growth inhibition assay, performed on bacterial cultures of *S. aureus* and *E. coli*. Results showed that the released cefazolin obtained from both HG and HG + *C. reinhardtii* after 8 and 72 hours was as effective as the freshly prepared antibiotic (control), while photosynthetic or control hydrogels did not have an antibiotic effect by themselves (Fig. 7**C**).

4. Discussion

Traditional wound dressings act mainly as barriers to keep wounds protected from the environment, preventing tissue infection and absorbing exudate. However, over the last decade, bioac-

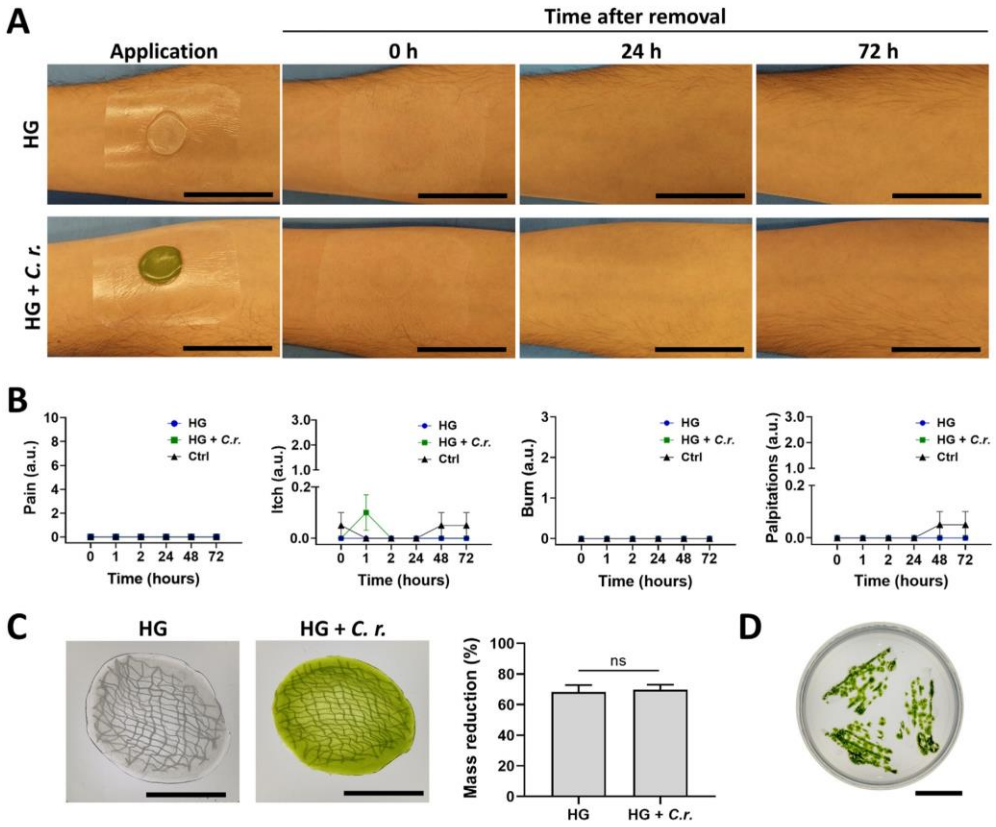

Fig. 5. Hydrogel application on healthy skin of human volunteers. (**A**) Representative images of the forearms of a single volunteer at the moment of application of the control hydrogels (HG) or hydrogels containing *C. reinhardtii* (HG + *C.r.*) at 0, 24 and 72 hours after removal. (**B**) Self-evaluation of pain intensity (0-10), itch, burning and palpitation sensation (0-3) at the different treated sites were completed by volunteers at all time points. (**C**) After hydrogel application, both HG and HG + *C.r.* were recovered to evaluate integrity (left) and mass reduction (right). (**D**) HG + *C.r.* hydrogels were plated in TAP agar to evaluate microalgae viability after application. Scale bars in A represent 5 cm, while in C and D represent 1 cm. Data are expressed as mean ± SEM; N = 20 in (B), N=15 in (C); ns: non-significant (t-test).

tive materials emerged as a powerful tool to modulate the wound microenvironment, promoting wound healing and tissue regeneration. Following this aim, in this work, alginate was chosen as the base material to establish a photosynthetic hydrogel-based wound dressing. Among other advantages, due to its mechanical and chemical properties, alginate is capable of absorbing wound exudate, maintaining a physiologically moist environment [48]. Moreover, because it does not stick to the wound bed, it allows a painless and clean removal and replacement during wound care, therefore being commonly used in clinics [49]. Finally, several studies have previously shown that alginate hydrogels are biocompatible with the microalgae *C. reinhardtii* [33,35,50,51].

Most of the therapeutic potential of hydrogels rely on their mechanical and structural properties, which are mainly given by crosslinking. Alginate can be crosslinked by external or internal gelation. External gelation is usually performed to create droplets by immersion in $CaCl_2$, where quick polymerization occurs. On the other hand, an insoluble calcium salt must be added to the alginate mixture for internal gelation, which upon acidification releases calcium ions from the insoluble salt and crosslinks alginate [52]. This method ensures more homogeneous and less dense matrices with larger pores that increase permeability. Therefore, in this work, hydrogels were first internally crosslinked by combining alginate, $CaCO_3$ and GDL, ensuring a homogeneous hydrogel density, pore size and distribution of microalgae. Then, in order to improve the mechanical properties and hence stability and ease of handling of the dressing, an additional external crosslinking was performed. Interestingly, although microalgae could have had interfered at several steps of the process by, for instance, affecting hydrogel polymerization or further inducing mechanical or enzymatic degradation, none of the analyzed structural and mechanical features of the hydrogel were affected. Similarly, other key functional features such as growth factors and antibiotics release were also unaffected by the presence of the microalgae.

While high proliferation rates of microalgae had been described in several biomaterials such as collagen [31] and fibrin [53] scaffolds or surgical sutures [34], the results obtained here revealed that the number of seeded microalgae remained constant overtime, agreeing with previous works which have also described low proliferation rates of microalgae embedded in alginate hydrogels [54,55]. This observation could be partially explained by the high crosslinking density and compressive young modulus, which causes mechanical constrain for cell division.

Transport and storage of living biomaterials, i.e. which contain cells, is difficult as they need optimal culture conditions for cell survival [56]. However, because microalgae are autotrophic systems

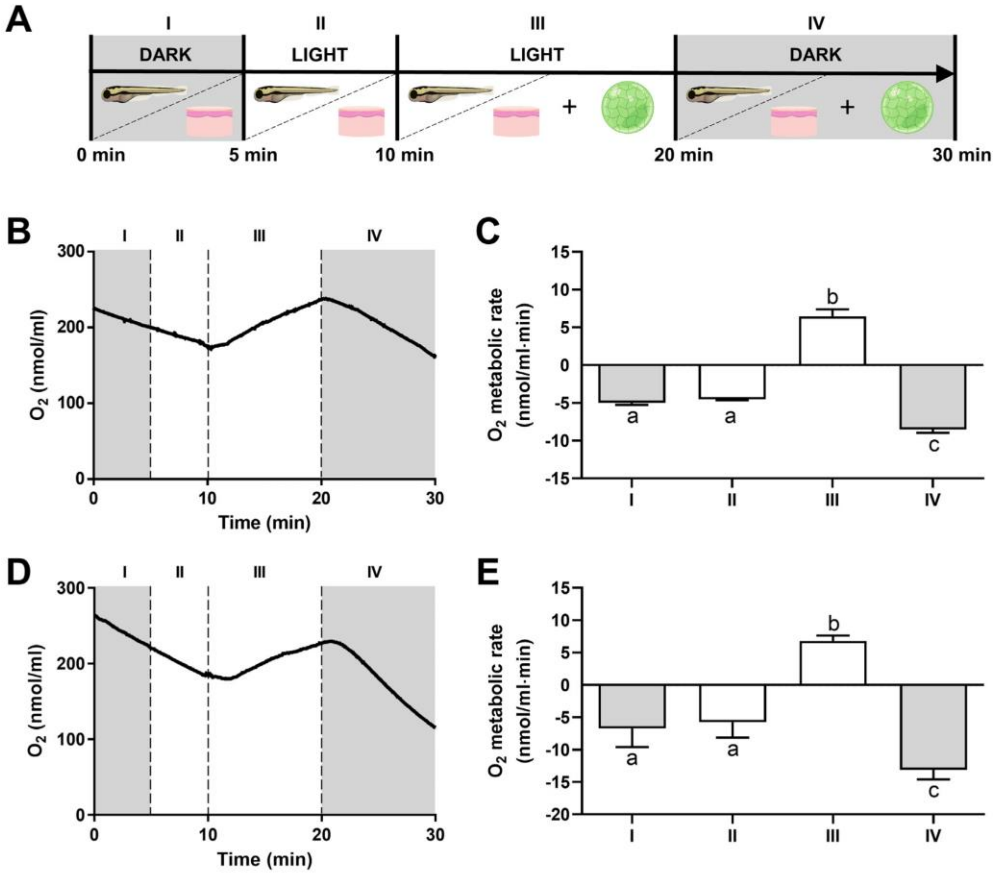

Fig. 6. Oxygenation capacity of the photosynthetic hydrogels. (**A**) Schematic of the experimental setting. Oxygen concentrations were measured for 5 min in darkness (I, DARK) or light (II, LIGHT) with the presence of either zebrafish (**B, C**) or skin explants (**D, E**). Next, hydrogels were incorporated and oxygen concentration was measured for 10 min in the presence (III, LIGHT) or absence (IV, DARK) of light. Schematic in (A) was created using Biorender (https://biorender.com/). Data are expressed as mean ± SEM; N ≥ 3; different letters in C and E indicate significant differences with $p < 0.05$ (one-way ANOVA followed by Tukeyś test).

and hydrogels can be loaded with large amounts of culture media, photosynthetic hydrogels showed to be metabolically stable for at least seven days at room temperature and in the absence of additional nutritional supplementation, enhancing the potential clinical translation for this kind of photosynthetic wound dressings.

Biocompatibility is the main requirement for biomaterials. In this work, photosynthetic hydrogels showed to be innocuous *in vitro* and *in vivo*. Human dermal fibroblasts were used for *in vitro* assays as they are one of the main cell types of the dermis. Transwell inserts were chosen to mimic the molecular interchange between the photosynthetic dressing and the wound bed in a clinical context, and to avoid potential mechanical damage in cells cultured as monolayers in plastic dishes. For *in vivo* assays, zebrafish larvae were chosen as they are a highly validated and characterized vertebrate model broadly described for biomedical toxicity assays [43,57]. In fact, a recently published article showed that high concentrations of *C. reinhardtii* (10^8 and 10^9 cells/ml) can be toxic for the larvae [29]. Interestingly, photosynthetic hydrogels fulfilled the oxygen metabolic requirement of two highly relevant biological models. Here, zebrafish larvae were chosen as they present a high metabolic rate, performing gas exchange by bulk diffusion through their body surface [58], while freshly isolated skin explants were chosen as they represent a functional wound model in their edges, which were co-incubated with photosynthetic hydrogels of equal surface. This last model provides important data about the oxygenation capacity of photosynthetic hydrogels in a more relevant clinical scenario, and agree with recently published articles describing that microalgae were able to sustain the metabolic requirements of rat kidney slices [29], as well as brain functionality both *in vitro* [26] and *in vivo* [27]. A positive correlation between oxygen concentration and better clinical outcomes has been broadly described for wounds [59], however the exact oxygen requirements vary depending on wound etiology and healing phase. In this work, the microalgae density was defined performing preliminary experiments where lower densities showed a reduced oxygen production, while at higher densities a decreased oxygenation was observed. This last can be attributed to the increased oxygen consumption of the microalgae to support their own metabolism and the well-known and described self-shading effect of photosynthetic microorganisms [60]. In this regard, an advantage of the photosynthetic hydrogels presented in this work is that the oxygen production rates can be easily adjusted for each

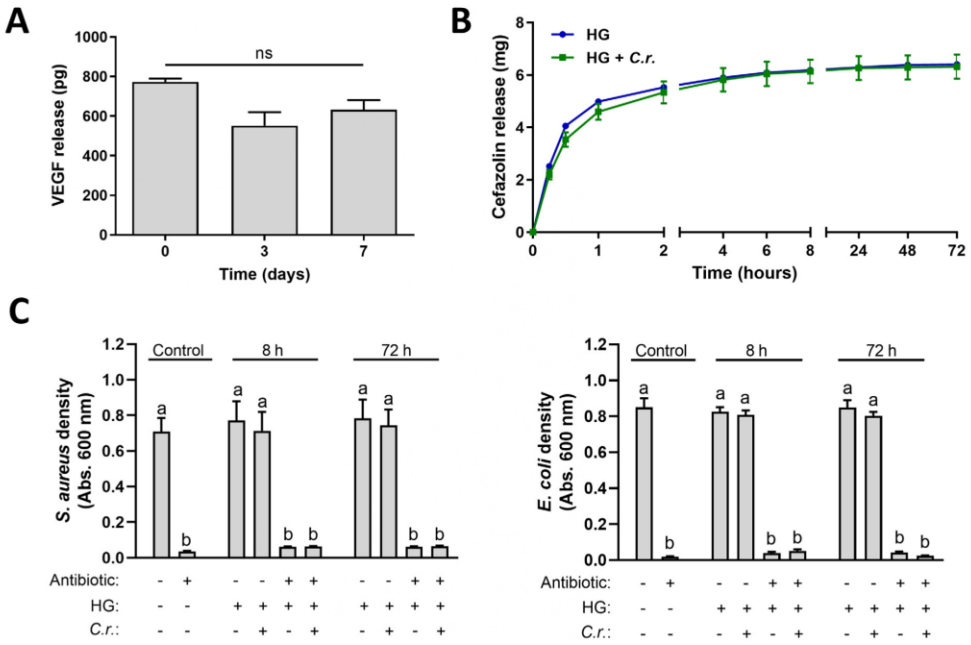

Fig. 7. Recombinant growth factor and antibiotic release. (**A**) VEGF release from hydrogels prepared with genetically modified microalgae was quantified after 0, 3 and 7 days of fabrication. (**B**) Control hydrogels (HG) or seeded with *C. reinhardtii* (HG + *C.r.*) were loaded with 1% cefazolin (8 mg total), and cumulative release in 0.9% saline was quantified for up to 72 hours. (**C**) Functionality of the released cefazolin from HG and HG + *C.r.* was studied by co-incubation with *S. aureus* and *E. coli* and quantification of the optical density after 24 hours. 1% cefazolin in 0.9% saline was used as control. Data are expressed as mean ± SEM; N ≥ 3; ns: non-significant (one-way ANOVA); different letters in C indicate significant differences with $p < 0.05$ (two-way ANOVA followed by Tukeyś test).

wound by modulating the illumination setting. As well as for other photosynthetic therapies, the development of such sophisticated illumination devices represents a challenge in the field and therefore a current limitation for the clinical use of the photosynthetic hydrogels presented here.

Due to major differences in several key aspects, it is difficult to compare the oxygenation capacity of the photosynthetic hydrogel presented here with traditional wound oxygenation therapies. For instance, HBOT provides systemic oxygenation and therefore the availability of oxygen depends on arterial pO_2, vascular supply, local capillary structures and the diffusion distance from the capillaries to the cells in the wound [59]. Moreover, such oxygenation is not permanent and typically occurs in session of about 90 minutes, which differs from the photosynthetic hydrogels that provide local and sustained oxygen release. In contrast to traditional TOT, where oxygen diffusion takes place through a gas phase, in photosynthetic hydrogels it occurs in a moisture environment with simultaneous active removal of CO_2 by carbon fixation, affecting the diffusion constants for local gas interchange.

Alginate dressings are extensively used for the treatment of wounds [48], and *C. reinhardtii* have shown to be safe both in animal models [36] and in humans [37]. Therefore, in this work, the use of animal models to assess its safety in wounds was not considered. However, as the combination of alginate, $CaCO_3$, GDL and *C. reinhardtii* had not been described previously, irritation was studied on healthy skin of human volunteers, showing negligible irritation and an irritation index lower than commercially available dressings. Although these results are critical for clinical translation, further studies should address safety and efficacy of photosynthetic hydrogels in different types of wounds. From the biomaterial side, it is important to note that hydrogels maintained their integrity and microalgae viability after 24-hour application, but lost around 60% of their initial mass. As hydrogels were applied on healthy skin and covered with a semi-occlusive transparent dressing (waterproof but permeable to water vapor and oxygen), water loss from the hydrogel might have occurred by evaporation and skin absorption. However, because hydrogels have shown to be a great option for exudate absorption in wounds, drying of the hydrogel is not expected to happen in a clinical context [13]. Moreover, and as shown by swelling assays, in a clinical setting, hydrogels could be dried to half their water content after fabrication and subsequently applied onto wounds for an improved exudate absorption, functioning as a wound cleaning system.

Wound healing is a multifactorial process that relies on several molecules, therefore the ability of the photosynthetic hydrogels to release freshly produced recombinant growth factors and bioactive drugs was demonstrated in this work, where saline was used to resemble the moist environment of exudative wounds. The use of genetically engineered microalgae has been suggested to provide a constant source of freshly produced bioactive recombinant molecules in wounds [34,36,38], but the potential effect of the hydrogel in their release kinetics and production had not been tested before. VEGF was chosen in this study, as it is the most important proangiogenic growth factor, being essential for proper wound healing. Indeed, patients with chronic wounds present very low levels of active VEGF [61]. Therefore, functionalized dressings able to deliver VEGF *in situ* represent a promising platform for a more efficient wound closure, and several *in vivo* approaches have shown its clinical potential [36,62,63]. Interestingly, compared to other growth factor delivering therapies, the presented photosynthetic hydrogels are able to continuously produce and deliver VEGF, and dosage can be further controlled by varying the cell density or

Table 1
Scores of skin irritation test performed on healthy skin of human volunteers. Skin reaction score for every volunteer at each time point was studied and classified as absent (0), very slight (1), defined (2), moderate (3) or severe (4) erythema and/or edema at the treated sites with either control hydrogel (HG) or hydrogel containing *C. reinhardtii* (HG + *C.r.*), and control site (Ctrl). Score of primary irritation (SPI) was calculated for the treated sites. Primary Irritation Index (PII) of the hydrogels was calculated as the mean of the SPI values from all volunteers.

	0 h			1 h			2 h			24 h			48 h			72 h			SPI		PII	
	HG	HG + *C.r.*	Ctrl	HG	HG + *C.r.*	Ctrl	HG	HG + *C.r.*	Ctrl	HG	HG + *C.r.*	Ctrl	HG	HG + *C.r.*	Ctrl	HG	HG + *C.r.*	Ctrl	HG	HG + *C.r.*	HG	HG + *C.r.*
V1	0	0	1	0	1	0	0	0	0	0	0	0	0	0	0	0	0	0	-0.17	0.00		
V2	1	0	0	0	0	0	0	0	0	0	0	1	0	0	1	0	0	1	-0.33	-0.50		
V3	0	0	0	0	0	0	0	0	0	0	0	0	0	0	0	0	0	0	0.00	0.00		
V4	0	0	0	0	0	1	0	0	0	0	0	0	0	3	0	2	3	0	0.17	0.83		
V5	0	1	1	0	0	0	0	0	0	0	0	0	0	0	0	0	0	0	-0.17	0.00		
V6	1	1	1	0	0	0	0	0	0	1	1	0	0	0	0	0	0	0	0.17	0.17		
V7	0	0	1	0	0	0	0	0	0	0	0	0	0	0	0	0	0	0	-0.17	-0.17		
V8	0	0	0	0	0	0	0	0	0	0	0	0	0	0	0	0	0	0	0.00	0.00	-0.06	-0.01
V9	0	0	1	0	0	0	0	0	0	0	0	0	0	0	0	0	0	0	-0.17	-0.17		
V10	0	0	1	0	0	0	0	0	0	0	0	0	0	0	0	0	0	0	-0.17	-0.17		
V11	0	0	0	0	0	0	0	0	0	0	0	0	1	1	0	1	1	0	0.50	0.33		
V12	0	0	1	0	0	0	0	0	0	0	1	0	0	0	0	0	0	0	-0.17	0.00		
V13	0	0	1	0	0	0	0	0	0	0	0	0	0	0	1	0	0	1	-0.50	-0.50		
V14	0	0	0	0	0	0	0	0	0	0	0	0	0	0	0	0	0	0	0.00	0.00		
V15	0	0	1	0	0	0	0	1	0	0	0	0	0	0	0	0	0	0	-0.17	0.00		
V16	0	0	0	0	0	0	0	0	0	0	0	0	0	0	0	0	0	0	0.00	0.00		
V17	0	0	0	0	0	0	0	0	0	0	0	0	0	0	0	0	0	0	0.00	0.00		
V18	0	0	0	0	0	0	0	0	0	0	0	0	0	0	0	0	0	0	0.00	0.00		
V19	0	0	0	0	0	0	0	0	0	0	0	0	0	0	0	0	0	0	0.00	0.00		
V20	0	0	0	0	0	0	0	0	0	0	0	0	0	0	0	0	0	0	0.00	0.00		

illumination parameters. Additionally, the released VEGF could act optimally, since angiogenesis is dependent on oxygen availability, which would be provided by the photosynthetically active microalgae cells [64]. As hydrogels are also clinically used for local and controlled drug release, it was crucial to evaluate if the presence of the microalgae affected the release kinetics and bioactivity of the loaded drugs. The choice of cefazolin as a model for antibiotic release was based on its broad-spectrum activity against Gram-positive and Gram-negative bacteria. Moreover, as cefazolin binds and inactivates penicillin-binding proteins from the inner membrane of the bacterial cell wall, a direct impact against *C. reinhardtii* was not expected [65]. The hydrogel was able to release about 75% of the total loaded antibiotic, showing the same high functionality against *E. coli* and *S. aureus* as the freshly prepared antibiotic solution. Because a very quick burst of initial release was observed, it could be hypothesized that the remaining 25% of the loaded antibiotic was released during the $CaCl_2$ coating. The release rate of cefazolin or other small molecules could be further optimized by modifying the structural properties of the hydrogels [66]. Nevertheless, it is important to mention that VEGF and cefazolin were chosen only as proof-of-concept molecules, but such molecules could be further replaced by other therapeutic agents depending on the clinical needs, employing the photosynthetic hydrogel as a customizable platform.

Recently, previous works have also proposed the use of photosynthetic hydrogels for wound healing, by combining microalgae or cyanobacteria with different materials, manufacturing techniques, and final presentation including wound patches [33], topical gels [67], or *in situ* bioprinted hydrogels [35]. However, and in comparison to such previous works, *C. reinhardtii* was chosen here as it is the only photosynthetic microorganism that has shown clinical safety when implanted in human patients [37]. Moreover, an unconventional strategy to improve the mechanical properties of the hydrogel is described in this study, where a single layer of sterile gauze was embedded within the alginate mixture, which optimized the strength and handling of the dressing by acting as a secondary network. In addition, this work described for the first time the development of a customizable platform in the form of an oxygen-releasing photosynthetic hydrogel, showing its safety in human skin and its potential to further release therapeutic drugs and recombinant growth factors.

Altogether, the work presented here supports the use of photosynthetic biomaterials in regenerative medicine, and proposed the use of living hydrogels as wound dressings that may locally act as personalized bioreactors to promote wound healing by the controlled delivery of oxygen and other bioactive molecules *in situ*. Although the results presented here are promising, further studies need to be done to evaluate efficacy of these photosynthetic dressings in relevant preclinical wound models such as diabetic mice, and in human patients with different types of wounds.

Funding

This project was financed by CORFO grant 18PIDE98887, Fondecyt 1200280 and Amarena VC.

Data and materials availability

All data and materials associated with this study are in this manuscript, and can be shared with approved outside collaborators under a materials transfer agreement; requests should be sent to JTE., jte@uc.cl.

Declaration of Competing Interest

JTE is CSO and co-founder of SymbiOx Inc., a start-up company that owns IP in the field of this work. During the conduct of this project, RC-O and CV were employees of SymbiOx Inc. All other authors declare that they have no competing interests.

Acknowledgments

We thank Mario Faúndez (Pontificia Universidad Católica de Chile) for the use of Cytation 5 instrument, Pedro Bouchon (Pontificia Universidad Católica de Chile) for the access to the texture analyzer, and César Ramírez (Pontificia Universidad Católica de Chile) for the access to V-730 spectrophotometer. We are thankful to the Advanced Microscopy Facility UMA UC for their support in SEM imaging, to Marianne Brenet for her support obtaining preliminary data, to Pablo Rozas for his critical review of the manuscript and to all the volunteers that participated in the skin irritation test.

Supplementary materials

Supplementary material associated with this article can be found, in the online version, at doi:10.1016/j.actbio.2022.11.036.

References

[1] C. Shi, C. Wang, H. Liu, Q. Li, R. Li, Y. Zhang, Y. Liu, Y. Shao, J. Wang, Selection of appropriate wound dressing for various wounds, Front. Bioeng. Biotechnol. 8 (2020) https://www.frontiersin.org/article/10.3389/fbioe.2020.00182. accessed March 8, 2022.
[2] I. Firlar, M. Altunbek, C. McCarthy, M. Ramalingam, G. Camci-Unal, Functional hydrogels for treatment of chronic wounds, Gels 8 (2022) 127, doi:10.3390/gels8020127.
[3] Y. Liang, J. He, B. Guo, Functional hydrogels as wound dressing to enhance wound healing, ACS Nano 15 (2021) 12687–12722, doi:10.1021/acsnano.1c04206.
[4] F. Fan, S. Saha, D. Hanjaya-Putra, Biomimetic hydrogels to promote wound healing, Front. Bioeng. Biotechnol. 9 (2021) 718377, doi:10.3389/fbioe.2021.718377.
[5] J. Su, J. Li, J. Liang, K. Zhang, J. Li, Hydrogel preparation methods and biomaterials for wound dressing, Life 11 (2021) 1016, doi:10.3390/life11101016.
[6] S. Jacob, A.B. Nair, J. Shah, N. Sreeharsha, S. Gupta, P. Shinu, Emerging role of hydrogels in drug delivery systems, tissue engineering and wound management, Pharmaceutics 13 (2021) 357, doi:10.3390/pharmaceutics13030357.
[7] M. Vigata, C. Meinert, D.W. Hutmacher, N. Bock, Hydrogels as drug delivery systems: a review of current characterization and evaluation techniques, Pharmaceutics 12 (2020) E1188, doi:10.3390/pharmaceutics12121188.
[8] H. Suo, M. Hussain, H. Wang, N. Zhou, J. Tao, H. Jiang, J. Zhu, Injectable and pH-sensitive hyaluronic acid-based hydrogels with on-demand release of antimicrobial peptides for infected wound healing, Biomacromolecules 22 (2021) 3049–3059, doi:10.1021/acs.biomac.1c00502.
[9] M. Contardi, D. Russo, G. Suarato, J.A. Heredia-Guerrero, L. Ceseracciu, I. Penna, N. Margaroli, M. Summa, R. Spanò, G. Tassistro, L. Vezzulli, T. Bandiera, R. Bertorelli, A. Athanassiou, I.S. Bayer, Polyvinylpyrrolidone/hyaluronic acid-based bilayer constructs for sequential delivery of cutaneous antiseptic and antibiotic, Chem. Eng. J. 358 (2019) 912–923, doi:10.1016/j.cej.2018.10.048.
[10] E. Wawrzyńska, D. Kubies, Alginate matrices for protein delivery - a short review, Physiol. Res. 67 (2018) S319–S334, doi:10.33549/physiolres.933980.
[11] Z. Wang, Z. Wang, W.W. Lu, W. Zhen, D. Yang, S. Peng, Novel biomaterial strategies for controlled growth factor delivery for biomedical applications, NPG Asia Mater. 9 (2017) e435–e435, doi:10.1038/am.2017.171.
[12] Z. Pan, H. Ye, D. Wu, Recent advances on polymeric hydrogels as wound dressings, APL Bioeng. 5 (2021) 011504, doi:10.1063/5.0038364.
[13] V. Brumberg, T. Astrelina, T. Malivanova, A. Samoilov, Modern wound dressings: hydrogel dressings, Biomedicines 9 (2021) 1235, doi:10.3390/biomedicines9091235.
[14] S. Schreml, R.M. Szeimies, L. Prantl, S. Karrer, M. Landthaler, P. Babilas, Oxygen in acute and chronic wound healing, Br. J. Dermatol. 163 (2010) 257–268, doi:10.1111/j.1365-2133.2010.09804.x.
[15] W.L. Yip, Influence of oxygen on wound healing, Int. Wound J. 12 (2014) 620–624, doi:10.1111/iwj.12324.
[16] H.M. Kimmel, A. Grant, J. Ditata, The presence of oxygen in wound healing, Wounds 28 (2016) 264–270.
[17] O. Al-Jalodi, M. Kupcella, K. Breisinger, T.E. Serena, A multicenter clinical trial evaluating the durability of diabetic foot ulcer healing in ulcers treated with topical oxygen and standard of care versus standard of care alone 1 year post healing, Int. Wound J. (2022), doi:10.1111/iwj.13789.
[18] D.L. Moreira DA Cruz, J. Oliveira-Pinto, A. Mansilha, The role of hyperbaric oxygen therapy in the treatment of diabetic foot ulcers: a systematic review with meta-analysis of randomized controlled trials on limb amputation and ulcer healing, Int. Angiol. 41 (2022) 63–73, doi:10.23736/S0392-9590.21.04722-2.
[19] D.-J. Lim, I. Jang, Oxygen-releasing composites: a promising approach in the management of diabetic foot ulcers, Polymers 13 (2021) 4131, doi:10.3390/polym13234131.
[20] J.S. Ortega, R. Corrales-Orovio, P. Ralph, J.T. Egaña, C. Gentile, Photosynthetic microorganisms for the oxygenation of advanced 3D bioprinted tissues, Acta Biomater. (2022) S1742-7061(22)00278–1, doi:10.1016/j.actbio.2022.05.009.
[21] Y. Qiao, F. Yang, T. Xie, Z. Du, D. Zhong, Y. Qi, Y. Li, W. Li, Z. Lu, J. Rao, Y. Sun, M. Zhou, Engineered algae: a novel oxygen-generating system for effective treatment of hypoxic cancer, Sci. Adv. 6 (2020) eaba5996, doi:10.1126/sciadv.aba5996.
[22] M. Huo, L. Wang, L. Zhang, C. Wei, Y. Chen, J. Shi, Photosynthetic tumor oxygenation by photosensitizer-containing cyanobacteria for enhanced photodynamic therapy, Angew. Chem. Int. Ed. Engl. 59 (2020) 1906–1913, doi:10.1002/anie.201912824.
[23] H. Wang, H. Liu, Y. Guo, W. Zai, X. Li, W. Xiong, X. Zhao, Y. Yao, Y. Hu, Z. Zou, J. Wu, Photosynthetic microorganisms coupled photodynamic therapy for enhanced antitumor immune effect, Bioact Mater. 12 (2022) 97–106, doi:10.1016/j.bioactmat.2021.10.028.
[24] M. Chang, W. Feng, L. Ding, H. Zhang, C. Dong, Y. Chen, J. Shi, Persistent luminescence phosphor as in-vivo light source for tumoral cyanobacterial photosynthetic oxygenation and photodynamic therapy, Bioact. Mater. 10 (2022) 131–144, doi:10.1016/j.bioactmat.2021.08.030.
[25] J. Wang, Q. Su, Q. Lv, B. Cai, X. Xiaohalati, G. Wang, Z. Wang, L. Wang, Oxygen-generating cyanobacteria powered by upconversion-nanoparticles-converted near-infrared light for ischemic stroke treatment, Nano Lett. 21 (2021) 4654–4665, doi:10.1021/acs.nanolett.1c00719.
[26] L.J. Voss, M. Plouviez, N. Whittle, Microalgae-based photosynthetic strategy for oxygenating avascularised mouse brain tissue – an in vitro proof of concept study, Brain Res. 1768 (2021) 147585, doi:10.1016/j.brainres.2021.147585.
[27] S. Özugur, M.N. Chávez, R. Sanchez-Gonzalez, L. Kunz, J. Nickelsen, H. Straka, Green oxygen power plants in the brain rescue neuronal activity, IScience 24 (2021) 103158, doi:10.1016/j.isci.2021.103158.
[28] J.E. Cohen, A.B. Goldstone, M.J. Paulsen, Y. Shudo, A.N. Steele, B.B. Edwards, J.B. Patel, J.W. MacArthur, M.S. Hopkins, C.E. Burnett, K.J. Jaatinen, A.D. Thakore, J.M. Farry, V.N. Truong, A.T. Bourdillon, L.M. Stapleton, A. Eskandari, A.S. Fairman, W. Hiesinger, T.V. Esipova, W.L. Patrick, K. Ji, J.A. Shizuru, Y.J. Woo, An innovative biologic system for photon-powered myocardium in the ischemic heart, Sci Adv. 3 (2017) e1603078, doi:10.1126/sciadv.1603078.
[29] V. Veloso-Giménez, R. Escamilla, D. Necuñir, R. Corrales-Orovio, S. Riveros, C. Marino, C. Ehrenfeld, C.D. Guzmán, M.P. Boric, R. Rebolledo, J.T. Egaña, Development of a novel perfusable solution for ex vivo preservation: towards photosynthetic oxygenation for organ transplantation, Front. Bioeng. Biotechnol. 9 (2021) 1287, doi:10.3389/fbioe.2021.796157.
[30] I. Yamaoka, T. Kikuchi, T. Arata, E. Kobayashi, Organ preservation using a photosynthetic solution, Transplant. Res. 1 (2012) 2, doi:10.1186/2047-1440-1-2.
[31] U. Hopfner, T.-L. Schenck, M.-N. Chávez, H.-G. Machens, A.-V. Bohne, J. Nickelsen, R.-E. Giunta, J.-T. Egaña, Development of photosynthetic biomaterials for in vitro tissue engineering, Acta Biomater. 10 (2014) 2712–2717, doi:10.1016/j.actbio.2013.12.055.
[32] T.L. Schenck, U. Hopfner, M.N. Chávez, H.-G. Machens, I. Somlai-Schweiger, R.E. Giunta, A.V. Bohne, J. Nickelsen, M.L. Allende, J.T. Egaña, Photosynthetic biomaterials: a pathway towards autotrophic tissue engineering, Acta Biomater. 15 (2015) 39–47, doi:10.1016/j.actbio.2014.12.012.
[33] H. Chen, Y. Cheng, J. Tian, P. Yang, X. Zhang, Y. Chen, Y. Hu, J. Wu, Dissolved oxygen from microalgae-gel patch promotes chronic wound healing in diabetes, Sci. Adv. 6 (2020) eaba4311, doi:10.1126/sciadv.aba4311.
[34] C. Centeno-Cerdas, M. Jarquín-Cordero, M.N. Chávez, U. Hopfner, C. Holmes, D. Schmauss, H.-G. Machens, J. Nickelsen, J.T. Egaña, Development of photosynthetic sutures for the local delivery of oxygen and recombinant growth factors in wounds, Acta Biomater. 81 (2018) 184–194, doi:10.1016/j.actbio.2018.09.060.
[35] X. Wang, C. Yang, Y. Yu, Y. Zhao, Situ 3D bioprinting living photosynthetic scaffolds for autotrophic wound healing, Research 2022 (2022), doi:10.34133/2022/9794745.
[36] M.N. Chávez, T.L. Schenck, U. Hopfner, C. Centeno-Cerdas, I. Somlai-Schweiger, C. Schwarz, H.-G. Machens, M. Heikenwalder, M.R. Bono, M.L. Allende, J. Nickelsen, J.T. Egaña, Towards autotrophic tissue engineering: photosynthetic gene therapy for regeneration, Biomaterials 75 (2016) 25–36, doi:10.1016/j.biomaterials.2015.10.014.
[37] M.L. Obaíd, J.P. Camacho, M. Brenet, R. Corrales-Orovio, F. Carvajal, X. Martorell, C. Werner, V. Simón, J. Varas, W. Calderón, C.D. Guzmán, M.R. Bono, S. San Martín, A. Eblen-Zajjur, J.T. Egaña, A first in human trial implanting microalgae shows safety of photosynthetic therapy for the effective treatment of full thickness skin wounds, Front. Med. 8 (2021) 2088, doi:10.3389/fmed.2021.772324.
[38] M.N. Chávez, B. Fuchs, N. Moellhoff, D. Hofmann, L. Zhang, T.T. Selão, R.E. Giunta, J.T. Egaña, J. Nickelsen, T.L. Schenck, Use of photosynthetic transgenic cyanobacteria to promote lymphangiogenesis in scaffolds for dermal regeneration, Acta Biomater. 126 (2021) 132–143, doi:10.1016/j.actbio.2021.03.033.
[39] J. Neupert, D. Karcher, R. Bock, Generation of Chlamydomonas strains that efficiently express nuclear transgenes, Plant J. 57 (2009) 1140–1150, doi:10.1111/j.1365-313X.2008.03746.x.

[40] E.H. Harris, Introduction to Chlamydomonas and its laboratory use, The Chlamydomonas Sourcebook, 2008.
[41] J. Schindelin, I. Arganda-Carreras, E. Frise, V. Kaynig, M. Longair, T. Pietzsch, S. Preibisch, C. Rueden, S. Saalfeld, B. Schmid, J.-Y. Tinevez, D.J. White, V. Hartenstein, K. Eliceiri, P. Tomancak, A. Cardona, Fiji: an open-source platform for biological-image analysis, Nat. Methods 9 (2012) 676–682, doi:10.1038/nmeth.2019.
[42] J.D. Barnes, L. Balaguer, E. Manrique, S. Elvira, A.W. Davison, A reappraisal of the use of DMSO for the extraction and determination of chlorophylls a and b in lichens and higher plants, Environ. Exp. Bot. 32 (1992) 85–100, doi:10.1016/0098-8472(92)90034-Y.
[43] T.-Y. Choi, T.-I. Choi, Y.-R. Lee, S.-K. Choe, C.-H. Kim, Zebrafish as an animal model for biomedical research, Exp. Mol. Med. 53 (2021) 310–317, doi:10.1038/s12276-021-00571-5.
[44] M. Alvarez, N. Reynaert, M. Chavez, G. Aedo, F. Araya, U. Hopfner, J. Fernández, M. Allende, J. Egaña, Generation of viable plant-vertebrate chimeras, PLoS One 10 (2015), doi:10.1371/journal.pone.0130295.
[45] G. Aedo, M. Miranda, M. Chavez, M. Allende, J. Egaña, A reliable preclinical model to study the impact of cigarette smoke in development and disease, Curr. Protocols Toxicol. 80 (2019), doi:10.1002/cptx.78.
[46] I.O. for StandardizationBiological Evaluation of Medical Devices, Part 10: Tests for Irritation and Skin Sensitization, ISO Geneva, Switzerland, 2010 ISO 10993-102010.
[47] M.K.A. Md, Z.S. Md, C.G. Md, O.E. Md, G.S. PhD, S.Ç. PhD, vitro potency and stability of fortified ophthalmic antibiotics, Aust. N. Zeal. J. Ophthalmol. 27 (1999) 426–430, doi:10.1046/j.1440-1606.1999.00239.x.
[48] A. Barbu, B. Neamtu, M. Zăhan, G.M. Iancu, C. Bacila, V. Mireşan, Current trends in advanced alginate-based wound dressings for chronic wounds, J. Personal. Med. 11 (2021) 890, doi:10.3390/jpm11090890.
[49] B.A. Aderibigbe, B. Buyana, Alginate in wound dressings, Pharmaceutics 10 (2018) 42, doi:10.3390/pharmaceutics10020042.
[50] A. Lode, F. Krujatz, S. Brüggemeier, M. Quade, K. Schütz, S. Knaack, J. Weber, T. Bley, M. Gelinsky, Green bioprinting: fabrication of photosynthetic algae-laden hydrogel scaffolds for biotechnological and medical applications, Eng. Life Sci. 15 (2015) 177–183, doi:10.1002/elsc.201400205.
[51] S. Maharjan, J. Alva, C. Cámara, A.G. Rubio, D. Hernández, C. Delavaux, E. Correa, M.D. Romo, D. Bonilla, M.L. Santiago, W. Li, F. Cheng, G. Ying, Y.S. Zhang, Symbiotic photosynthetic oxygenation within 3D-bioprinted vascularized tissues, Matter 4 (2021) 217–240, doi:10.1016/j.matt.2020.10.022.
[52] K.I. Draget, K. Østgaard, O. Smidsrød, Alginate-based solid media for plant tissue culture, Appl. Microbiol. Biotechnol. 31 (1989) 79–83, doi:10.1007/BF00252532.
[53] T.L. Schenck, U. Hopfner, M.N. Chávez, H.G. Machens, I. Somlai-Schweiger, R.E. Giunta, A.V. Bohne, J. Nickelsen, M.L. Allende, J.T. Egaña, Photosynthetic biomaterials: a pathway towards autotrophic tissue engineering, Acta Biomater. 15 (2015), doi:10.1016/j.actbio.2014.12.012.
[54] H. Lee, D. Shin, J. Choi, C.S. Ki, J. Hyun, Mimicry of the plant leaf with a living hydrogel sheet of cellulose nanofibers, Carbohydr. Polym. 290 (2022) 119485, doi:10.1016/j.carbpol.2022.119485.
[55] S. Malik, J. Hagopian, S. Mohite, C. Lintong, L. Stoffels, S. Giannakopoulos, R. Beckett, C. Leung, J. Ruiz, M. Cruz, B. Parker, Robotic extrusion of algae-laden hydrogels for large-scale applications, Glob Chall. 4 (2020) 1900064, doi:10.1002/gch2.201900064.
[56] L. Wang, X. Guo, J. Chen, Z. Zhen, B. Cao, W. Wan, Y. Dou, H. Pan, F. Xu, Z. Zhang, J. Wang, D. Li, Q. Guo, Q. Jiang, Y. Du, J. Yu, B.C. Heng, Q. Han, Z. Ge, Key considerations on the development of biodegradable biomaterials for clinical translation of medical devices: with cartilage repair products as an example, Bioact. Mater. 9 (2021) 332–342, doi:10.1016/j.bioactmat.2021.07.031.
[57] G. Lieschke, P. Currie, Animal models of human disease: zebrafish swim into view, Nat. Rev. Genet. (2007), doi:10.1038/nrg2091.
[58] B. Pelster, B. Bagatto, 7 - Respiration, in: S.F. Perry, M. Ekker, A.P. Farrell, C.J. Brauner (Eds.), Fish Physiology, Academic Press, 2010, pp. 289–309, doi:10.1016/S1546-5098(10)02907-9.
[59] A.R. Oropallo, T.E. Serena, D.G. Armstrong, M.Q. Niederauer, Molecular biomarkers of oxygen therapy in patients with diabetic foot ulcers, Biomolecules 11 (2021) 925, doi:10.3390/biom11070925.
[60] D. Wangpraseurt, S. You, F. Azam, G. Jacucci, O. Gaidarenko, M. Hildebrand, M. Kühl, A. Smith, M. Davey, A. Smith, D. Deheyn, S. Chen, S. Vignolini, Bionic 3D printed corals, Nat. Commun. 11 (2020) 1748, doi:10.1038/s41467-020-15486-4.
[61] K. Zhou, Y. Ma, M.S. Brogan, Chronic and non-healing wounds: the story of vascular endothelial growth factor, Med. Hypotheses 85 (2015) 399–404, doi:10.1016/j.mehy.2015.06.017.
[62] Q. He, Y. Zhao, B. Chen, Z. Xiao, J. Zhang, L. Chen, W. Chen, F. Deng, J. Dai, Improved cellularization and angiogenesis using collagen scaffolds chemically conjugated with vascular endothelial growth factor, Acta Biomater. 7 (2011) 1084–1093, doi:10.1016/j.actbio.2010.10.022.
[63] K.Y. Lee, M.C. Peters, K.W. Anderson, D.J. Mooney, Controlled growth factor release from synthetic extracellular matrices, Nature 408 (2000) 998–1000, doi:10.1038/35050141.
[64] H.W. Hopf, J.J. Gibson, A.P. Angeles, J.S. Constant, J.J. Feng, M.D. Rollins, M. Zamirul Hussain, T.K. Hunt, Hyperoxia and angiogenesis, Wound Repair Regen. 13 (2005) 558–564, doi:10.1111/j.1524-475X.2005.00078.x.
[65] National Center for Biotechnology InformationPubChem Compound Summary for CID 33255, Cefazolin, 2022 https://pubchem.ncbi.nlm.nih.gov/compound/Cefazolin.
[66] A. Sabu, P. Vijayaraghavan, R. Nair, F. Cheruvathoor, Effect of structural properties of hydrogel in controlled drug delivery, in: 2021: pp. 205–211. doi:10.1007/978-981-15-7138-1_11.
[67] Y. Zhu, J. Jung, S. Anilkumar, S. Ethiraj, S. Madira, N.A. Tran, D.M. Mullis, K.M. Casey, S.K. Walsh, C.J. Stark, A. Venkatesh, A. Boakye, H. Wang, Y.J. Woo, A novel photosynthetic biologic topical gel for enhanced localized hyperoxygenation augments wound healing in peripheral artery disease, Sci. Rep. 12 (2022) 10028, doi:10.1038/s41598-022-14085-1.

4. Paper II

Title	Development of a Hibernation-Inspired Preservation Strategy to Enhance the Clinical Translation of Photosynthetic Biomaterials**.**
Authors	Corrales-Orovio R, Castillo V, Rozas P, Schenck TL, Egaña JT.
Journal	Advanced Therapeutics
Year	2023
Volume	6
Issue	12
Pages	2300299
DOI	10.1002/adtp.202300299

Copyright notices

The following pages present a publication as originally published, reprinted with permission from the corresponding publisher. The copyright of the original publications is held by the respective copyright holders:

© 2023 John Wiley & Sons, Inc. Reprinted with permission. The original publication is available at: https://onlinelibrary.wiley.com/doi/10.1002/adtp.202300299.

Check for updates

RESEARCH ARTICLE

ADVANCED THERAPEUTICS
www.advtherap.com

Development of a Hibernation-Inspired Preservation Strategy to Enhance the Clinical Translation of Photosynthetic Biomaterials

*Rocío Corrales-Orovio, Valentina Castillo, Pablo Rozas, Thilo L. Schenck, and José Tomás Egaña**

Photosynthetic biomaterials have emerged as a promising approach for delivering oxygen and other bioactive molecules in several biomedical applications. This technology is based on the use of standard biomaterials loaded with photosynthetic cells for the controlled release of oxygen at the target site. However, as well as for other cell-based approaches, a main drawback for their clinical translation is the low shelf-life of living materials. Here, the potential of inducing a dormant hibernation-inspired state to preserve photosynthetic biomaterials for clinical applications is explored. First, a protocol to preserve microalgae *Chlamydomonas reinhardtii* is optimized and then applied to photosynthetic scaffolds, showing that the viability and functionality of the biomaterial is preserved for up to 6 weeks. To evaluate the clinical viability of this approach, both fresh and preserved photosynthetic scaffolds are implanted in a full-skin defect mouse model. The safety of this approach is evaluated and confirmed by several means, including clinical parameters, histological assays, and local and systemic molecular analysis. Altogether, for the first time the successful preservation of photosynthetic biomaterials through a hibernation-inspired strategy is described here, which could have a tremendous impact for the clinical translation of these materials as well as other photosynthetic therapies.

1. Introduction

One of the main limitations in the success of regenerative therapeutics is the lack of oxygenation of the wound site due to hypoxic conditions.[1] Molecular oxygen is known to be critical in wound healing, as it is required for angiogenesis, cell proliferation, extracellular matrix synthesis, |and bacterial defense.[2] Therefore, extensive efforts have been made in the development of new therapies that can provide oxygen to the wounds, either systemically or locally.[3] Systemic therapies, such as hyperbaric oxygen therapy, have shown inconsistent results to date and represent a complex and expensive clinical approach.[4] On the other hand, local oxygen therapies, including mechanical devices or oxygen delivering dressings, have shown to alleviate this problem by avoiding cell death and promoting cell proliferation as well as vascularization.[5,6]

In this context, the use of photosynthetic microorganisms has been proposed in order to increase local tissue oxygenation in wounds via photosynthetic oxygenation in situ upon light stimulation.[7,8] Compared to other approaches, photosynthetic microorganisms have the advantage of enabling constant production and delivery of oxygen in situ, with the ability to adjust oxygen levels based on the illumination settings. These photosynthetic therapies have gained increased attention in the last decade, and different biomaterials have been designed so far, including scaffolds,[9–13] topical hydrogels,[14–18] patches,[19] and sutures.[20] Several of these approaches have shown their biocompatibility in vitro and in vivo. Furthermore, an ongoing Phase I clinical trial (NCT03960164) has shown the safety of implanting photosynthetic scaffolds containing the microalgae *Chlamydomonas reinhardtii* in human full-thickness skin wounds.[21,22]

Although the use of photosynthetic biomaterials is promising and could have a tremendous impact in several fields of medicine, their potential use is currently highly limited by the intrinsic low half-life of the photosynthetic microorganisms in the materials, which require specific and strictly controlled culture and transport conditions to maintain their viability until clinical use. This limitation also applies to other living engineered constructs, such as fresh cellularized skin substitutes, which have shelf-lives of under 1 week,[23] limiting their applicability and commercialization. Consequently, the development of cryopreservation methods for human cells has been extensively

R. Corrales-Orovio, T. L. Schenck
Division of Hand
Plastic and Aesthetic Surgery
University Hospital
Ludwig Maximilian University of Munich
81377 Munich, Germany

V. Castillo, P. Rozas, J. T. Egaña
Institute for Biological and Medical Engineering
Schools of Engineering, Medicine and Biological Sciences
Pontificia Universidad Católica de Chile
Santiago 7820436, Chile
E-mail: jte@uc.cl

The ORCID identification number(s) for the author(s) of this article can be found under https://doi.org/10.1002/adtp.202300299

DOI: 10.1002/adtp.202300299

 © 2023 Wiley-VCH GmbH

23663987, 2023, 12, Downloaded from https://onlinelibrary.wiley.com/doi/10.1002/adtp.202300299 by Pontificia Universidad Catolic De Chile, Wiley Online Library on [12/12/2023]. See the Terms and Conditions (https://onlinelibrary.wiley.com/terms-and-conditions) on Wiley Online Library for rules of use; OA articles are governed by the applicable Creative Commons License

studied and implemented in the last decades,[24] facilitating the widespread adoption of different innovative translational approaches by enabling the preparation of larger quantities, advanced quality control, and longer shelf-lives, which ultimately result in more reliable, scalable, and cost-effective technologies.[25] Indeed, several Food and Drug Administration (FDA)-approved cellular scaffolds have implemented cryopreservation as a storage method to increase their shelf-life from days to months and even years.[26] However, cryopreservation methods involves the use of cryoprotective agents like dimethyl sulfoxide, which are highly toxic and need to be removed before cell or biomaterial use.[24]

In terms of microalgae preservation, several techniques have been described to date, which include cryopreservation, vitrification or lyophilization among others. However, these methods are not compatible with every microalgae strain, and many efforts have been made to stablish preservation methods for specific photosynthetic microorganisms.[27] Cryopreservation has been the preferred method for the long term storage of *C. reinhardtii*;[28,29] however, the use of chemical cryoprotectants and the need of freezing facilities highly limit their applicability in the biomedical field.

In contrast to human cells, photosynthetic microorganisms have evolved to inhabit most of the environments and ecosystems on Earth, relying on their own metabolic and molecular tools to survive to different environmental stresses.[30] Photosynthetic cells such as microalgae *C. reinhardtii* have the ability to enter a dormant or hibernation state under harsh environmental conditions, which include lack of light, nutrients, and low temperatures.[31,32] Previous studies have shown that immobilizing *C. reinhardtii* on a solid support enables the storage of these photosynthetic cells for extended periods of time.[33,34] However, no previous works have described a preservation method for photosynthetic biomaterials based on hibernation-inspired conditions. Therefore, in this work, a protocol for the preservation of photosynthetic biomaterials in a clinically compatible setting was established for the first time, based on hibernation conditions such cold temperatures, lack of nutrients and darkness. The functionality of the photosynthetic biomaterial was maintained in vitro and their safety in vivo was confirmed using a full-skin defect mouse model.

The strategy presented in this work enables to increase the operational timeframe of photosynthetic biomaterials without the need of toxic cryopreservation chemicals, therefore reducing their preservation complexity. Moreover, the described method has the potential to reduce manufacturing times and costs, enabling mass production, standardization, and significantly increasing the shelf-life and applicability of photosynthetic biomaterials in a clinical context. Altogether, these results provide a promising platform that could have a tremendous impact on the clinical translation of photosynthetic biomaterials.

2. Results

2.1. Preservation of Isolated Microalgae

Microalgae *C. reinhardtii* were isolated from their culture media and stored in darkness. The effect of temperature in the preservation process (room temperature, RT or 4 °C) was evaluated for up to 8 weeks (**Figure 1**). At different time points, cells were resuspended in media and allowed to recover for 72 h in the presence of light. The overall morphology of the microalgae was assessed by optical microscopy, showing a clear deterioration of cells stored at RT compared to those stored at 4 °C. The latter maintaining their characteristic round shape and green color even after 8 weeks of storage (Figure 1A). To quantify and compare the effect of the different preservation settings on cell morphology, the diameter of microalgae was evaluated by flow cytometry using calibrated beads (Figure 1B). The results showed a diameter of ≈8 µm before preservation (fresh), which remained constant throughout storage at 4 °C. However, for microalgae stored at RT, cell diameter was increased after 2 weeks of storage, while significantly decreased at week 4. At weeks 6 and 8, no microalgae could be detected and quantified. To determine the effect of preservation on the photosynthetic capacity of the cells, oxygen production was quantified (Figure 1C). At all measured times, results showed that the oxygen production rate was unaffected after storage at 4 °C, while from week 4 to 8, no production was detected in the group stored at RT. Similar results were obtained when evaluating the growth capacity of the preserved cells, as proliferation on agar plates could not be detected after preservation at RT for 4 to 8 weeks (Figure 1D). Finally, cell viability was quantified and compared by flow cytometry (Figure 1E). The results showed that the effect of temperature was not significant after 2 weeks of preservation. However, for the group preserved at RT, a significant reduction of about 60–70% was observed after 4 weeks, while no survival was detected at subsequent time points. On the other hand, when cells were preserved at 4 °C, no significant differences were detected among all the time points.

2.2. Preservation of Photosynthetic Scaffolds

After demonstrating that isolated *C. reinhardtii* can be preserved through a hibernation-inspired strategy, photosynthetic scaffolds were prepared as described in the Experimental Section and subjected to the same hibernation-inspired protocol. Scaffolds' structure and composition were analyzed at different preservation time points for up to 8 weeks (**Figure 2**). A macroscopic evaluation of the preserved scaffolds did not show overall differences compared to freshly prepared scaffolds. The characteristic green color of the microalgae and its distribution within the scaffold remained unaffected for up to 6 weeks. However, a reduction in color intensity was consistently observed after 8 weeks of preservation (Figure 2A). To better study this phenomenon, fluorescent microscopy was performed to visualize the autofluorescence of collagen and chlorophyll, thereby examining the interaction between the scaffold and microalgae (Figure 2B). Results showed that the overall structure of the scaffold appeared to be unaffected by the hibernation-inspired process, as no obvious differences in the density and distribution of the collagen sheets were observed. As for the microalgae, chlorophyll was detected throughout the analyzed times, exhibiting the characteristic shape of the *C. reinhardtii* chloroplast. Since the microalgae were seeded and attached to the scaffolds with fibrin, scanning electron microscopy (SEM) imaging was performed to observe the microstructure and integrity of all components within the preserved scaffolds (Figure 2C). The SEM images of fresh and

 © 2023 Wiley-VCH GmbH

ADVANCED SCIENCE NEWS
www.advancedsciencenews.com

ADVANCED THERAPEUTICS
www.advtherap.com

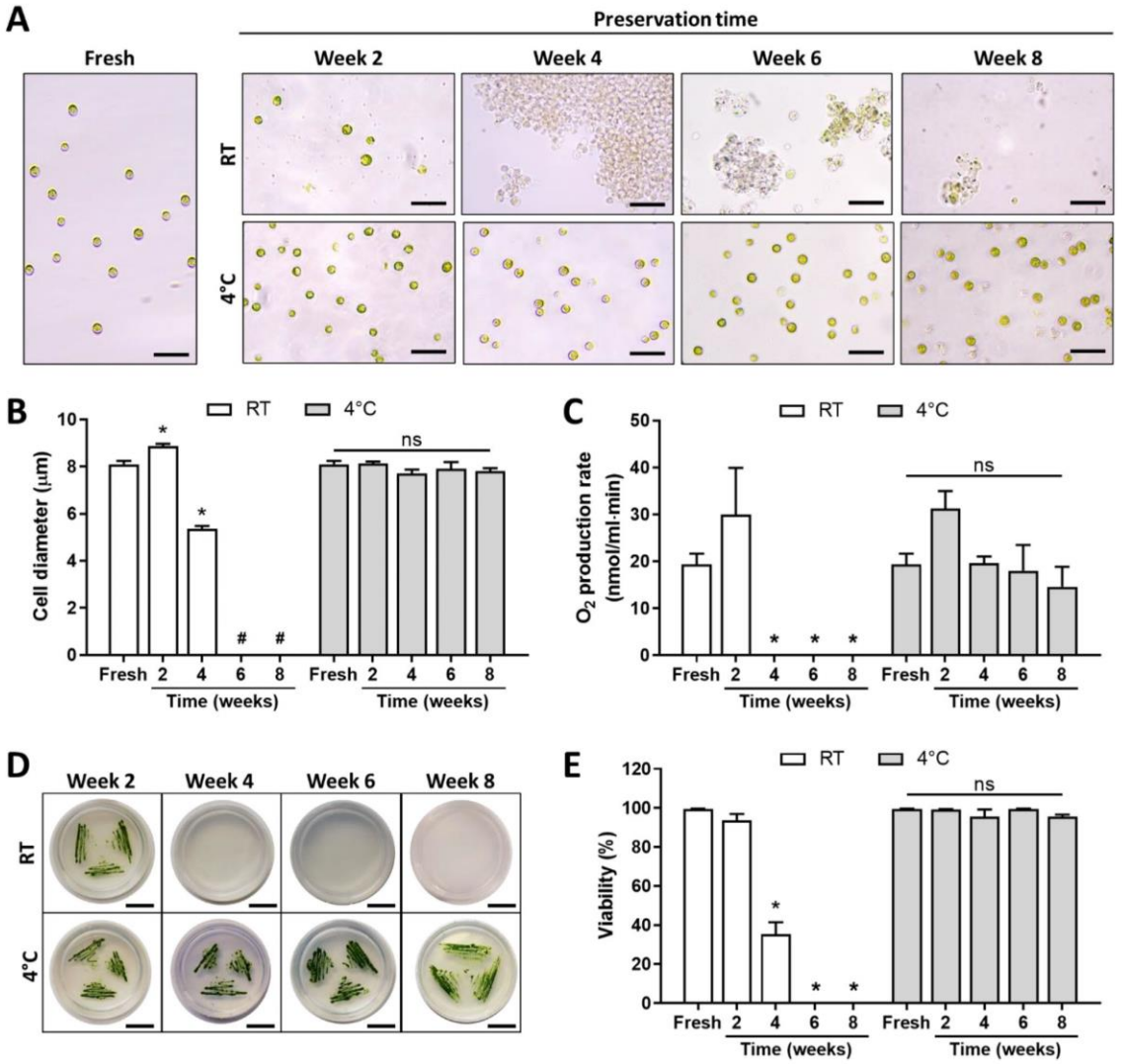

Figure 1. Preservation of microalgae *C. reinhardtii*. Microalgae were stored either at 4 °C or RT, in darkness for up to 8 weeks, and then recovered during 72 h of light exposure at RT. A) Overall appearance and morphology of the microalgae is shown after preservation and compared to fresh microalgae. B) Cell diameter was quantified by flow cytometry before and after preservation at RT or 4 °C. C) Metabolic activity or photosynthetic oxygen production of the microalgae is shown before (fresh) and after preservation at RT or 4 °C. D) Microalgae growth capacity in agar plates after inoculation of preserved microalgae is shown. E) Assessment of microalgae viability after preservation at RT or 4 °C was also assessed by flow cytometry. Scale bars in (A) and (D) represent 50 µm and 1 cm, respectively. Data are expressed as mean + SEM; $N = 3$; number signs (#) indicate no value for that time point due to absence of chlorophyll positive cells; asterisks (*) indicate significant differences compared to fresh microalgae with $p < 0.05$; ns: nonsignificant (one-way ANOVA, Tukey's posteriori comparison).

preserved scaffolds clearly showed microalgae surrounded by fibrin fibers distributed in the pores of the collagen scaffold. However, at week 8, fibrin fibers were scarce within the scaffold.

After evaluating the effect of the preservation on the overall morphology and structure of photosynthetic scaffolds, other key features related to their functionality were assessed. The impact of preservation on the chlorophyll content was first examined (**Figure 3**A) and the results showed that the chlorophyll content remained stable for up to 6 weeks after hibernation-inspired preservation of the scaffolds. However, a significant decrease was observed after 8 weeks. Then, the photosynthetic capacity of the microalgae was evaluated by quantifying the oxygen production rate of the scaffold upon illumination (Figure 3B). The results showed that the photosynthetic capacity was maintained

© 2023 Wiley-VCH GmbH

23663987, 2023, 12, Downloaded from https://onlinelibrary.wiley.com/doi/10.1002/adtp.202300299 by Pontificia Universidad Catolic De Chile, Wiley Online Library on [12/12/2023]. See the Terms and Conditions (https://onlinelibrary.wiley.com/terms-and-conditions) on Wiley Online Library for rules of use; OA articles are governed by the applicable Creative Commons License

ADVANCED SCIENCE NEWS
www.advancedsciencenews.com

ADVANCED THERAPEUTICS
www.advtherap.com

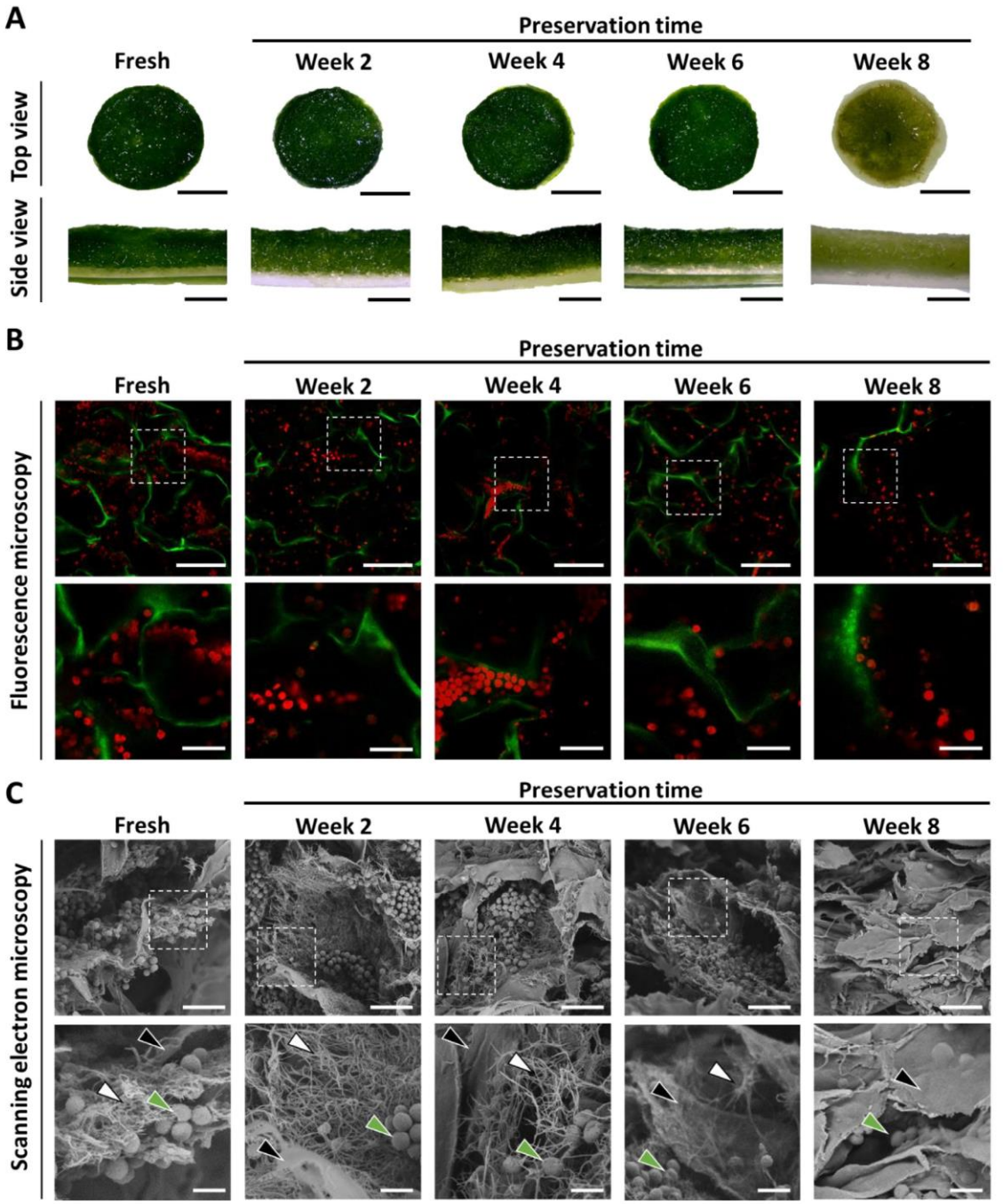

Figure 2. Morphology and structure of preserved photosynthetic scaffolds. Photosynthetic scaffolds were preserved for up to 8 weeks at 4 °C. A) Macroscopic imaging from the top and side view of the scaffolds. B) Scaffolds were analyzed by fluorescence microscopy, where microalgae and collagen autofluorescence are observed in red and green, respectively. C) SEM images were obtained to observe microalgae (green arrows), collagen sheets (black arrows), and fibrin fibers (white arrows). Dotted-line boxes in (B) and (C) indicate magnified areas shown below. Scale bars represent A) 5 mm, B, upper) 100 µm, B, lower) 25 µm, C, upper) 20 µm, C, lower) and 5 µm.

© 2023 Wiley-VCH GmbH

23663987, 2023, 12, Downloaded from https://onlinelibrary.wiley.com/doi/10.1002/adtp.202300299 by Pontificia Universidad Catolic De Chile, Wiley Online Library on [12/12/2023]. See the Terms and Conditions (https://onlinelibrary.wiley.com/terms-and-conditions) on Wiley Online Library for rules of use; OA articles are governed by the applicable Creative Commons License

ADVANCED SCIENCE NEWS
www.advancedsciencenews.com

ADVANCED THERAPEUTICS
www.advtherap.com

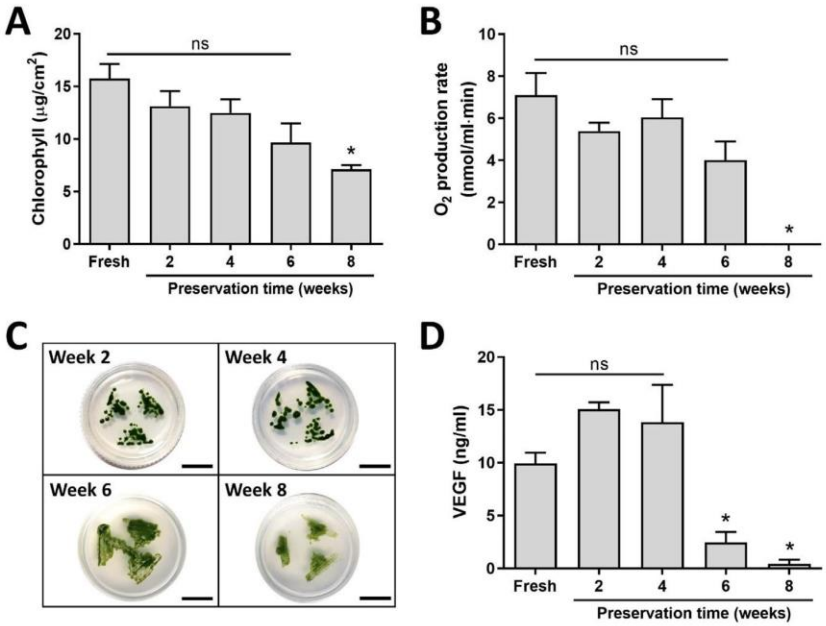

Figure 3. Functional characterization of preserved photosynthetic scaffolds. Photosynthetic scaffolds were stored for up to 8 weeks at 4 °C. A) Chlorophyll content of photosynthetic scaffolds was quantified before and after preservation. B) Oxygen production of the photosynthetic scaffolds was also studied before and after preservation. C) Growth capacity of microalgae in photosynthetic scaffolds after preservation was assessed by agar plating and imaged after 7 d. D) Production of VEGF from preserved photosynthetic scaffolds fabricated with genetically modified microalgae expressing recombinant VEGF was assessed and compared to freshly prepared scaffolds. Scale bars in (C) indicate 1 cm. Data are expressed as mean + SEM; A,B) $N = 4$ and D) $N = 3$; asterisks (*) indicate significant differences compared to fresh photosynthetic scaffolds with $p < 0.05$; ns: nonsignificant (one-way ANOVA, Tukey's posteriori comparison).

for up to 6 weeks, but no oxygen production was detected after 8 weeks of scaffold preservation. Additionally, the proliferation capacity of the microalgae was studied and it was found that cells were able to grow on agar plates at all the measured time points (Figure 3C). Finally, photosynthetic scaffolds were seeded with genetically modified microalgae, and the release of recombinant vascular endothelial growth factor (VEGF) after preservation was examined (Figure 3D), showing a stable release after 2 and 4 weeks of preservation, but a significant decrease after 6 and 8 weeks.

2.3. Safety of Preserved Photosynthetic Scaffolds In Vivo

As the safety of this preservation approach is crucial for its clinical translation, hibernation-inspired preserved photosynthetic scaffolds (P-PS) were implanted in a bilateral full-skin defects mouse model. Control scaffolds without microalgae (CS) and freshly prepared photosynthetic scaffolds (F-PS) were also implanted and several parameters were studied and compared. Over the course of the following 10 d, animals were closely monitored and weight, temperature, and overall health were daily measured (**Figure 4**). After surgery, all groups of animals showed a temporary decrease in weight, which was rapidly recovered in the following days (Figure 4A). Normal temperatures were observed at all time points; however, differences were observed at day 3 between groups implanted with control and fresh photosynthetic scaffolds (Figure 4B). The health score was calculated as described in the Experimental Section, where a score of 15 represented the humanitarian endpoint for the experiment. Animals showed a slight increase in health score during the initial days after surgery, but decreased to 0 in all groups before the end of the experiment. Statistical difference was observed between groups receiving fresh and preserved photosynthetic scaffolds at day 3; however, health score was low for both groups (Figure 4C). On day 10, animals were imaged to evaluate the general appearance of the wounds (Figure 4D). The results indicated that in all groups, scaffolds adhered to the wound bed without any signs of local inflammation, infection, or contraction. Furthermore, both fresh and hibernation-inspired preserved photosynthetic scaffolds maintained their original green color and no macroscopic differences could be observed between these groups.

On day 10 postimplantation, animals were euthanized and the presence of viable microalgae in the photosynthetic scaffolds (either fresh or preserved) was evaluated (**Figure 5**). Optical microscopy showed that microalgae in both groups appeared intact, exhibiting their characteristic green color and round shape (Figure 5A). To assess the viability of these microalgae, the presence of mRNA from the RuBisCO large subunit (RBCL) was assessed by reverse transcription polymerase chain reaction (RT-PCR;Figure 5B). RuBisCO mRNA was found in seven out of eight samples of the photosynthetic scaffold group, and in all samples

 © 2023 Wiley-VCH GmbH

23663987, 2023, 12, Downloaded from https://onlinelibrary.wiley.com/doi/10.1002/adtp.202300299 by Pontificia Universidad Catolic De Chile, Wiley Online Library on [12/12/2023]. See the Terms and Conditions (https://onlinelibrary.wiley.com/terms-and-conditions) on Wiley Online Library for rules of use; OA articles are governed by the applicable Creative Commons License

ADVANCED SCIENCE NEWS
www.advancedsciencenews.com

ADVANCED THERAPEUTICS
www.advtherap.com

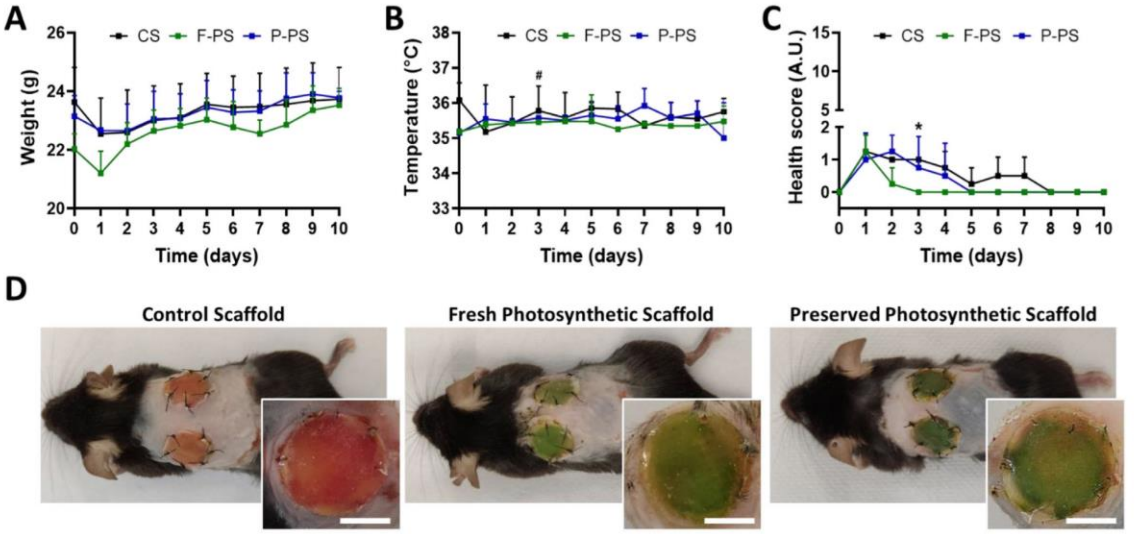

Figure 4. Scaffold implantation in full-skin defect in vivo. Control, fresh photosynthetic, and hibernated photosynthetic scaffolds (CS, F-PS, and P-PS respectively) were implanted on mice full-skin defects and animals were monitored for 10 d. A) Body weight, B) body temperature, and C) health scores were monitored daily to assess overall mice wellness. D) General aspect of mice and implanted scaffolds after 10 d is shown. Data in (A)–(C) are expressed as mean + SD; $N = 4$; number signs (#) and asterisks (*) indicate differences between F-PS and P-PS groups and between CS and F-PS groups respectively, with $p < 0.05$ (two-way ANOVA, Tukey's posteriori comparison). Scale bars in (D) represent 5 mm.

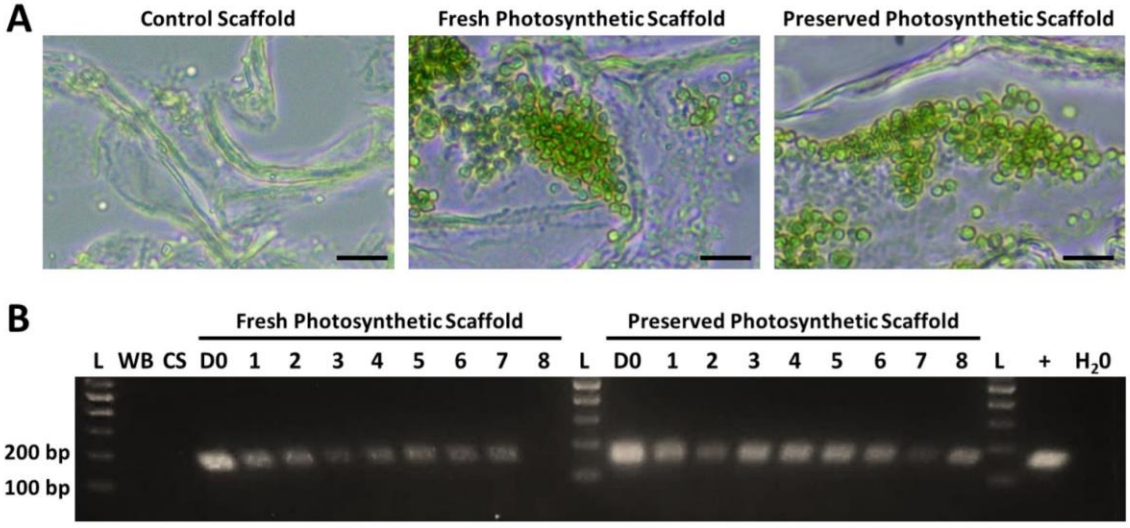

Figure 5. Microalgae presence and viability after scaffold implantation. A) After scaffold removal at 10 d post implantation, optical microscopy of control, fresh and preserved photosynthetic scaffolds (PS) was performed to evaluate the presence of microalgae. B) Microalgae viability was assessed by RT-PCR testing RBCL mRNA expression (154 bp) at 10 d after implantation. Abbreviations: L, ladder; WB, wound bed before scaffold implantation; CS, control scaffold after 10 d of implantation; D0, scaffolds at day 0 before implantation; 1–8, individual scaffolds after 10 d of implantation on mice; +, positive *C. reinhardtii* control. Scale bars in (A) represent 25 µm.

© 2023 Wiley-VCH GmbH

23663987, 2023, 12, Downloaded from https://onlinelibrary.wiley.com/doi/10.1002/adtp.202300299 by Pontificia Universidad Catolica De Chile, Wiley Online Library on [12/12/2023]. See the Terms and Conditions (https://onlinelibrary.wiley.com/terms-and-conditions) on Wiley Online Library for rules of use; OA articles are governed by the applicable Creative Commons License

ADVANCED SCIENCE NEWS
www.advancedsciencenews.com

ADVANCED THERAPEUTICS
www.advtherap.com

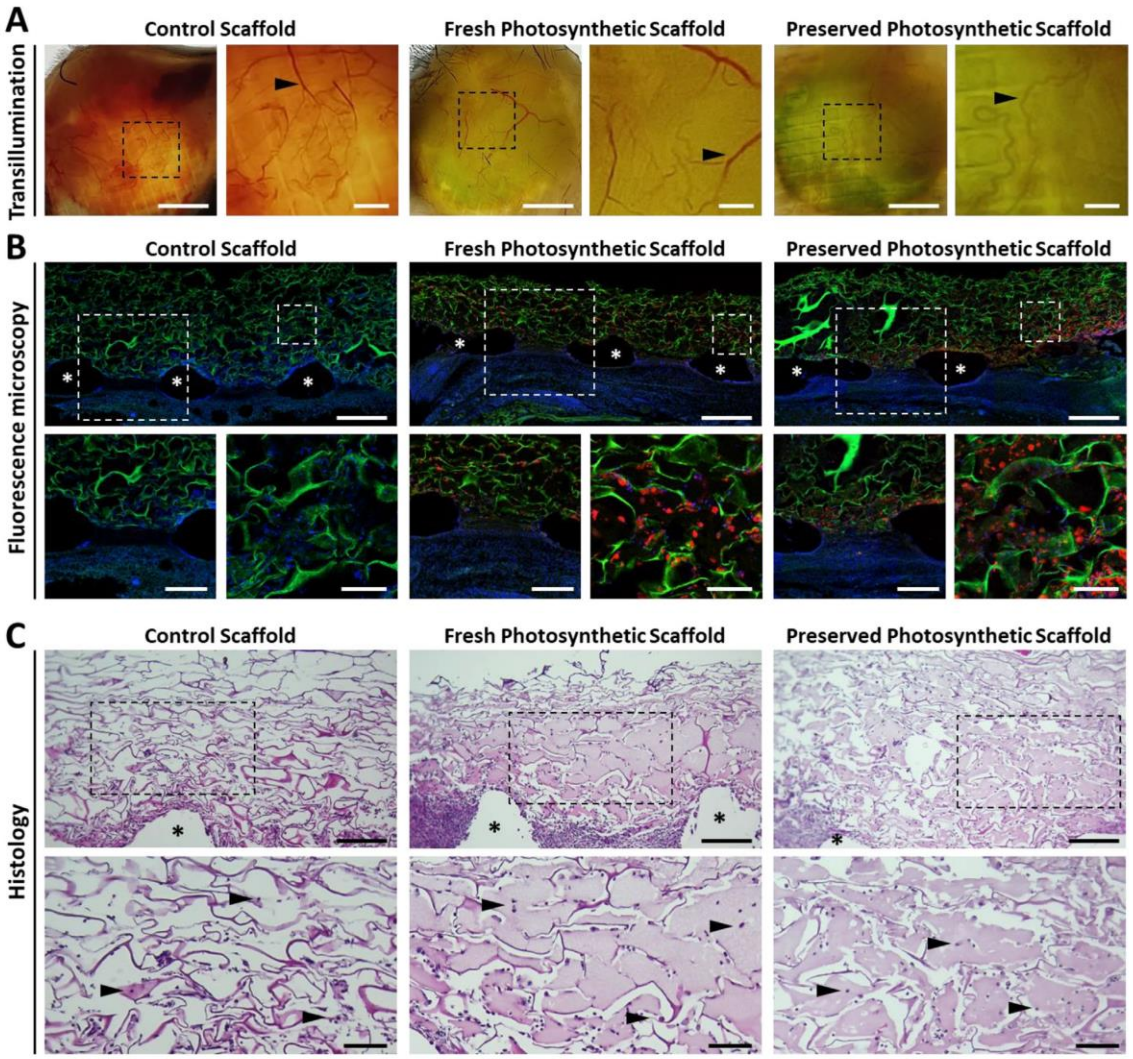

Figure 6. Macro and microscopic analysis of scaffolds after 10 d of implantation. A) Control scaffolds and fresh and preserved photosynthetic scaffolds were excised after 10 d and macroscopically imaged using a transilluminator to evaluate the presence of vascular structures. B) Scaffolds were stained with Hoechst 33342 nuclear staining and visualized by fluorescence microscopy. Collagen from the scaffold (green autofluorescence), microalgae (red autofluorescence) and mice cell nuclei (blue) can be observed. C) Scaffolds were evaluated histologically by hematoxylin and eosin staining. Black arrows in (A) and (C) indicate vascular structures and cell nuclei, respectively. Asterisks (*) in (B) and (C) indicate titanized mesh used between the scaffold and the wound bed. Dotted-line boxes indicate magnified areas. Scale bars represent A, left images) 2.5 mm, A, right magnified areas; B, upper) 500 µm, B, lower left magnified areas; C, upper) 250 µm, and B, lower right magnified areas; C, lower) 100 µm.

from the group which received preserved photosynthetic scaffolds.

Once the presence of viable microalgae was confirmed in both the fresh and preserved photosynthetic scaffolds, it was important to assess the local interaction between the photosynthetic microorganisms and host tissue (**Figure 6**). For this purpose, the scaffolds were harvested and imaged using a transilluminator. Except for the color, no main differences were observed among groups and newly formed vessels were observed in all individuals (Figure 6A). Subsequently, scaffolds were fixed and processed as described in the Experimental Section. Cryosections of the scaffolds were stained and examined using fluorescence microscopy to visualize the infiltrating cells (Figure 6B) and images showed proper biomaterial integration and cellular infiltration in all groups. Furthermore, in both fresh and preserved photosynthetic groups, microalgae were found throughout the entire scaffold, showing colocalization with the host cells. To further study in more detail scaffold composition

 © 2023 Wiley-VCH GmbH

23663987, 2023, 12, Downloaded from https://onlinelibrary.wiley.com/doi/10.1002/adtp.202300299 by Pontificia Universidad Catolic De Chile, Wiley Online Library on [12/12/2023]. See the Terms and Conditions (https://onlinelibrary.wiley.com/terms-and-conditions) on Wiley Online Library for rules of use; OA articles are governed by the applicable Creative Commons License

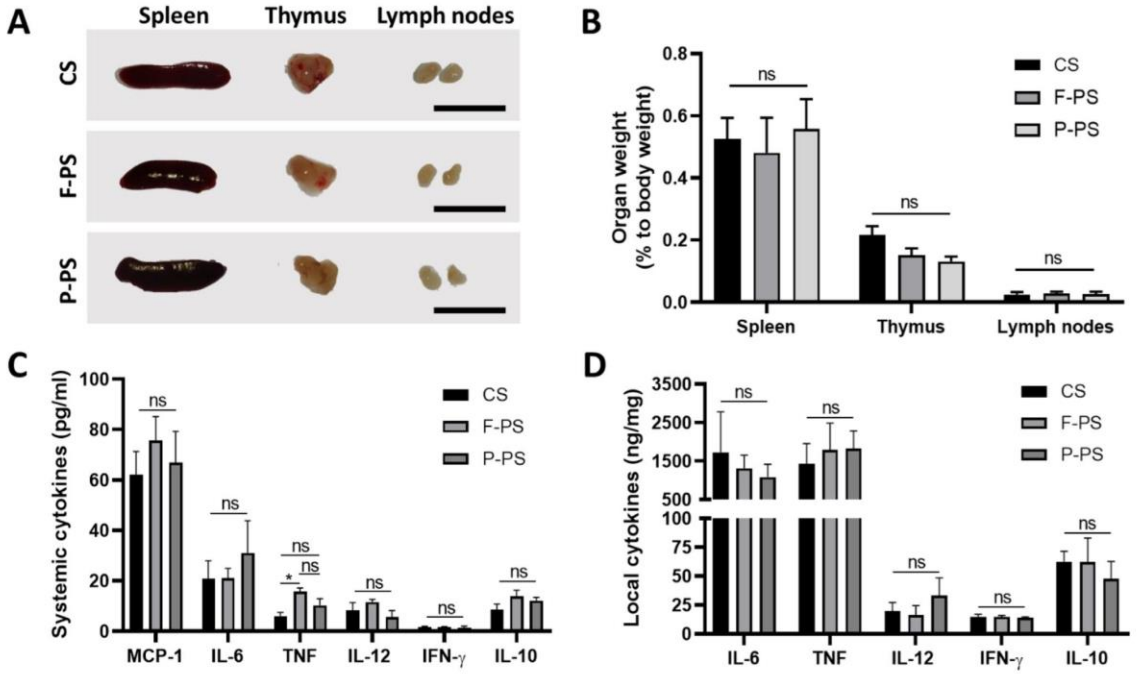

Figure 7. Inflammatory response of mice after scaffold implantation. A) After euthanasia at day 10, lymphatic organs (spleen, thymus, and lymph nodes) were recovered from animals that received control scaffold (CS), fresh photosynthetic scaffolds (F-PS), or preserved photosynthetic scaffolds (P-PS). B) Organ weight relative to total animal body weight was calculated. C) Systemic and D) local inflammatory cytokines were quantified from serum and tissue samples by flow cytometry, respectively. Scale bars in (A) represent 1 cm. Data are expressed as mean + SEM; B,C) $N = 4$, D) $N = 8$; ns: nonsignificant (one-way ANOVA, Tukey's posteriori comparison).

and appearance after implantation, hematoxylin and eosin staining was performed (Figure 6C). Compared to the control group, the presence of fibrin used to encapsulate the microalgae in the scaffolds was clearly observed in the sections obtained from the photosynthetic scaffolds. The images showed that the overall appearance and density of collagen were similar across the different groups. Collagen fibers and fibrin did not exhibit any clear differences after hibernation-inspired preservation when compared to nonpreserved fresh photosynthetic group. Additionally, in accordance with fluorescence microscopy data, infiltration of cells from native tissue was detected throughout the scaffolds in all groups.

To evaluate the potential effects of scaffold preservation on inflammation, both systemic and local parameters were examined (**Figure 7**). In order to assess systemic inflammation, lymphatic organs and blood were extracted. When comparing the spleen, thymus and lymphatic nodes among groups, no macroscopic differences were observed in terms of size, structure, and color (Figure 7A). The organs were weighted and normalized to the body weight of the corresponding mice and no statistical differences were found among the groups (Figure 7B). Systemic inflammatory cytokines, including monocyte chemoattractant protein 1 (MCP-1), interferon γ (IFN-γ), tumor necrosis factor (TNF) and interleukin (IL) 6, 10 and 12, were quantified in the blood serum by flow cytometry (Figure 7C). TNF showed a slight increase in animals implanted with fresh photosynthetic scaffolds, while the rest of the measured cytokines showed no significant differences between the groups. Similarly, the inflammatory cytokines (IL-6, TNF, IL-12, INF-γ, and IL-10) present in the scaffolds were quantified and no significant differences were observed among the groups (Figure 7D).

3. Discussion

While photosynthetic biomaterials offer a promising platform for the local production and delivery of oxygen in tissues,[7] their potential clinical impact is currently limited due to the lack of preservation protocols. Therefore, this study aimed to investigate the possibility of extending the shelf-life of these biomaterials by inducing microalgae to enter a dormant state through a hibernation like-protocol, obtaining a more reliable, scalable, and cost-effective technology.

C. reinhardtii are known to reduce their metabolic activity under harsh conditions, such as low temperatures, lack of nitrogen and darkness.[31,32] Hence, the impact of these factors on the preservation of the microalgae was studied here. Previous works have described the possibility of storing *Chlamydomonas* for extended periods by placing the microalgae on solid cotton support.[34] These studies reported a loss in the photosynthetic potential of algae after storage in the dark at either RT or 4 °C, which was subsequently recovered after several days in standard culture conditions. Contrarily to the aforementioned findings,

© 2023 Wiley-VCH GmbH

23663987, 2023, 12, Downloaded from https://onlinelibrary.wiley.com/doi/10.1002/adtp.202300299 by Pontificia Universidad Catolic De Chile, Wiley Online Library on [12/12/2023]. See the Terms and Conditions (https://onlinelibrary.wiley.com/terms-and-conditions) on Wiley Online Library for rules of use; OA articles are governed by the applicable Creative Commons License

23663987, 2023, 12, Downloaded from https://onlinelibrary.wiley.com/doi/10.1002/adtp.202300299 by Pontificia Universidad Catolic De Chile, Wiley Online Library on [12/12/2023]. See the Terms and Conditions (https://onlinelibrary.wiley.com/terms-and-conditions) on Wiley Online Library for rules of use; OA articles are governed by the applicable Creative Commons License

the results presented here showed that effective storage of isolated microalgae *C. reinhardtii* was strongly dependent on the preservation temperature, as cell integrity and functionality were completely lost after storage at RT, but maintained for at least 8 weeks at 4 °C. Therefore, a storage temperature of 4 °C was chosen to set up a hibernation-inspired protocol for the preservation of photosynthetic biomaterials.

A previously described photosynthetic biomaterial was chosen for this study due to its in vitro and in vivo validations,[10,12] as well as its ongoing evaluation in a human phase I clinical trial.[21,22] This biomaterial is composed of a collagen-glycosaminoglycan matrix, fibrin glue, and *C. reinhardtii* as a photosynthetic oxygen generator. This microalga has been used as model for studying cold stress adaptation in plants,[32] and abundant literature describes changes in cell proliferation,[35] oxidative status,[36] and photosynthetic rate[33,37] induced by low temperatures, which can be potentially recovered after restoring optimal culture conditions.[32] Therefore, it represents a good candidate for hibernation-inspired protocols aiming to preserve photosynthetic capabilities of the biomaterials.

Interestingly, the results obtained in this work showed that microalgae seeded on the collagen-based scaffolds maintained their growth capacity for at least 8 weeks and their oxygen-producing capacity for up to 6 weeks of preservation, which is shorter compared to isolated microalgae that maintained functionality for at least 8 weeks. Although more studies should be performed to fully address this point, this could be explained by the higher density of cells in the pellets compared to the scaffolds, which has been previously shown to play a key role in protecting other microorganisms from environmental stress.[38] Moreover, the formation of multicellular structures such as palmelloids or aggregates are highly described as a strategy used by *Chlamydomonas* to survive environmental stress.[39] However, the fact that cells within the photosynthetic scaffolds are trapped in a fibrin matrix may be negatively affecting this survival strategy. Additionally, besides oxygen, the preservation protocol described here allowed for the maintenance of the biomaterial's capacity to release recombinant growth factors for up to 4 weeks of storage. As photosynthesis and protein synthesis and secretion rely on different cell mechanisms, this result may hint that storage of microalgae under harsh conditions causes specific effects among different cellular structures, affecting diverse signaling pathways. Moreover, it has been broadly described that the expression of recombinant proteins in certain microorganisms induces high metabolic stress for the cells.[40] Therefore, additional cold stress might have caused a reduction in protein yield to optimize the essential metabolic pathways.

It has been described that in response to certain environmental stressors, some microalgae produce harmful compounds such as microcystins and saxitoxins.[41,42] In the case of *C. reinhardtii*, some effects of cold exposure are unknown and remain to be elucidated.[32] However, many others have already been described. These effects include the secretion of specific proteins (such as cold-shock proteins), changes in the cell membrane, and overaccumulation of oxygen species, among others.[35,37] Due to the potential implications of these factors in the clinical translation of this preservation approach, one of the main objectives of this work was to evaluate the safety of hibernation-inspired preserved photosynthetic biomaterials in vivo.

After implanting the photosynthetic scaffolds (both freshly prepared and preserved) in an already established full-skin wound model,[10,12,43] high biocompatibility was observed between the biomaterials and mice, as no overall changes in the health of the animal and viability of the microalgae were detected. These observations agree with previous work implanting fresh photosynthetic scaffolds,[12] suggesting that preserved biomaterials through a hibernation-inspired strategy can produce and deliver oxygen to tissues for at least 10 d as well. Moreover, the proper interaction between preserved microalgae and the host tissue was confirmed by histology, and similar cell migration levels were observed in both of the implanted photosynthetic biomaterials, showing colocalization of microalgae and autologous cells within the regenerating tissue. Additionally, a more in-depth study of the local and systemic effects of the implanted mice supports the conclusion that no toxic stress-related proteins or compounds were present in the preserved scaffold, as no differences were observed in the immune organs of animals or the levels of local inflammatory cytokines. Regarding systemic inflammatory cytokines, no differences were observed among them, except for TNF, which presented increased values in animals implanted with fresh photosynthetic scaffolds. However, the values obtained lay within the normal ranges of TNF plasma levels in C57BL/6 mice.[44,45] This agrees with previous studies showing that certain fresh microalga and cyanobacteria can be safely delivered or implanted into mice,[11,12,46] and even humans.[21] However, such a similar response for preserved photosynthetic biomaterials had never been described before.

As scaffold integrity and its further biodegradation are essential for tissue repair,[47] these aspects were also investigated in vitro and in vivo and no differences could be observed among the analyzed groups. This is important not only for the clinical translation of the approach but also because it shows that when *C. reinhardtii* are subjected to different stresses, they do not modify their microenvironment in a clinically relevant manner, emphasizing the short-term potential applicability of this preservation platform in a clinical context.

While this protocol has been validated in a specific photosynthetic scaffold that is already being tested in human patients,[21] this technology could be adapted to different photosynthetic biomaterials, such as perfusable photosynthetic solutions,[48] sutures,[20] patches,[19] or hydrogels.[11,14,15] Therefore, a broader validation should be conducted, where different photosynthetic microorganisms that have also shown to be promising for photosynthetic therapies could be evaluated.[49] Additionally, since there are several differences between skin structure and physiology between mice and humans,[50] the preservation approach described here should be further validated in a phase I clinical trial before its implementation.

Altogether, the results presented here describe a simple and cost-effective approach to significantly enhance the shelf-life of photosynthetic biomaterials. Despite the fact that cryopreservation protocols using cryoprotective agents have been described for the storage of microalgae,[28,29] the presented work enables to increase the operational window of photosynthetic biomaterials without the need of additional reagents, which are known to be toxic and therefore have to be removed before biomaterial use. This work optimizes the overall photosynthetic biomaterial fabrication process, allowing the standardization, mass

 © 2023 Wiley-VCH GmbH

ADVANCED SCIENCE NEWS
www.advancedsciencenews.com

ADVANCED THERAPEUTICS
www.advtherap.com

23663987, 2023, 12, Downloaded from https://onlinelibrary.wiley.com/doi/10.1002/adtp.202300299 by Pontificia Universidad Catolic De Chile, Wiley Online Library on [12/12/2023]. See the Terms and Conditions (https://onlinelibrary.wiley.com/terms-and-conditions) on Wiley Online Library for rules of use; OA articles are governed by the applicable Creative Commons License

production, and transport of these biomaterials, thereby supporting the worldwide implementation of photosynthetic therapies in clinics.

4. Experimental Section

Microalgae Culture: Cell-wall deficient UVM4 *C. reinhardtii* strain[51] was grown photomixotrophically at 24 °C in sterile liquid tris-acetate-phosphate medium (TAP) with constant agitation and kept always in the exponential growth phase and constant illumination (30 μE m^{-2} s^{-1}). A genetically modified *C. reinhardtii* UVM4 human-VEGF producing strain was used only for growth factor release assay[12] and cultured as described above.

Photosynthetic Scaffold Fabrication: Photosynthetic scaffolds were fabricated as previously described.[10,21] Briefly, biopsy punches of Integra matrix (Integra Life Science Corporation) were cut and slightly dried on a sterile gauze. For 1 cm^2 scaffolds, 5×10^6 microalgae were resuspended in 68 μL of TAP medium mixed with human fibrinogen (EVICEL, Johnson and Johnson) in a 1:1 ratio. UVM4 *C. reinhardtii* strain were used for all in vitro and in vivo experiments, except for growth factor release assay, where a genetically modified *C. reinhardtii* UVM4 human-VEGF producing strain was used. The mixture of microalgae and fibrin was seeded in the scaffolds, followed by the addition of 34 μL of human thrombin (EVICEL, Johnson and Johnson). In order to ensure fibrinogen conversion to fibrin, scaffolds were left undisturbed for 1 h, and further covered with sterile TAP medium. Photosynthetic scaffolds were cultured under constant illumination for 72 h until use.

Microalgae and Photosynthetic Scaffold Preservation: Microalgae were maintained in exponential growth phase. Cells were counted and adjusted to a final concentration of 10^7 microalgae mL^{-1}. Next, microalgae suspensions of 10^7 cells were centrifuged at 2000 rpm for 5 min. The supernatant was discarded and microalgae were washed by adding 1 mL of TAP medium, resuspending, and centrifuging. The supernatant was discarded and tubes containing pellets of 10^7 microalgae cells were stored either at RT (24 °C) or 4 °C, protected from direct light for up to 8 weeks. At each specific time point (2, 4, 6, or 8 weeks), microalgae were "woken up" by adding 1 mL of TAP per tube (at the same storage temperature, RT, or 4 °C), gently resuspending, and incubating them at RT with constant illumination for 72 h.

For the preservation of the photosynthetic scaffolds, these were prepared as described above. After 72 h of culture with TAP medium and constant light exposure, scaffolds were placed in 1.5 mL tubes without TAP, and stored at 4 °C, protected from direct light for up to 8 weeks. At each specific time point (2, 4, 6, and 8 weeks), scaffolds were placed on 35 mm plates and were "woken up" by adding 3 mL of TAP per plate and incubating them at RT with constant illumination for 72 h. For in vivo experiments, scaffolds were preserved for 5 weeks, and "woken up" as described before implantation.

In Vitro Microalgae Viability Assays: Several assays were performed to assess microalgae viability, depending on the sample. For microalgae in suspension or for photosynthetic scaffolds in vitro, viability was determined by examining microalgae growth after 7 d of inoculation in agar plates. Additionally, as viability probe of microalgae in suspension, *C. reinhardtii* were incubated for 1 h with 25 μM of fluorescein diacetate (F1303, Life Technologies) and analyzed by flow cytometry. A death control was performed by heating *C. reinhardtii* at 85 °C for 10 min. 10^5 events per sample were acquired in BD FACSCanto II analyzer (Becton Dickinson). Data were analyzed with FlowJo software (Becton Dickinson).

Microalgae Morphology and Diameter: General morphology of the microalgae was evaluated by optical microscopy (DM500, Leica) as well as by flow cytometry (BD FACSCanto II analyzer, Becton Dickinson). In order to calculate cell diameter, marker beads of 4, 6, and 10 μm were used (Life Technologies) and 10^5 events were recorded in the chlorophyll positive microalgae gate. Data were analyzed with FlowJo software (Becton Dickinson).

Optical Microscopy: Imaging of microalgae was performed by optical microscopy (DM500, Leica). For in vitro assays, photosynthetic scaffolds were macroscopically imaged using a standard stereoscope (Leica S6D). Moreover, in vivo implanted scaffolds were fixed in 4% paraformaldehyde (PFA) for 24 h. Next, samples were stored in 30% sucrose for at least 24 h and then mounted in Tissue-Tek O.C.T. (Sakura). Cryosections of 20 μm were obtained (Cryostat CM1520, Leica) and visualized using optical microscope (Primovert, Zeiss).

Confocal Microscopy: For in vitro experiments, scaffolds were stored in 4% PFA, and further analyzed by confocal microscopy (Airyscan, Zeiss), where chlorophyll and collagen autofluorescence were observed in red and green channels, respectively.

Confocal microscopy was also performed on implanted scaffolds. Scaffolds were fixed in 4% PFA for 24 h. Next, samples were stored in 30% sucrose for at least 24 h and further mounted in Tissue-Tek O.C.T. (Sakura). Cryosections of 20 μm were obtained (Cryostat CM1520, Leica) and stained with Hoechst 33342 (1:5000, Life Technologies) for 10 min. Cryosections were mounted with Fluoromount (Sigma) and stored at 4 °C until microscopy. Images were obtained with Airyscan microscope (Zeiss).

SEM: Scaffolds were fixed in 2% glutaraldehyde for 24 h and dehydrated with graded ethanol solutions and final 100% acetone. Samples were then air-dried overnight, sputtered with 20 nm gold (Varian Vacuum Evaporator PS10E), and analyzed using an acceleration voltage of 15 kV (TM3000, Hitachi).

Oxygraphy: Metabolic activity of the microalgae was measured using a Oxygraph+ System (Hansatech Instruments). Samples (microalgae suspension, or 8 mm in diameter scaffolds) were introduced in the electrode chamber with 1 mL of TAP medium, and subjected to 10 min of darkness, followed by 10 min of illumination. Dissolved oxygen concentration was recorded over time. Metabolic rates were calculated from the slopes of the oxygen concentration curves.

Chlorophyll Quantification: Microalgae pellets or photosynthetic scaffolds were stored individually at −20 °C until analysis. Samples were thawed and 500 μL of dimethyl sufoxide (DMSO; Sigma) was added. Samples were then vortexed and disrupted with a plastic pestle following incubation at RT for 40 min, covered from direct light. Finally, supernatant absorbance was measured at 665 and 648 nm using a microplate reader (Epoch, BioTek) and total chlorophyll content was calculated as[52]

$$\text{Chlorophyll}\left(\frac{\mu g}{mL}\right) = 7.49 \cdot A^{665} + 20.34 \cdot A^{648} \quad (1)$$

Growth Factor Release: Photosynthetic scaffolds (8 mm in diameter) fabricated with *C. reinhardtii* expressing recombinant human-VEGF protein were prepared and preserved as described in the sections above. At each specific time point (0, 2, 4, 6, or 8 weeks), scaffolds were washed to remove any possible remaining VEGF and "woken up" for 72 h at RT with TAP medium and constant illumination. Next, the medium was discarded, and scaffolds were placed in 12-well culture plates, and covered with 400 μL of phosphate buffer saline (PBS) 1X. Scaffolds were then incubated for 1 h at RT, with constant illumination and gentle agitation (110 rpm). PBS 1X supernatant was removed from the wells and stored at −80 °C until analysis. For growth factor release quantification, Human VEGF Quantikine ELISA kit (R&D Systems) was used, following the manufacturer's instructions.

Mouse Breeding and Procedures: All the experimental animal procedures were previously approved by the Scientific Ethical Committee for Animal Care at Pontificia Universidad Católica de Chile (Approval number: 220106001). Female C57BL/6 mice (10–15 weeks old) were bred at the institutional animal facilities and maintained under standard conditions (12/12 h of light/dark cycles, 20–24 °C) until experimental procedures.

Scaffold Implantation in Full-Skin Defect In Vivo: Surgical procedures were carried out as previously reported.[12,43] Briefly, animals were anesthetized by inhalation of 1–2% isoflurane (Baxter). Animal dorsal hair was removed using a shaving machine followed by shaving cream (Veet, Reckitt Benckiser) and skin was properly rinsed with lukewarm sterile water and cleaned with 2% chlorhexidine gluconate solution (Difem Laboratories). To maintain animal wellness during surgery, ophthalmic gel was applied to prevent eye damage (Nicotears, Saval Laboratories) and 300 μL of meloxicam (5 mg kg^{-1}) in saline solution was subcutaneously injected for analgesic treatment and to avoid dehydration. Next, two 10 mm in di-

© 2023 Wiley-VCH GmbH

23663987, 2023, 12, Downloaded from https://onlinelibrary.wiley.com/doi/10.1002/adtp.202300299 by Pontificia Universidad Catolic De Chile, Wiley Online Library on [12/12/2023]. See the Terms and Conditions (https://onlinelibrary.wiley.com/terms-and-conditions) on Wiley Online Library for rules of use; OA articles are governed by the applicable Creative Commons License

ameter full-skin defects were surgically created at the back of the animals, using fine surgical tweezers and scissors. 12 mm in diameter titanized meshes (TiMesh, Pfm medical) were placed on the wound sites, under the wound edges. Control, photosynthetic, and preserved scaffolds (for 5 weeks) were placed on top of the mesh and sutured to the wound edges with six single knots using nonabsorbable surgical sutures (Ethilon 5/0, Johnson and Johnson). The back of the animal was then covered with a transparent dressing (Tegaderm, 3 M). For each experimental group, four animals were used (eight independent scaffolds per group).

Animal Maintenance and Health Assessment: Animals were maintained individually in cages after surgery. In order to promote the photosynthetic activity of the microalgae, red light-emitting diode (LED) lights were adapted to the animal cages. Animals were subjected to circadian cycles of 12/12 h of red light/darkness. During the next 3 d postsurgery, 300 µL of meloxicam (5 mg kg^{-1}) in saline solution was subcutaneously injected for analgesic treatment and to avoid dehydration. Moreover, temperature and animal weight were monitored for up to 10 d. General health was assessed based on Grimace Scale, quantifying weight loss, general aspect of hair, wound aspect, spontaneous behavior, and behavior in response to manipulation. These parameters were scored between 0 and 3 as previously described.[44]

Euthanasia and Tissue Samples Collection: After 10 d of scaffold implantation, animals were euthanized by intraperitoneal overdose of ketamine/xylazine (30/300 mg kg^{-1} respectively). Blood was collected via cardiac puncture, allowed to clot at RT for 1 h, and further centrifuged at 1500 g for 10 min. Blood serum was then stored at −80 °C until analysis. Tegaderm dressing was removed and skin defects were imaged. Scaffolds were harvested and divided for protein extraction (immediately immersed in dry ice and stored at −80 °C), microscopy (fixed in 4% PFA), oxygraphy (stored in saline solution), and RNA quantification (stored in RNAlater solution, Thermo Fisher Scientific). Lymphatic organs, including spleen, thymus and lymph nodes, were also harvested, weighted, and imaged.

In Vivo Microalgae Viability Assessment: After 10 d of implantation, scaffold biopsies were preserved in RNAlater solution (Thermo Fisher Scientific) at 4 °C. RNA was isolated using TRIzol reagent (Thermo Fisher Scientific) following manufacturer's instructions. RNA samples were treated with 1 U of DNase I (Thermo Fisher Scientific) in the presence of 2.5 mM $MgCl_2$ at 37 °C for 30 min. A total of 0.5 µg of RNA was used for cDNA synthesis using MultiScribe reverse transcriptase with random primers p(dN)6 (Thermo Fisher Scientific) according to manufacturer's instructions. Conventional PCR was performed using SapphireAmp Fast PCR Master Mix (Takara Bio). Specific primers for *C. reinhardtii* RBCL subunit gene were used. Primer sequences for RBCL were: forward 5′-ACGCATGTCTTCAGTTCGGT-3′ and reverse 5′-GCTGAACGAATTACGTCGCC-3′.

Histology of the Scaffolds: Scaffolds were harvested after 10 d of implantation and fixed in 4% PFA for 24 h. Next, samples were dehydrated in 70% ethanol and embedded in Paraplast (Leica Biosystems) at 60 °C. Microsections of 4 µm were obtained and stained with Hematoxylin–Eosin. Images were obtained using Primovert optical microscope (Zeiss).

Cytokine Quantification: Cytokines were quantified from serum and harvested tissue samples. In order to extract proteins from tissues, these were weighted and disrupted with a plastic pestled in 300 µL of lysis buffer (150 mM NaCl, 1% v/v Triton X-100, 0.5% w/v sodium deoxycholate and 50 mM Tris) on ice. Next, samples were sonicated for 15 s twice and incubated at 4 °C for 1 h. Finally, samples were centrifuged at 13 000 × *g* for 20 min at 4 °C and supernatants were collected. Cytokines from serum samples and tissue protein extracts were quantified using Mouse Inflammation Kit (BD Cytometric Bead Array) following manufacturer's instructions. For tissue samples, data were normalized to the weight of each sample.

Statistical Analysis: All in vitro assays were performed in at least three independent experiments. For in vivo experiments, four animals with two implanted scaffolds each were used per group. Data in graphs are presented as mean + SEM or mean + standard deviation (SD), and comparison of conditions was performed by *t*-test, One-way or Two-way analysis of variance (ANOVA) followed by a Tukey's multiple comparison test when necessary (details are specified at each figure legend). In all cases, significance was defined as $p < 0.05$. Statistical analysis was carried out using GraphPad Prism 8 software.

Acknowledgements

The authors thank the Advanced Microscopy Facility UMA UC for their help in confocal and SEM imaging, and Felipe Carvajal and Valentina Veloso for their experimental support. The authors also thank Nicholas Möllhoff for his guidance and support in this work. This project was financed by CORFO grant 18PIDE98887, FONDECYT 1200280 and Amarena Venture Capital. In the introduction section the sentence "Indeed, several fluorescein diacetate (FDA)-approved cellular scaffolds have implemented cryopreservation as a storage method to increase their shelf-life from days to months and even years." was corrected to "Indeed, several Food and Drug Administration (FDA)-approved cellular scaffolds have implemented cryopreservation as a storage method to increase their shelf-life from days to months and even years." on December 15, 2023.

Conflict of Interest

J.T.E. is Chief Scientific Officer and co-founder of SymbiOx Inc., a start-up company that owns intellectual property in the field of this work. R.C.-O. and P.R. are employees of SymbiOx Inc. All other authors declare that they have no competing interests.

Data Availability Statement

The data that support the findings of this study are available from the corresponding author upon reasonable request.

Keywords

biomaterial preservation, microalgae, oxygen therapy, photosynthetic biomaterials

Received: August 24, 2023
Revised: October 16, 2023
Published online: October 26, 2023

[1] J. Malda, T. J. Klein, Z. Upton, *Tissue Eng.* **2007**, *13*, 2153.
[2] S. Schreml, R. M. Szeimies, L. Prantl, S. Karrer, M. Landthaler, P. Babilas, *Br. J. Dermatol.* **2010**, *163*, 257.
[3] G. H. J. De Smet, L. F. Kroese, A. G. Menon, J. Jeekel, A. W. J. Van Pelt, G.-J. Kleinrensink, J. F. Lange, *Wound Repair Regener.* **2017**, *25*, 591.
[4] D. L. Moreira Da Cruz, J. Oliveira-Pinto, A. Mansilha, *Int. Angiol.* **2022**, *41*, 63.
[5] R. G. Frykberg, *Medicina (Kaunas)* **2021**, *57*, 917.
[6] T. Agarwal, S. Kazemi, M. Costantini, F. Perfeito, C. R. Correia, V. Gaspar, L. Montazeri, C. De Maria, J. F. Mano, M. Vosough, P. Makvandi, T. K. Maiti, *Mater. Sci. Eng., C* **2021**, *122*, 111896.
[7] S. Liu, H. Yang, M. Y. Ho, B. Xing, *Adv. Opt. Mater.* **2023**, *n/a*, 2203038.
[8] J. Ma, Y. Fang, H. Yu, J. Yi, Y. Ma, P. Lei, Q. Yang, L. Jin, W. Wu, H. Li, D. Sun, *Adv. Funct. Mater.* **2023**, *n/a*, 2308387.
[9] U. Hopfner, T.-L. Schenck, M.-N. Chávez, H.-G. Machens, A.-V. Bohne, J. Nickelsen, R.-E. Giunta, J.-T. Egaña, *Acta Biomater.* **2014**, *10*, 2712.
[10] T. L. Schenck, U. Hopfner, M. N. Chávez, H.-G. Machens, I. Somlai-Schweiger, R. E. Giunta, A. V. Bohne, J. Nickelsen, M. L. Allende, J. T. Egaña, *Acta Biomater.* **2015**, *15*, 39.
[11] X. Wang, C. Yang, Y. Yu, Y. Zhao, *Research* **2022**, *2022*, 9794745.

 © 2023 Wiley-VCH GmbH

[12] M. N. Chávez, T. L. Schenck, U. Hopfner, C. Centeno-Cerdas, I. Somlai-Schweiger, C. Schwarz, H.-G. Machens, M. Heikenwalder, M. R. Bono, M. L. Allende, J. Nickelsen, J. T. Egaña, *Biomaterials* **2016**, *75*, 25.
[13] M. N. Chávez, B. Fuchs, N. Moellhoff, D. Hofmann, L. Zhang, T. T. Selão, R. E. Giunta, J. T. Egaña, J. Nickelsen, T. L. Schenck, *Acta Biomater.* **2021**, *126*, 132.
[14] R. Corrales-Orovio, F. Carvajal, C. Holmes, M. Miranda, S. González-Itier, C. Cárdenas, C. Vera, T. L. Schenck, J. T. Egaña, *Acta Biomater.* **2023**, *155*, 154.
[15] Y. Zhu, J. Jung, S. Anilkumar, S. Ethiraj, S. Madira, N. A. Tran, D. M. Mullis, K. M. Casey, S. K. Walsh, C. J. Stark, A. Venkatesh, A. Boakye, H. Wang, Y. J. Woo, *Sci. Rep.* **2022**, *12*, 10028.
[16] G. Chen, F. Wang, X. Zhang, Y. Shang, Y. Zhao, *Sci. Adv.* **2023**, *9*, eadg3478.
[17] W. Li, S. Wang, D. Zhong, Z. Du, M. Zhou, *Adv. Ther.* **2021**, *4*, 2000107.
[18] H. Wu, P. Yang, A. Li, X. Jin, Z. Zhang, H. Lv, *Acta Pharm. Sin. B* **2023**, *13*, 410.
[19] H. Chen, Y. Cheng, J. Tian, P. Yang, X. Zhang, Y. Chen, Y. Hu, J. Wu, *Sci. Adv.* **2020**, *6*, eaba4311.
[20] C. Centeno-Cerdas, M. Jarquín-Cordero, M. N. Chávez, U. Hopfner, C. Holmes, D. Schmauss, H.-G. Machens, J. Nickelsen, J. T. Egaña, *Acta Biomater.* **2018**, *81*, 184.
[21] M. L. Obaíd, J. P. Camacho, M. Brenet, R. Corrales-Orovio, F. Carvajal, X. Martorell, C. Werner, V. Simón, J. Varas, W. Calderón, C. D. Guzmán, M. R. Bono, S. San Martín, A. Eblen-Zajjur, J. T. Egaña, *Front. Med.* **2021**, *8*, 2088.
[22] M. L. Obaíd, F. Carvajal, J. P. Camacho, R. Corrales-Orovio, X. Martorell, J. Varas, W. Calderón, C. D. Guzmán, M. Brenet, M. Castro, C. Orlandi, S. San Martín, A. Eblen-Zajjur, J. T. Egaña, *Front. Bioeng. Biotechnol.* **2022**, *10*.
[23] A. L. Clement, G. D. Pins, in *Wound Healing Biomaterials* (Ed: M. S. Ågren), Woodhead Publishing, Sawston, UK **2016**, pp. 253–275.
[24] T. H. Jang, S. C. Park, J. H. Yang, J. Y. Kim, J. H. Seok, U. S. Park, C. W. Choi, S. R. Lee, J. Han, *Integr. Med. Res.* **2017**, *6*, 12.
[25] J. Meneghel, P. Kilbride, G. J. Morris, *Front. Med.* **2020**, *7*, https://doi.org/10.3389/fmed.2020.592242.
[26] C. Bay, Z. Chizmar, E. M. Reece, J. Z. Yu, J. Winocour, J. Vorstenbosch, S. Winocour, *Semin. Plast. Surg.* **2021**, *35*, 171.
[27] S. C. Foo, C. Y. Mok, S. Y. Ho, N. M. H. Khong, *Algal Res.* **2023**, *71*, 103007.
[28] J. Boswell, C. R. Lindsey, E. Cook, F. Rosenzweig, M. Herron, *Biol. Methods Protoc.* **2021**, *6*, bpab011.
[29] C. Scarbrough, M. Wirschell, *Cryobiology* **2016**, *73*, 291.
[30] A. Hopes, T. Mock, in *Encyclopedia of Life Sciences*, John Wiley and Sons, Ltd, Hoboken, NJ **2015**, p. 1.
[31] S. Sasso, H. Stibor, M. Mittag, A. R. Grossman, *Elife* **2018**, *7*, e39233.
[32] E. Ermilova, *Front. Plant Sci.* **2020**, *11*, 569437.
[33] R. Prasad, P. Pardha-Saradhi, *Phytomorphology* **2017**, *67*, 59.
[34] R. Prasad, N. Shabnam, P. Pardha-Saradhi, *Algal Res.* **2016**, *20*, 172.
[35] L. Li, H. Peng, S. Tan, J. Zhou, Z. Fang, Z. Hu, L. Gao, T. Li, W. Zhang, L. Chen, *Genomics* **2020**, *112*, 1128.
[36] Z. M. Zalutskaya, U. S. Skryabina, E. V. Ermilova, *Russ. J. Plant Physiol.* **2019**, *66*, 223.
[37] L. Valledor, T. Furuhashi, A.-M. Hanak, W. Weckwerth, *Mol. Cell. Proteomics* **2013**, *12*, 2032.
[38] E. Parrilli, M. L. Tutino, G. Marino, *Rend. Fis. Acc. Lincei* **2022**, *33*, 527.
[39] F. De Carpentier, S. D. Lemaire, A. Danon, *Cells* **2019**, *8*, 1307.
[40] I. Shachrai, A. Zaslaver, U. Alon, E. Dekel, *Mol. Cell* **2010**, *38*, 758.
[41] J. S. M. Pimentel, A. Giani, *Appl. Environ. Microbiol.* **2014**, *80*, 5836.
[42] S. P. Melegari, F. Perreault, S. Moukha, R. Popovic, E. E. Creppy, W. G. Matias, *Chemosphere* **2012**, *89*, 38.
[43] T. L. Schenck, M. N. Chávez, A. P. Condurache, U. Hopfner, F. Rezaeian, H.-G. Machens, J. T. Egaña, *J. Visualized Exp.* **2014**, *90*, e51428.
[44] C. Cárdenas-Calderón, V. Veloso-Giménez, T. González, A. Wozniak, P. García, S. S. Martín, J. F. Varas, I. Carrasco-Wong, M. Vera, J. T. Egaña, *Sci. Rep.* **2022**, *12*, 21846.
[45] M. Abram, D. Vuckovic, B. Wraber, M. Doric, *Mediators Inflammation* **2000**, *9*, 229.
[46] K. M. Williams, H. Wang, M. J. Paulsen, A. D. Thakore, M. Rieck, H. J. Lucian, F. Grady, C. E. Hironaka, A. J. Chien, J. M. Farry, H. Sook Shin, K. J. Jaatinen, A. Eskandari, L. M. Stapleton, A. N. Steele, J. E. Cohen, Y. J. Woo, *Microb. Biotechnol.* **2020**, *13*, 1780.
[47] M. I. Echeverria Molina, K. G. Malollari, K. Komvopoulos, *Front. Bioeng. Biotechnol.* **2021**, *9*, 617141.
[48] V. Veloso-Giménez, R. Escamilla, D. Necuñir, R. Corrales-Orovio, S. Riveros, C. Marino, C. Ehrenfeld, C. D. Guzmán, M. P. Boric, R. Rebolledo, J. T. Egaña, *Front. Bioeng. Biotechnol.* **2021**, *9*, 1287.
[49] M. N. Chávez, N. Moellhoff, T. L. Schenck, J. T. Egaña, J. Nickelsen, *Front. Bioeng. Biotechnol.* **2020**, *8*, 1158.
[50] D. S. Masson-Meyers, T. A. M. Andrade, G. F. Caetano, F. R. Guimaraes, M. N. Leite, S. N. Leite, M. A. C. Frade, *Int. J. Exp. Pathol.* **2020**, *101*, 21.
[51] J. Neupert, D. Karcher, R. Bock, *Plant J.* **2009**, *57*, 1140.
[52] J. D. Barnes, L. Balaguer, E. Manrique, S. Elvira, A. W. Davison, *Environ. Exp. Bot.* **1992**, *32*, 85.

 © 2023 Wiley-VCH GmbH

23663987, 2023, 12, Downloaded from https://onlinelibrary.wiley.com/doi/10.1002/adtp.202300299 by Pontificia Universidad Catolic De Chile, Wiley Online Library on [12/12/2023]. See the Terms and Conditions (https://onlinelibrary.wiley.com/terms-and-conditions) on Wiley Online Library for rules of use; OA articles are governed by the applicable Creative Commons License

References

1. Corrales-Orovio R, Carvajal F, Holmes C, Miranda M, González-Itier S, Cárdenas C, Vera C, Schenck TL, Egaña JT. Development of a photosynthetic hydrogel as potential wound dressing for the local delivery of oxygen and bioactive molecules. *Acta Biomaterialia* (2023) 155:154–166. doi: 10.1016/j.actbio.2022.11.036

2. Corrales-Orovio R, Castillo V, Rozas P, Schenck TL, Egaña JT. Development of a Hibernation-Inspired Preservation Strategy to Enhance the Clinical Translation of Photosynthetic Biomaterials. *Advanced Therapeutics* (2023) 6:2300299. doi: 10.1002/adtp.202300299

3. Kujath P, Michelsen A. Wounds – From Physiology to Wound Dressing. *Dtsch Arztebl Int* (2008) 105:239–248. doi: 10.3238/arztebl.2008.0239

4. Burgess M, Valdera F, Varon D, Kankuri E, Nuutila K. The Immune and Regenerative Response to Burn Injury. *Cells* (2022) 11:3073. doi: 10.3390/cells11193073

5. Nguyen HM, Le TTN, Nguyen AT, Le HNT, Pham TT. Biomedical materials for wound dressing: recent advances and applications. *RSC Adv* (2023) 13:5509–5528. doi: 10.1039/D2RA07673J

6. Eming SA, Martin P, Tomic-Canic M. Wound repair and regeneration: mechanisms, signaling, and translation. *Sci Transl Med* (2014) 6:265sr6. doi: 10.1126/scitranslmed.3009337

7. Gurtner GC, Werner S, Barrandon Y, Longaker MT. Wound repair and regeneration. *Nature* (2008) 453:314–321. doi: 10.1038/nature07039

8. Guo S, DiPietro LA. Factors Affecting Wound Healing. *J Dent Res* (2010) 89:219–229. doi: 10.1177/0022034509359125

9. Rezvani Ghomi E, Khalili S, Nouri Khorasani S, Esmaeely Neisiany R, Ramakrishna S. Wound dressings: Current advances and future directions. *Journal of Applied Polymer Science* (2019) 136:47738. doi: 10.1002/app.47738

10. Da Silva J, Leal EC, Carvalho E, Silva EA. Innovative Functional Biomaterials as Therapeutic Wound Dressings for Chronic Diabetic Foot Ulcers. *International Journal of Molecular Sciences* (2023) 24:9900. doi: 10.3390/ijms24129900

11. Kimmel HM, Grant A, Ditata J. The Presence of Oxygen in Wound Healing. *Wounds* (2016) 28:264–270.

12. Schreml S, Szeimies RM, Prantl L, Karrer S, Landthaler M, Babilas P. Oxygen in acute and chronic wound healing. *British Journal of Dermatology* (2010) 163:257–268. doi: 10.1111/j.1365-2133.2010.09804.x

13. de Smet GHJ, Kroese LF, Menon AG, Jeekel J, van Pelt AWJ, Kleinrensink G-J, Lange JF. Oxygen therapies and their effects on wound healing. *Wound Repair Regen* (2017) 25:591–608. doi: 10.1111/wrr.12561

14. Moreira DA Cruz DL, Oliveira-Pinto J, Mansilha A. The role of hyperbaric oxygen therapy in the treatment of diabetic foot ulcers: a systematic review with meta-analysis of randomized controlled trials on limb amputation and ulcer healing. *Int Angiol* (2022) 41:63–73. doi: 10.23736/S0392-9590.21.04722-2

15. Agarwal T, Kazemi S, Costantini M, Perfeito F, Correia CR, Gaspar V, Montazeri L, De Maria C, Mano JF, Vosough M, et al. Oxygen releasing materials: Towards addressing the hypoxia-related issues in tissue engineering. *Materials Science and Engineering: C* (2021) 122:111896. doi: 10.1016/j.msec.2021.111896

16. Frykberg RG. Topical Wound Oxygen Therapy in the Treatment of Chronic Diabetic Foot Ulcers. *Medicina (Kaunas)* (2021) 57:917. doi: 10.3390/medicina57090917

17. Ma J, Fang Y, Yu H, Yi J, Ma Y, Lei P, Yang Q, Jin L, Wu W, Li H, et al. Recent Advances in Living Algae Seeding Wound Dressing: Focusing on Diabetic Chronic Wound Healing. *Advanced Functional Materials* (2023) n/a:2308387. doi: 10.1002/adfm.202308387

18. Chávez MN, Schenck TL, Hopfner U, Centeno-Cerdas C, Somlai-Schweiger I, Schwarz C, Machens H-G, Heikenwalder M, Bono MR, Allende ML, et al. Towards autotrophic tissue engineering: Photosynthetic gene therapy for regeneration. *Biomaterials* (2016) 75:25–36. doi: 10.1016/j.biomaterials.2015.10.014

19. Chávez MN, Fuchs B, Moellhoff N, Hofmann D, Zhang L, Selão TT, Giunta RE, Egaña JT, Nickelsen J, Schenck TL. Use of photosynthetic transgenic cyanobacteria to promote lymphangiogenesis in scaffolds for dermal regeneration. *Acta Biomaterialia* (2021) 126:132–143. doi: 10.1016/j.actbio.2021.03.033

20. Centeno-Cerdas C, Jarquín-Cordero M, Chávez MN, Hopfner U, Holmes C, Schmauss D, Machens H-G, Nickelsen J, Egaña JT. Development of photosynthetic sutures for the local delivery of oxygen and recombinant growth factors in wounds. *Acta Biomater* (2018) 81:184–194. doi: 10.1016/j.actbio.2018.09.060

21. Liu S, Yang H, Ho MY, Xing B. Recent Advances of Material-Decorated Photosynthetic Microorganisms and Their Aspects in Biomedical Applications. *Advanced Optical Materials* (2023) n/a:2203038. doi: 10.1002/adom.202203038

22. Hopfner U, Schenck T-L, Chávez M-N, Machens H-G, Bohne A-V, Nickelsen J, Giunta R-E, Egaña J-T. Development of photosynthetic biomaterials for in vitro tissue engineering. *Acta Biomater* (2014) 10:2712–2717. doi: 10.1016/j.actbio.2013.12.055

23. Schenck TL, Hopfner U, Chávez MN, Machens H-G, Somlai-Schweiger I, Giunta RE, Bohne AV, Nickelsen J, Allende ML, Egaña JT. Photosynthetic biomaterials: a pathway towards autotrophic tissue engineering. *Acta Biomater* (2015) 15:39–47. doi: 10.1016/j.actbio.2014.12.012

24. Obaíd ML, Camacho JP, Brenet M, Corrales-Orovio R, Carvajal F, Martorell X, Werner C, Simón V, Varas J, Calderón W, et al. A First in Human Trial Implanting Microalgae Shows Safety of Photosynthetic Therapy for the Effective Treatment of Full Thickness Skin Wounds. *Frontiers in Medicine* (2021) 8:2088. doi: 10.3389/fmed.2021.772324

25. Obaíd ML, Carvajal F, Camacho JP, Corrales-Orovio R, Martorell X, Varas J, Calderón W, Guzmán CD, Brenet M, Castro M, et al. Case report: Long-term follow-up of a large full-thickness skin defect treated with a photosynthetic scaffold for dermal regeneration. *Frontiers in Bioengineering and Biotechnology* (2022) 10: https://www.frontiersin.org/articles/10.3389/fbioe.2022.1004155 [Accessed January 23, 2023]

26. Wang X, Yang C, Yu Y, Zhao Y. In Situ 3D Bioprinting Living Photosynthetic Scaffolds for Autotrophic Wound Healing. *Research* (2022) 2022: doi: 10.34133/2022/9794745

27. Zhu Y, Jung J, Anilkumar S, Ethiraj S, Madira S, Tran NA, Mullis DM, Casey KM, Walsh SK, Stark CJ, et al. A novel photosynthetic biologic topical gel for enhanced localized hyperoxygenation augments wound healing in peripheral artery disease. *Sci Rep* (2022) 12:10028. doi: 10.1038/s41598-022-14085-1

28. Li W, Wang S, Zhong D, Du Z, Zhou M. A Bioactive Living Hydrogel: Photosynthetic Bacteria Mediated Hypoxia Elimination and Bacteria-Killing to Promote Infected Wound Healing. *Advanced Therapeutics* (2021) 4: doi: 10.1002/adtp.202000107

29. Hu H, Zhong D, Li W, Lin X, He J, Sun Y, Wu Y, Shi M, Chen X, Xu F, et al. Microalgae-based bioactive hydrogel loaded with quorum sensing inhibitor promotes infected wound healing. *Nano Today* (2022) 42:101368. doi: 10.1016/j.nantod.2021.101368

30. Wu H, Yang P, Li A, Jin X, Zhang Z, Lv H. Chlorella sp.-ameliorated undesirable microenvironment promotes diabetic wound healing. *Acta Pharm Sin B* (2023) 13:410–424. doi: 10.1016/j.apsb.2022.06.012

31. Chen G, Wang F, Zhang X, Shang Y, Zhao Y. Living microecological hydrogels for wound healing. *Sci Adv* (2023) 9:eadg3478. doi: 10.1126/sciadv.adg3478

32. Chen H, Cheng Y, Tian J, Yang P, Zhang X, Chen Y, Hu Y, Wu J. Dissolved oxygen from microalgae-gel patch promotes chronic wound healing in diabetes. *Science Advances* (2020) 6:eaba4311. doi: 10.1126/sciadv.aba4311

33. Zhao E, Xiao T, Tan Y, Zhou X, Li Y, Wang X, Zhang K, Ou C, Zhang J, Li Z, et al. Separable Microneedles with Photosynthesis-Driven Oxygen Manufactory for Diabetic Wound Healing. *ACS Appl Mater Interfaces* (2023) 15:7725–7734. doi: 10.1021/acsami.2c18809

34. Firlar I, Altunbek M, McCarthy C, Ramalingam M, Camci-Unal G. Functional Hydrogels for Treatment of Chronic Wounds. *Gels* (2022) 8:127. doi: 10.3390/gels8020127

35. Clement AL, Pins GD. "10 - Engineering the tissue–wound interface: Harnessing topography to direct wound healing.," In: Ågren MS, editor. *Wound Healing Biomaterials*. Woodhead Publishing (2016). p. 253–275 doi: 10.1016/B978-1-78242-455-0.00010-0

36. Jang TH, Park SC, Yang JH, Kim JY, Seok JH, Park US, Choi CW, Lee SR, Han J. Cryopreservation and its clinical applications. *Integrative Medicine Research* (2017) 6:12–18. doi: 10.1016/j.imr.2016.12.001

37. Bay C, Chizmar Z, Reece EM, Yu JZ, Winocour J, Vorstenbosch J, Winocour S. Comparison of Skin Substitutes for Acute and Chronic Wound Management. *Semin Plast Surg* (2021) 35:171–180. doi: 10.1055/s-0041-1731463

38. Meneghel J, Kilbride P, Morris GJ. Cryopreservation as a Key Element in the Successful Delivery of Cell-Based Therapies—A Review. *Frontiers in Medicine* (2020) 7: https://www.frontiersin.org/articles/10.3389/fmed.2020.592242 [Accessed February 23, 2023]

39. Foo SC, Mok CY, Ho SY, Khong NMH. Microalgal culture preservation: Progress, trends and future developments. *Algal Research* (2023) 71:103007. doi: 10.1016/j.algal.2023.103007

40. Boswell J, Lindsey CR, Cook E, Rosenzweig F, Herron M. Cryopreservation of clonal and polyclonal populations of Chlamydomonas reinhardtii. *Biology Methods and Protocols* (2021) 6:bpab011. doi: 10.1093/biomethods/bpab011

41. Scarbrough C, Wirschell M. Comparative analysis of cryopreservation methods in Chlamydomonas reinhardtii. *Cryobiology* (2016) 73:291–295. doi: 10.1016/j.cryobiol.2016.07.011

42. Ermilova E. Cold Stress Response: An Overview in Chlamydomonas. *Front Plant Sci* (2020) 11:569437. doi: 10.3389/fpls.2020.569437

43. Sasso S, Stibor H, Mittag M, Grossman AR. From molecular manipulation of domesticated Chlamydomonas reinhardtii to survival in nature. *eLife* (2018) 7:e39233. doi: 10.7554/eLife.39233

44. Schenck TL, Chávez MN, Condurache AP, Hopfner U, Rezaeian F, Machens H-G, Egaña JT. A full skin defect model to evaluate vascularization of biomaterials in vivo. *J Vis Exp* (2014) doi: 10.3791/51428